ABSTRACT

GIL, EUN SEOK: STIMULI-RESPONSIVE PROTEIN-BASED HYDROGELS BY UTILIZING β-SHEET CONFORMATION OF SILK FIBROIN AS CROSS-LINKS. (Under the direction of Dr. Samuel M. Hudson and Dr. Richard J. Spontak)

Stimuli responsive polymers can provide a variety of applications for biomedical fields such as drug delivery, biotechnology, and chromatography. The interest in these polymers has exponentially increased due to their promising potential. Stimuli-responsive polymers have been utilized in various forms: hydrogels, micelles, modified interfaces, and conjugated solutions. Among them, hydrogels have gained strong attention as biomaterials due to their biocompatibility and biodegradability in the swollen state. The introduction of stimuli-responsive characteristic into hydrogels should provide more versatile applications such as targeted drug delivery, micro or nano scale actuating valves, artificial organs responding to stimuli, and protein or DNA purification. In many applications, better biological materials are needed, particularly the incorporation of two or more functionalities into one material.

One strategy is to develop interpenetrating polymer networks (INPs) in hydrogels. Novel protein-based complex hydrogels were prepared by blending gelatin (Gel) with Bombyx mori silk fibroin (SF) and introducing β-sheet conformation of SF in their complex networks. The influence of solvent-induced SF crystallization on the properties and structures of these binary protein complexes was determined as functions of blend composition and preparation history. Rheological tests confirmed that the fine β-sheet crystalline structure successfully governed the Gel/SF complex networks, increasing their viscoelastic properties and sustaining their physical form as hydrogels even at body

temperature. The helix-coil transition of gelatin in the Gel/SF complex hydrogels was determined by DSC and rheological tests to be reversible between ambient and body temperatures, so these hydrogels exhibit reversible IPNs/semi-IPNs transitions. This reversible temperature-responsive conformational change of gelatin molecules in Gel/SF complex hydrogels could promote an abrupt swelling increase and a temperature-triggered protein release from the networks at body temperature, which could be utilized for a targeted drug delivery.

These hydrogels show a temperature-responsive gelatin release profile: at 20 °C they exhibited no gelatin release and maintained their hydrogel dimensions, but at 37 °C they showed time-dependent gelatin release and their hydrogel dimensions decreased.

Protein-synthetic polymer hybrid interpenetrating networks (IPNs) of poly(*N*-isopropylacrylamide) (PNIPAAm) with *Bombyx mori (B. mori)* silk fibroin (SF) are described. In these IPNs, SF has the β-sheet crystalline structure, and shows improved storage and loss moduli. The IPN hydrogels show volume phase transition behavior at the same temperature and NaCl concentration as pure PNIPAAm hydrogels. The PNIPAAm/SF IPNs retain the swelling kinetics of PNIPAAm and show increased deswelling kinetics, with a mechanism whereby the internal water molecules are rapidly released through the induced β-sheet networks. The IPNs with SF β-sheet structure successfully decrease the formation of a skin layer observed in conventional PNIPAAm hydrogels. Therefore, the proposed IPN hydrogels can provide three benefits; improved mechanical property, biocompatibility, and deswelling rates.

STIMULI-RESPONSIVE PROTEIN-BASED HYDROGELS BY UTILIZING β-SHEET CONFORMATION OF SILK FIBROIN AS CROSS-LINKS

By

Eun Seok Gil

A dissertation submitted to Graduate Faculty
of North Carolina State University
in partial fulfillment of the requirements
for the degree of Doctor of Philosophy

FIBER AND POLYMER SCIENCE

Raleigh

Dec 2004

Approved By

_____	_____
_____	_____
Co-Chair of Advisory Committee	**Chair of Advisory Committee**

BIOGRAPHY

Eun Seok Gil was born on January 3, 1972 in Seoul, South Korea as a son of Gi Hong Gil, and Bang Ran Tak. He attended both elementary and junior high school in Seoul, South Korea. In 1990, he graduated from Hong-ik High School in Seoul, South Korea. In March 1990, Eun Seok attended Hanyang University. He received a Bachelor of Science in Fiber and Polymer Engeening from Hanyang University, 1994. He continued his study in Fiber and Polymer Engineering and received a Master's degree from Hanyang University in 1996. After his graduation, he worked as a researcher for 2 years in Advanced Industrial Science Research Center in Hanyang University. Also, he had worked for his family business of constructing and managing a commercial building until he began new study in America. In August 2000, he enrolled in the Fiber and Polymer Science program in the College of Textile at North Carolina State University, where he began training under the direction of Dr. Samuel M. Hudson.

ACKNOWLEDGMENTS

Completing the requirements for the doctoral degree in Fiber and Polymer Science program has been one of the most challenging endeavors of my life. I have had to overcome many obstacles throughout this experience. I would like to thank God for continuing to pursue this goal. It would not have been possible for me to achieve this goal had it not been for the many people that have supported me and prayed for me during this period of my life. I could not possibly list all of the people that have inspired or encouraged and supported me during this time.

First, I would like to thank members of my family beginning with my wife, Kang Mi Lee, for her continued patience and support for the past four years, while pursuing her own Ph.D program of Immunology at NCSU. I would also like to acknowledge my father and mother, Gi Hong Gil and Bang Ran Tak, for their endless praying, encouragement, and unselfish support in whole my life time. I would also like to thank mother-in-law, Jong Sun Kim, for her concern and love. I acknowledge my elder brother, Jun Seok Gil, for his love and advices through my life. Finally, of my family members, I would like to acknowledge my elder sister in heaven, Hye Seon Gil. I always remember her smartness and brilliance. She deserves this degree rather than me. Please, God bless her forever.

Secondly, I would like to thank members of my graduate advisory committee, Dr. Richard Spontak, Dr. Alan Tonelii, and Dr. Richard Kotek. They have all been very helpful, supportive, and have each provided excellent advice during my training period. I am thankful to work with Dr. Spontak, who always encouraged and helped me as my co-advisor. Most of all, I would like to thank my advisor, Dr. Samuel Hudson. Dr. Hudson

encouraged me to achieve high standards in research and academics. He has been helpful, supportive, encouraging, and most of all, patient. Besides the excellent training I received under his supervision, I am especially thankful to him for his parental cares. I will never forget his graceful financial support in my second semester through a loan from the department. I am sure that his love will affect me to love other people without condition.

I would like to thank other faculty members in college of textile to include, Dr. Keith Beck, Dr. Brent Smith, Dr, Harold Freeman, Dr. Wendy Klause, and Dr. Russel Gorga. I would like to acknowledge my lab mates, David Jenkins, Sang Hun Lim, Sung Won Ha, Khaled El-Tahlawy, Dong Wook Jung, Kyeong Pang, Ji Sang Hwang and a new member Mai Yamazaki. They were all supportive and a pleasure to work with.

Finally, I would like to thank all church members including Chang Gu Kang in Duraleigh Presbyterian Church, especially, Pastor. Su MyungWoo, Pastor. Byeong Jin Woo, and Pastor. Se Jong Cheon.

TABLE OF CONTENTS

LIST OF TABLES

LIST OF FIGURES

1. BACK GROUND REVIEW

STIMULI-RESPONSIVE POLYMERS AND THEIR BIOCONJUGATES

1.1. Introduction

Polymers such as proteins, polysaccharides, and nucleic acids are present as basic components in living organic systems. Synthetic polymers, which are designed to mimic these biopolymers, have been developed into a very active field due to their industrial and scientific value. They have been progressively developed from the description of the unique properties of biopolymers.

One approach involves the response of a polymer system to stimuli, which is a common process for biopolymers in living organisms. These properties of biopolymers are based on highly cooperative interactions, which can provide significant driving forces for the responses caused by small environmental changes. For the past several decades, the concept of cooperative interactions between the functional segments of biopolymer has led to the creative idea to invent novel synthetic polymer systems that are environmentally responsive to stimuli in some controlled ways [1-4].

Stimuli-responsive polymers are defined as polymers that undergo relatively large and abrupt, physical or chemical changes in response to small external changes in the environmental conditions. Names coined for 'stimuli-responsive' polymers have been given as stimuli-sensitive [4], intelligent [5], smart [6, 7], or environmentally sensitive polymers [8]. These polymer systems might recognize a stimulus as a signal, judge the magnitude of this signal, and then change their chain conformation in direct response [1]. There are many different stimuli to modulate the response of polymer systems.

These stimuli could be classified as either physical or chemical stimuli. Chemical stimuli, such as pH, ionic factors and chemical agents, will change the interactions between polymer chains or between polymer chains and solvents at the molecular level. The physical stimuli, such as temperature, electric or magnetic fields, and mechanical stress, will affect the level of various energy sources and alter molecular interactions at critical onset points. These responses of polymer systems are very useful in bio-related applications such as drug delivery [3, 4, 8-13], biotechnology [4, 7, 14], and chromatography [5, 15, 16]. Some systems have been developed to combine two or more stimuli-responsive mechanisms into one polymer system. For instance, temperature-sensitive polymers may also respond to pH changes [17-20]. On the other hand, some workers have reported that two or more signals could be simultaneously applied in order to induce response in so-called dual-responsive polymer systems [21]. Recently, biochemical stimuli have been considered as another category, which involves the responses to antigen, enzyme, ligand, and biochemical agents [6].

1.2. Physical forms of stimuli-responsive polymers

Stimuli-responsive polymers have been utilized in various forms as follows;

1. Cross-linked (permanently) hydrogels
2. Reversible hydrogels
3. Micelles
4. Modified interfaces
5. Conjugated solutions

Hydrogels are formed with a three- dimensional network of polymer chains,

where some parts are solvated by water molecules but the other parts are chemically or physically linked with each other. This structure gives the interesting property that they swell, but do not dissolve in aqueous environment. Therefore, hydrogels can come from a cross-linked network of hydrophilic polymers in water as the meaning of the prefix 'hydro' is 'aqueous' and they maintain their 3-dimensional (3D) structure after absorbing large amounts water and swelling. Based on these cross-linked networks of hydrogels, the dimensions of stimuli-responsive hydrogels could be dramatically changed by an alternative change of hydrophobicity and hydrophilicity in the molecular structure of the swollen polymer chains [3, 22-25]. This type of hydrogel has a cross-linked network structure containing the stimuli-responsive component in the polymer chains, which causes dramatic swelling/deswelling according to the change in stimuli.

Other forms of stimuli-responsive hydrogels could be reversibly transformed to solutions due to environmental stimuli changes, showing solution-gelation (sol-gel) transition by altering the hydrophobic interactions of cross-linked areas in an aqueous system [26- 31]. Therefore, this type of stimuli responsive polymer has been developed for a phase change rather than a dimension change, to be used for example, as injectable hydrogels [32].

Polymeric micelles can be another form of stimuli-responsive polymer system. Micelles form by aggregation of amphiphilically combined block or terminally modified polymers in aqueous medium, and originated from a hydrophobic effect. Stimuli responsive micelles can be designed by two methodologies. Firstly, amphiphilic blocks in one structure undergo the micellization/demicellization by the alternation of balance between hydrophilicity

and hydrophobicity, which can be modulated by stimuli (mostly temperature) [31, 33-35]. Secondly, one or both hydrophilic and hydrophobic segments would be replaced by stimuli responsive component, resulting in stimuli responsive outer shells or inner cores in micelle structures [36-38]. However, it is ambiguous to distinguish these micelle structures from reversible hydrogels, because micelles can form hydrogels above a specific high concentration (micelle gelation concentration) [31, 39].

Also, matrix surfaces, such as polymer [18, 40-42], silica [43], and metal [44], could be functionalized with stimuli-responsive polymers to produce highly responsive interfaces between solid and liquid (mostly water) phases. The property of the modified interface can give a dynamic on-off system by changing the hydrophobic/hydrophilic surface function and the pore size of porous membranes.

The solubility of stimuli responsive polymers can be controlled by changing stimuli. As a result, its conjugates can be modulated to have stimuli responsive solubility. The conjugation can be obtained by a covalent bond [43- 47] or secondary bond such as hydrophobic interactions [48, 49] and electrostatic forces [50, 51]. Once the conjugation of stimuli responsive polymer and conjugates such as drugs and proteins is developed, the activity of the conjugates depends on the hydrophobic and hydrophilic changes of the polymer chain induced by stimuli.

1.3. Temperature responsive polymers

1.3.1. Concept of temperature responsive polymers

Temperature is the most widely used stimulus in environmentally responsive polymer systems. The change of temperature is not only relatively easy to control, but also easily

applicable both *in vitro* and *in vivo*. For example, temperature-responsive dishes can be utilized as a cell sheet manipulation techniques *in vitro* [52-56] and temperature-responsive hydrogels or micelles containing drug can be applied *in vivo* [11, 13, 30, 57]. One of the unique properties of temperature-responsive polymers is the presence of a critical solution temperature. Critical solution temperature is the temperature at which the phase of polymer and solution (or the other polymer) is discontinuously changed according to their composition. If the polymer solution (mostly water) has one phase below a specific temperature, which depends on the polymer concentration, and are phase-separated above this temperature, these polymers generally have a lower critical solution temperature (LCST), the lowest temperature of the phase separation curve on concentration-temerature diagram. Otherwise, it is called a higher critical solution temperature (HCST) or upper critical solution temperature (UCST). However, most applications are related to LCST-based polymer systems [58]. For example, poly(*N*-isopropylacrylamide) (PNIPAAm) has a LCST, at which it undergoes a reversible volume phase transition caused by the coil-to-globule transition [184]. Intramolecular collapse occurs before intermolecular aggregation through LCST and the collapse of individual polymer chains increases the scattering of light in solution (cloud point). Phase separation between the collapsed polymer molecules and the expelled water follows this cloud point [59].

Besides the relationship between polymer and water molecules, there is another important characteristic of a temperature-responsive polymer. This is the intermolecular interaction in water medium, which might create hydrogel shrinkage, micelle aggregation or the physical cross-links. Generally, two types of intermolecular forces can be

considered; hydrogen bonding and hydrophobic interactions. One example of an intermolecular association based on hydrogen bonding is a random coil-to-helix transition, at which by lowering the temperature, two or three biopolymer chains (e.g. gelatin) form a helix conformation that generates physical junctions to make a gel network [60]. Another example is the hydrogen bonding association/dissociation between different pendant groups, which can be controlled by temperature. Through this mechanism, reversible swelling/deswelling of hydrogels around a critical temperature was reported in random copolymer or interpenetrating polymer networks (IPNs) composed of polyacids (proton donor at low pH) and polyacrylamide (proton accepter) [61, 62]. On the other hand, intermolecular association can be controlled by the balance of hydrophobic interactions and temperature. For example, triblock PEO-PPO-PEO copolymers (Pluronics, or Poloxamers) form a micelle structure above a critical micelle temperature on the basis of hydrophobic effects of the PPO blocks (hydrophobic junction domain) that aggregate to form a core [63].

1.3.2. Classification of temperature responsive polymers

1.3.2.1. Polymers based on LCST

Poly(*N*-substituted acrylamide) is representative of the group of temperature-responsive polymers which have a LCST, defined as the critical temperature at which a polymer solution undergoes phase transition from a soluble to an insoluble state above the critical temperature. Figure 1-1 shows respective *N*-substituted polyamides according to the substitution groups.

Poly(*N*-isopropylacrylamide) (PNIPAAm) (Figure 1-1a) is the most popular temperature-responsive polymer since it exhibits a sharp phase transition in water

(LCST) at around 32°C [59]. The fundamental behavior of PNIPAAm has been extensively studied not only to understand the mechanism itself but also to develop specific technological applications. The *N*-isopropylacrylamide (NIPAAm) segment has been designed at the molecular level to control the LCST and the response kinetics. The advances of PNIPAAm-based molecular designs to adjust the temperature sensitivity into desirable applications will be discussed in section 3.3.1.. Poly(*N,N'*-diethylacrylamide) (PDEAAm) (Figure 1-1b), which has a LCST in the range of 25-35°C, is an other popular temperature responsive polymer [8].

Poly(2-carboxyisopropylacrylamide) (PCIPAAm) (Figure 1-1c) is composed of a vinyl group, isopropylacrylamide gourp, and carboxyl group, which can give two benefits; the analogous temperature responsive behavior as PNIPAAm and the additional functionality in its pendant groups [64].The PNIPAAm-co-PCIPAAm was reported to have a similar LCST and sensitivity as PNIPAAm [64,65]. PNIPAAm-co-PCIPAAm is distinct from the PNIPAAm-co-Poly(acrylic acid), because the former has continuous isopropylacrylamide pendant groups in its chain. The continuous pendant groups did not change the temperature responsive behavior of PNIPAAm in spite of the additional carboxyl pendant groups.

Poly(*N*-(L)-(1-hydroxymethyl) propylmethacrylamide) (P(L-HMPMAAm)) (Figure 1-1d) is another specific temperature responsive polymer that is designed to also have optical activity associated with a single unit. This novel macromolecule in an aqueous milieu showed a quite different thermo-sensitive phase transition from that of optically inactive P(DL-HMPMAAm) [66].

Poly(*N*-acryloyl-*N'*-alkylpiperazine) (Figure 1-1e) was recently reported as another new temperature and pH responsive polymer [20, 67]. Poly(*N*-acryloyl-*N'*-propyllpiperazine) showed a LCST at 37°C, while introducing methyl or ethyl groups instead of the propyl group resulted in the loss of a LCST [20]. In another report, a series of copolymers of *N*-acryloyl-*N'*-alkylpiperazine (methyl and ethyl) with polymethacrylamide (PMAAm) was investigated for their temperature and pH sensitivity [67]. Even though the homopolymers based on methylpiperazine and ethylpiperazine did not exhibit the LCST due to their weak hydrophobicity [20], incorporating the methacrylamide group induced an LCST for these copolymers by increasing hydrophobicity in their structures [67].

Other temperature responsive synthetic polymers showing the LCST were enlisted in Table 1-1. However, these polymers have been less extensively investigated than poly(*N*-substituted acrylamide) (mostly PNIPAAm).

Table 1-1 Other temperature responsive synthetic polymers showing the LCST

Polymers	References
Poly(*N*-vinylisobutylamide)	[68]
Poly(vinyl methyl ether)	[69]
Poly(*N*-vinylcaprolactam)	[70]
Poly(dimethylaminoethyl methacrylate)	[40]

1.3.2.2. Polymers based on amphiphilic balance

A series of amphiphilic block copolymers were reported to have temperature responsive

micellization behavior and to form hydrogels above a critical gelation temperature (cgt) [12]. Representatively, poly(ethylene oxide)-poly(propylene oxide)- poly(ethylene oxide) (PEO-PPO-PEO) triblock copolymers exhibit the temperature responsive micellization and gelation. They have their sol-gel phase transition under body temperature and gel-sol phase transition around 50°C in the relatively high concentration range [71]. PEO, PPO, and PEO-PPO-PEO block copolymers have their respective LCSTs (e.g. cloud point) [12]. However, the sol-gel transition of PEO-PPO-PEO should be separated from their LCSTs, because the temperature responsive gelation occurs by the three dimensional packing of micelles, which form by the hydrophilic-hydrophobic balance.[72] The mechanism of sol-gel transition was elucidated as an increased micelle volume change, which caused crystal-like packing of micelles [73]. For example, P105 (EO_{37}-PO_{56}-EO_{37}) shows a cloud point (e.g. LCST) at 91°C and micellization at 12-18°C [74]. As the temperature increased over the other critical threshold, the micelle structure was changed from spherical to cylindrical with associated release of packing constraints [75].

The PPO block can be replaced with other hydrophobic groups. As one example, Poly(1,2-butylene oxide) (PBO) was introduced as a more hydrophobic group than PPO. Because of the hydrophobicity of the PBO unit, the critical micelle concentrations (cmc) of these copolymers were very low [76]. Copolymer PEO-*b*-PBO was prepared by sequential anionic polymerization of ethylene oxide followed by 1,2-butylene oxide, in order to obtain narrow block length distributions and avoid problems associated with the difference in reaction rates of ethylene oxide with secondary (PBO) oxyanions and primary (PEO)

oxyanions [77]. The PPO block can be also replaced with poly(L-lactic acid) (PLLA) [33] and (DL-lactic acid-co-glycolic acid) (PLGA) [34], which places a biodegradable ester group in its backbone.

The hydrophilic/hydrophobic balance can be adjusted by introducing two side chains that have hydrophilic and hydrophobic properties respectively. In this respect, poly(organophosphazene) bearing two side groups of poly(ethylene glycol) and amino acid esters were reported to exhibit temperature responsive behavior and have an easily hydrolyzed polymer back-bone (Figure 1-2a) [78-80]. In their first two reports [78, 79], the authors investigated the cloud point (e.g. LCST) of the modified poly(organophosphazene) with different side groups. The LCST of these polymers varied from 50 to 93°C, depending on the structure of the side groups. They also investigated the degradation rate of this series of polymers [78]. Interestingly, their recent report elucidated the sol-gel transition of these polymers [80]. They supposed that the sol-gel transtion was exhibited due to the hydrophilic/hydrophilic balance, where the hydrophobic interaction between the side-chain fragments (-$CH(CH_3)CH_2CH_3$) of hydrophobic L-isoleucine ethyl ester groups might act as the physical junction above critical gelation temperature. These authors reported another type of temperature responsive polymer, cyclotriphosphazenes with poly(ethyleneglycol) and amino acid esters as side groups and investigated their LCST according to different compositions of side groups (Figure 1-2b) [81,82]. However, the sol-gel behaviors of these polymers have not been reported yet.

1.3.2.3. Biopolymers and artificial polypeptides

Some biopolymers such as gelatin [83], agarose [84], and gellan benzyl ester [85] have been reported to exhibit temperature responsive behavior. They form helix conformations, leading to physical cross-linking. Gellan, a polysaccharide and its derivatives such as gellan benzyl ester have double helix conformations via hydrogen bonding in aqueous systems. The double helix domains aggregate to form physical cross-links due to hydrophobic interaction, resulting in gelation. These phase changes are controlled by temperature. Gelatin has a different mechanism for gelation. Gelatin is a protein that is obtained by breaking the triple-helix structure of collagen into single-strand molecules. Gelatin is a thermally reversible hydrogel, which means that it forms gels in aqueous solution by cooling the temperature as the chains transform their conformation from random coil to triple-helix, during which physical junctions are promoted and gel networks occur.

However, the physical properties of gelatins are not sufficiently stable at physiological temperature to use them in biomedical applications. Therefore, chemical cross-links have been introduced to form stable hydrogels of gelatin [83]. In this report, the temperature responsive behavior was investigated as affected by the chemical cross-linking densities. They also reported that the thermal transition of cross-linked gelatin was irreversible; once the helix structures were destroyed by heating, the helix structures were not observed when they were cooled. In the other report, gelatin was conjugated with chitosan to offer stable hydrogels based on gelatin [86]. The conjugation of gelatin and chitosan was performed by tyrosinases, which are oxidative enzymes converting accessible tyrosine residues of gelatin into reactive o-quinone moieties. Oxidized tyrosyl residues were expected to react with the amino groups of chitosan. From rheological measurements, the authors

showed the different thermal transition behaviors of this conjugated polymer from those of gelatin. Although the conjugated polymers exhibited a decrease of its rheological properties above 40°C, and reversibly returned its rheological properties under 20°C, this conjugated polymer conserved its hydrogel form over 50°C.

The complexation of two or more biopolymers [26, 27], salt [83], or surfactant [87-89] can be controlled by stimulus such as temperature. This complexation can offer thermal transition of the polymeric system in water, leading to volume change or sol-gel transition. Chitosan/polyol salt combinations were reported to be held liquid below room temperature and form monolithic gels at body temperature [27]. In this system, they did not use any synthetic chemical compounds. Therefore, they can provide a biodegradable and non-toxic system. They reported that the liquid formulations turn into gel implants *in situ* after the injection *in vivo*. They also suggested that chitosan/polyol salt combinations could be used for injectable drug delivery of biologically active growth factors *in vivo* as well as providing an encapsulating matrix for living chondrocytes for tissue engineering applications. Mixtures of pectin and chitosan were reported to form thermoreversible gels by lowering the temperature [26]. The gelation temperature was 30°C at 25 wt % of pectin and 48°C at 75 wt % of pectin. The possible mechanism of reversible gelation is that complexation of pectin and chitosan chains does not occur at higher temperature, while crosslinking junctions are developed by pectin-chitosan complexation under gelation temperature.

Recently, a novel synthetic approach was reported to provide the synthesis of block

copolypeptides with relatively low molecular weight and narrow molecular weight distribution [90-92]. In their reports, diblock copolypeptides, which have both hydrophobic and charged (hydrophilic) blocks, were designed to have a random coil secondary structure with poly(D/L-leusine), α-helix structure with poly(D/L-leusine) and β-sheet structure with poly(L-valine) as their hydrophobic segments. Diblock copolypeptides formed hydrogel via micellization similar to PEO-PPO block copolymers. However, these diblock copolypeptides showed a capability of forming hydrogels even at low concentration and rapidly rearranged to form micelles after physical deformation. They emphasized the secondary structure of the hydrophobic group. The α-helix structure was confirmed to be most effective for gelation of diblock copolypeptides.

Recent uses of recombinant DNA methods have opened a new approach to prepare artificial polypeptides that respond to temperature changes. The artificial protein was designed as a triblock copolypetides that consist of relatively short "leucine zipper" end blocks, which had α-helix structure and hydrophilic, charged middle blocks, which had random coil structure (Figure 1-3a) [93]. They reported the temperature and pH responsive coiled-coil aggregate of terminal domains enabled the formation of polymer networks, leading to hydrogels (Figure 1-3b). The leucine zipper motif is one specific example of the coiled coil motif characterized by amino-acid heptad repeating units designated as abcdefg with hydrophobic residues at a and d [93, 144]. In the case of the leucine zipper motif, hydrophobic residues are specifically occupied with leucine (especially at d position). When ionizable residues such as COOH-terminal cysteine are positioned usually at position

e and g, the coiled coil domains have pH sensitivity. The coiled coil, a well-defined protein-folding motif, undergoes conformational transition in response to temperature as well as pH changes.

Recombinant artificial elastin-like polypeptides (ELPs), which are composed of Val-Pro-Gly-Xaa-Gly amino acid repeat units (Xaa is a "guest residue" except proline), were reported to undergo a thermally reversible phase transition [94, 95]. Interestingly, ELPs are water-soluble under their transition temperature, but they precipitate due to their aggregation caused by hydrophobic interactions above the transition temperature. A block copolypeptide bearing ELPs segment and silk like segment, where the "guest residue" Xaa was valine, was reported to undergo sol-gel transition under physiological conditions [96]. Recently, applications of ELPs have broadened into protein purification [94, 95], nanosized metal-surface modification [44], and temperature responsive molecular valves in a porous membrane [97].

1.3.3. Recent advances of molecular designs

1.3.3.1. Designs for temperature sensitivity

Rapid sensitivity of temperature-responsive polymers should be considered for versatile applications such as biomimetic actuators. Macropore structures and phase-separated structures could lead to rapid swelling-deswelling sensitivity of hydrogels, by increasing the surface area [98, 99]. Also, the hydrogel microstructure structure could contribute to the increase of response time to stimuli [185]. These structures were given as examples of a change of physical form. Rapid responsive kinetics could be controlled by molecular design level. Hydrophilic moieties could increase the deswelling rate of PNIPAAm hydrogel

network, reducing the hydrophobic aggregation on the surface of the hydrogel, which suppresses the skin layer formation. Random copolymerization of NIPAAm with acrylic acid (AAc) or methacrylic acid (MAAc) gave hydrogels with faster deswelling kinetics than NIPAAm hydrogels [100]. Another strategy to obtain rapid deswelling was proposed by constructing the molecular architecture of PNIPAAm as a comb type instead of linear type structure (Figure 1- 4). Comb type PNIPAAm hydrogel exhibited a fast acceleration of the shrinking rate compared to that of a linear type PNIPAAm gel. Within its novel architecture, dangling PNIPAAm chains in a hydrogel can easily collapse above LCST due to the strong shrinking tendency of PNIPAAm chains that bear free ends [25].

More recently, the temporal change in the microenvironment of the dansyl-labeled comb type PNIPAAm hydrogels was compared with that of conventional linear type PNIPAAm hydrogels through fluorescence spectroscopy [24]. The change in microenvironment of the comb-type PNIPAAm gel due to a temperature jump revealed that it was altered hydrophobically more than 10 times faster than the linear type PNIPAAm gel. In this study, it was found that subsequent hydrophobic intermolecular aggregation occurred among dehydrated graft chains that had freely mobile characteristics. This created the hydrophobic cores, which accelerated the hydrophobic aggregation of the networks. The introduced freely mobile grafts also affected the mesh size of the gel networks, which was inferred thru the diffusivity of elutes [101]. The incorporation of PNIPAAm grafted chains into the molecular structure reduced the effective mesh size of the hydrogel network due to the additional friction between the probe molecule and gel network. In the case of surface-immobilized PNIPAAm, free mobile linear PNIPAAm showed more rapid

phase transition response than PNIPAAm randomly crosslinked onto the surface, due to their chain mobility [102, 103].

The modification of hydrophilic graft chains onto PNIPAAm hydrogel networks was reported to accelerate the temperature responsive hydrogel deswelling rates and it was compared with linear type poly(NIPAAm-co-AAc) [100]. Although the 1.3 wt % AAc-containing hydrogel showed more rapid deswelling than the PNIPAAm one, the deswelling rate decreased with increasing AAc-content above 1.3 wt %. Because the more AAc segments divided long linear NIPAAm segments into short ones, the hydrophobic aggregation forces decreased; therefore the deswelling rate rebounded over a certain threshold of AAc content, enough to suppress skin layer formation. It was also reported that the LCST of NIPAAm-co-AAc disappeared with too many AAc segments due to the weakened hydrophobic aggregation forces [6]. However, hydrophilic PEO grafts introduced onto the PNIPAAm back bone did not interfere with long PIPAAm sequences. Thus this structure could stand strong hydrophobic backbone aggregation between the long PIPAAm segments in spite of a large amount of the hydrophilic moiety in the network.

In a recent study, the sensitivity of hydrogels was promoted at the synthesis step of the hydrogel networks [104]. When P(NIPAAm-co-AAc) hydrogel network was synthesized at a weak alkaline condition (Tris/HCl solution, pH 8.8 and I = 0.5 M), it showed more rapid temperature sensitivity and improved oscillatory properties over small temperature cycles around the physiologic temperature of 37 °C. It was because the electrostatic repulsion between carboxylate anions led to the expanded conformations of polymer chains during the step of hydrogel network formation.

1.3.3.2. Designs for LCST control

The LCST of a temperature responsive polymer is influenced by hydrophobic or hydrophilic moieties in its molecular chains. In general, to increase the LCST of temperature responsive polymer (e.g. PNIPAAm), this polymer has been randomly copolymerized with a small ratio of hydrophilic monomers [105]. In contrast, a small ratio of hydrophobic constituent was reported to decrease the LCST of NIPAAm as well as to increase its temperature sensitivity [106]. More hydrophilic monomers such as acrylamide would make the LCST increase and even disappear, and more hydrophobic monomers such as *N*-butyl acrylamide would induce the LCST to decrease (Figure 1- 5) [6].

Therefore, the LCST could be controlled by incorporation of hydrophobic or hydrophilic moieties to adjust to a desired LCST. Adjustment of LCST near body temperature is essential especially for the drug delivery application. The influence of LCST of NIPAAm by random copolymerization with hydrophilic and hydrophobic monomers was investigated by varing the mole fractions between NIPAAm and incorporated monomers [1]. When ionizable groups such as AAc or *N,N'*-dimethylacrylamide (DMAAm) are copolymerized with NIPAAm, the LCST of NIPAAm shows a discontinuous alternation or even disappeared at the pK_a of the ionizble groups. This changeable LCST could be utilized in targeted drug delivery system (see section 3.4.1). However, when hydrophilic groups were grafted onto PNIPAAm chains, the LCST of PNIPAAm was independent of the content of hydrophilic groups such as AAc [106].

The hydrolytically sensitive lactate ester side group was introduced to control the LCST of temperature responsive NIPAAm-based random copolymer by hydrolysis of lactate

ester side groups [107]. Poly(NIPAAm-co-HEMA-lactate) showed increased hydrophilicity after the hydrolysis of the hydrophobic lactate groups changed it into (poly(NIPAAm-co-HEMA) which increased the LCST to above body temperature. On the basis of this concept, hydrolytically sensitive micelle formation was designed, where the critical micelle temperature (cmt) of this polymer system was controlled by the hydrolysis of lactate ester side groups [37]. Temperature sensitive group (NIPAAm-co- HEMA-lactate) (group A) was copolymerized as AB block copolymer type with a monomethoxy-PEG substituted macroinitiator (group B) (Mn=5000 g/mol). The structure of this polymer is shown in Figure 1- 6. After hydrolysis in aqueous solution, (NIPAAm-co-HEMA-lactate)-*b*-PEO block copolymer lost the lactate groups and showed an increased critical micelle temperature (cmt), which was interpreted as the increased LCST of poly(NIPAAm-co-HEMA). Therefore, this block copolymer system formed a micelle structure at physiological temperature but the micelle structure was destabilized after the hydrolysis of lactate groups.

Terminal-incorporation of hydrophilic and hydrophobic groups was reported to influence the LCST of temperature responsive polymers such as PNIPAAm, resulting in change of the thermodynamics of this unique position [36]. The effect of terminal modification on PIPAAm phase transition was more predominant in comparison with the random copolymers of NIPAAm and incorporated monomers at the same mole fraction. As described in section 3.3.1, free mobile PNIPAAm chains had a more rapid sensitivity to temperature than restricted ones, because the phase transition might be initiated at the ends of free mobile PNIPAAm [102, 103]. In their study [36], hydrophilic end groups

such as acrylic acid (AAc) and *N,N'*-dimethylacrylamide (DMAAm) more pronouncedly raised the LCST of PNIPAAm and slowed down the rate of the phase transition when it was compared with the effect of their random copolymers. However, when supramolecular association of hydrophobic end groups formed micellar structures, hydrophobic end modification of PNIPAAm did not change the LCST of PNIPAAm or the rate of the phase transition.

1.3.3.3. Designs of micelles based on amphiphilic balance

Amphiphilic block and graft copolymers are materials bearing a self-assembling property by which they can form polymeric micelles in aqueous solutions [36-38, 109-113]. Some of these micelles undergo transition of their physical form in response to temperature change. Recently, a model study of a amphiphilic block copolymer by small-angle neutron scattering investigated the thermoreversible morphological transitions of poly(2-ethoxyethyl vinyl ether-*b*-2-hydroxyethyl vinyl ether) (poly(EOVE-*b*-HOVE)) [39]. Figure 1- 7 shows the schematic representation of two different micelle structure transitions following a temperature change below or above the threshold concentration of block copolymers. Under the threshold concentration, molecular unimer mixtures in aqueous medium underwent an isolated micelle structure formation, while over this concentration the micelles underwent a crystal-like macro-lattice formation with body-centered cubic symmetry. In their report, the origin of the transition was explained to come from an association or a dissociation of hydrophobic structure. As a possible mechanism of thermo-gelling behavior, it has been generally proposed that the micelles contact neighboring micelles due to the increased interphase volume (the increased number of chains in

one micelle), and the hydrophilic chains in the corona interpenetrates between micelles, leading to crystal-like micelle packing. As the temperature increases in the gel phase, the miscibility between the hydrophobic and hydrophilic blocks increases, leading to dissociation of micelles [114].

Representative amphiphilic polymers that respond to thermal change are block copolymers of poly(ethylene oxide) (PEO) and poly(propylene oxide) (PPO) (Pluonics or poloxamers). Even though poloxamers are tremendously useful in many applications such as surfactants [115] and targeted drug delivery [116, 117], they have several drawbacks. One drawback is the high concentration of poloxamers required to form gel at body temperature [118]. To solve this problem, poloxamer was grafted onto the PAAc backbone [106, 119-121]. The graft copolymer of poloxamers and PAAc had several advantages; thermally reversible gelling behavior over a wide pH range, no phase separation, and bioadhesive property combined in a single molecule. First, Pluronic-graft-PAAc (onto PAAc backbone) was synthesized with 3 steps; 1) Oxidation of Pluronic with 4-nitrophenyl formate sites in the presence of triethylamine, 2) amino-terminated Pluronic by reaction with diaminoethylene, 3) conjugation of Pluronic onto PAAc via an amide bond using dicyclohexylcarbodiimide as a coupling agent [106].

More recently, a one-step procedure for PAAc-graft-poloxamer (onto poloxamer backbone) was conducted through radical polymerization of acrylic acid in the presence of poloxamer, which resulted in chain transfer reaction onto the methylene groups of poloxamer [119-121]. The graft copolymer containing PAAc and poloxamer could be obtained as an essentially monomer-free product by this chain transfer reaction

method. The sol-gel transition of these graft copolymers was reported to occur at the micelle critical temperature of poloxamer. This graft copolymer also showed gellation at a much lower concentration than poloxamer, because the PAAc-graft-poloxamer is more likely to form physical cross-links at dilute concentration due to its higher molecular weight.

In the case of injection of poloxamer into the body, the hydrogel structure of poloxamer was erodable from its surface into soluble unimers within 1 day [122, 123]. More durable and biocompatible block copolymers that undergo micelle aggregation and packing were obtained when the PPO block was replaced with poly(L-lactic acid) [33] and more recently with poly(DL-lactic acid-co-glycolic acid) (PLGA), which contains a biodegradable ester group in its backbone [34]. PEO-*b*-PLGA-*b*-PEO block copolymer also formed a micellar structure with a PLGA core and a PEG corona. A structure-property relationship, where transition temperatures were sensitive to the balance of hydrophobicity and hydrophilicity in PEG-PLGA-PEG triblock copolymers, was determined [34]. The control of hydrophobicity and hydrophilicity in this polymer was the important parameter to adjust the sol-gel transition. Increasing the length or ratio of hydrophobic group (PLGA) and increasing the DL-lactic acid group ratio to glycolic acid in the middle block led to decreases of the critical gelation concentration and critical gelation temperature [34]. After the degradation of middle block, short PEO chains (Mr < 5000) would be eliminated from the body without long-term accumulation.

Graft type copolymers of PEG and PLGA were reported to show more competitive thermogelling concentration and temperature ranges than linear type triblock copolymers [29]. The authors reported two types of graft copolymer containing PEG and PLGA;

PEG-*g*-PLGA (PEG backbone) and PLGA-*g*-PEG (PLGA backbone) (Figure 1- 8). Even though the two different type block copolymers have the same components, they showed different profiles of their degradability. PEG-*g*-PLGA, which contained hydrophilic backbones, degraded earlier, within a week. PLGA-*g*-PEG, however, formed more durable gels enduring for three months [29, 124]. Recently, a similar type of biodegradable triblock copolymer, poly(fumaric acid-co-propylene glycol)/PEG, was reported to undergo similar micellization and thermogelling behavior [125].

The application of poloxamers as nano-scale reservoirs of drugs encountered problems, in that the micelles disassociate at low concentration, which causes a failure for long-term circulation of micelles in blood. Recently, one approach to solve this problem was designed by incorporating an interpenetrating polymer network (IPN) of temperature responsive polymer and poloxamer (P-105) into a micelle core [126]. *N,N'*-diethylacrylamide (DEAAm) was polymerized in the presence of 10 % P-105 with a small ratio of *N,N'*-bis(acryoyl) cystamine (BAC) as a cross-linking agent. Above LCST of poly(DEAAm) (around 28 °C), IPN core containing DEAAm collapsed and became more hydrophobic. In this mechanism, the interpenetrating network of poly(DEAAm) within a micelle core, stabilized the micelles at concentrations below their critical micelle concentrations (cmc). The authors proposed that this novel micelle structure could be utilized for drug delivery in which the poly(DEAAm) IPN core stabilizes the micelle above LCST and releases the loaded drugs below LCST.

1.3.3.4. Designs of micelles based on the LCST

As described in section 3.2.1., temperature responsive polymers like PNIPAAm undergo LCST in aqueous medium, above which the behavior of these polymers changes from hydrophilic to hydrophobic. Interestingly, this swichable property has been utilized as a basic concept to manufacture an attractive polymer system that might loose or gain its amphiphilic property according to temperature changes around its LCST, resulting in temperature responsive micelle deformation or formation. Two types of micellar structures containing temperature responsive polymers (especially PNIPAAm) can be considered; thermosensitive outer corona and thermosensitive inner core. The schematic illustrations about these two types of block copolymers consisting of PNIPAAm-based blocks are shown in Figure 1- 9. In the former case, NIPAAm block has been usually copolymerized with hydrophobic blocks [127, 128]. In the latter case, NIPAAm and hydrophilic segments were combined as a block copolymer [129].

When the outer shells of micelles are designed with temperature responsive polymer (e.g. NIPAAm), micelles form below the LCST and intermicellar aggregation occurs above the LCST. The effects of two different hydrophobic segments were investigated as inner core model materials [113]. In this study, poly(butyl methacrylate) (PBMA) and polystyrene (PSt) were selected as flexible and rigid inner core segments respectively. PBMA exhibits a relatively flexible conformation compared with the outer PNIPAAm segment and low glass transition temperature (T_g under 20°C), while PSt shows a more rigid conformation and high T_g (100°C). From the dynamic light scattering and transmittance measurements, above LCST of PNIPAAm, PNIPAAm-*b*-PBMA underwent

the hydrophobic change of the PNIPAAm outer shell as well as inner core deformation, whereas PNIPAAm-*b*-PSt underwent only the hydrophobic change of the outer shell without inner core deformation, causing aggregation of micelles. These results were confirmed by the amount of Adriamycine (ADR) loaded into the micelle inner core that was released. Another aspect of the design of a hydrophobic inner core involves introducing a biodegradable segment to prevent toxicity due to the degraded short PNIPAAm chains which easily move out of the body without long term accumulation [112]. In their report, poly(DL-lactide) (PLA) was used as a hydrophobic and biodegradable segment. PNIPAAm-*b*-PLA was synthesized by ring-opening polymerization of DL-lactide using hydroxy-terminated PIPAAm as the ring-opening agent (Figure 1- 10). The authors reported that the micelles showed reversible thermal transition; below LCST, micelles were stable and formed with dimensions of approximately 40 nm diameter, and above LCST, the micelles aggregated by the association of the hydrophobic surfaces. However, fusion of micelles was not observed above LCST. To increase the transition temperature of PNIPAAm-*b*-PLA to above body temperature, PIPAAm block was modified with a hydrophilic group, *N,N'*-dimethylacrylamide (DMAAm) [38].

The other simple design of a hydrophobic inner core is the terminal incorporation of the hydrophobic group into one side of a temperature responsive polymer chain [36]. In aqueous media, micellar association was observed to form hydrophobic microdomains due to the hydrophobic effect of the end group. Alkyl terminated PNIPAAm were reported to form different core-shell micellar structure according to the length of the alkyl groups [132].

Combining a hydrophilic segment with a temperature responsive polymer segment

is another strategy to develop temperature responsive micellar structures. In this strategy, below the LCST, these polymer structures exhibit an amphiphilic property and lead to stable micellar formation bearing a temperature responsive core and hydrophilic outer shell. Whereas, above the LCST, the hydrophobic effect in the inner microdomain may disappear due to the hydrophilical change of the inner core, leading to micelle deformation.

From the poloxamer structure, a NIPAAm segment replaced the hydrophobic block PPO position [109, 130]. In these reports, block copolymers of PNIPAAm and PEG were synthesized by a ceric ion redox system yielding radicals at the terminal carbons of PEG. While the mechanism of poloxamer micelle aggregation is determined by the balence of the hydrophilic PEO and hydrophobic PPO segment, PEO-*b*-NIPAAm-*b*-PEO micellization is totally dependent on the temperature responsive behavior of the NIPAAm segment.

The effect of length and ratio of PEO with the respect to that of NIPAAm on the micellar structure and thermal transiton has been determined [111]. In this study, the LCST of NIPAAm and micellar formation of the block copolymers was investigated by static and dynamic light scattering and fluorescence spectroscopy. The LCST of NIPAAm was shifted to higher temperatures by a long PEO block (MW 1900 /mol), resulting in the increase of micellar formation temperature, whereas this shift of LCST was not observed with the short PEO block (MW 550 g/mol) regardless of NIPAAm length. The ratio NIPAAM/PEO negatively affected the LCST for the long PEO block. Above the LCST, the shape of the micellar structure was affected by the length of the PNIPAAm block, the molar ratio of the repeating units of PNIPA and PEO, and the polymer concentration.

In another study, *N*-(2- hydroxypropyl)methacrylamide (HPMA)

was selected as the hydrophilic monomer [129]. (PHPMA-*b*-PNIPAAm) diblock copolymer was also confirmed to show monodisperse particles above the LCST of PNIPAAm. The size and molecular weight of supramolecular nano-particles decreased with decreasing content of PHPMA in the block copolymer.

Instead of linear block copolymer type, graft copolymer was also investigated as a temperature responsive micelle [131] Poly(L-lysine) (PLL), which is a cationic polypeptide, was selected as the hydrophilic backbone. PLL-*g*-PNIPAAm was suggested to show micelle aggregation above the phase transition temperature of PNIPAAm blocks.

1.3.3.5. Designs of hydrogels

Since the first hydrogel was synthesized with copolymers of 2-hydroxyethyl methacrylate with ethylene dimethacrylate, hydrogels have been successfully utilized in commercial applications, such as contact lens and implant material due to the proven biocompatibility in their clinical uses [133, 134]. The tremendous interests in hydrogels were increased by introducing stimuli responsive properties. Of these properties, temperature responsive hydrogels have attracted the most interests with the incorporation of the interesting thermal sensitivity of PNIPAAm into hydrogels.

Commonly, temperature responsive hydrogels can be prepared by two different methods; one is polymerization starting from the temperature responsive monomers and cross-linking agents, and the other is introducing cross-links to a polymer solution by chemical reaction of side functional groups or by irradiation by γ-ray or electron beam. PNIPAAm, a representative temperature responsive polymer, is generally shaped to its

hydrogel form by the former method [135]. The cross-linking agent, methylenebis(acrylamide), raised the LCST of PNIPAAm to 34°C, resulting from its hydrophilic property. Recently, the structural inhomogeneities of PNIPAAm hydrogels were systemically investigated as a function of the gel preparation temperature and the cross-link density [136]. The inhomogeneities increased with increasing gel preparation temperature and cross-link density. These permanent inhomogeneities give limitations to PNIPAAm hydrogels. One approach to improve on this drawback was to introduce nano-size clay particles as a cross-linker in PNIPAAm hydrogels, and these nanocomposite (clay-PNIPAAm) hydrogels were compared with conventional PNIPAAm hydrogels [43]. Nanocomposite (clay-PNIPAAm) hydrogels were prepared by *in situ* free-radical polymerization of N-isopropylacrylamide (NIPAAm) in the presence of a water-swollen inorganic clay. In the case of (clay-PNIPAAm) hydrogels, deswelling rates and mechanical properties exhibited increases with increasing cross-linker (clay) contents.

On the other hand, there are still limitations to hydrogels composed of only PNIPAAm, such as biocompatibility, swelling/deswelling rate, and mechanical properties. The need to improve these required properties led to other functionalities being incorporated by copolymerization and interpenetrating polymer networks (IPNs). Interpenetrating polymer networks (INPs) are polymeric mixtures mainly formed by the permanent entanglement of two or more cross-linked networks [137]. Recently, the incorporation methods of the pH responsive component PMAAc into cross-linked PNIPAAm hydrogel networks was introduced by copolymerizing two monomers in the presence of a cross-linkable monomer

and forming interpenetrating polymer networks [22, 138]. Comb type graft hydrogel can give a combination of the required properties and also accelerate deswelling rates. For example, PNIPAAm grafted comb type alginate was reported to show more rapid swelling/deswelling kinetics than their semi-IPNs, as well as having both temperature and pH sensitivity [139].

Biodegradability can be given to the hydrogels, while keeping their temperature responsive properties. PNIPAAm chains were grafted to biodegradable biopolymers such as zein protein [140] and alginate [139]. IPNs of PNIPAAm with gelatin without covalent bonds between two components were investigated [141]. In this study, IPNs did not in anyway alter the chemistry of the PNIPAAm chain. To improve thermal, mechanical, and solvent-resistant properties of hydrogels, inorganic-organic hybrid hydrogels have been introduced as IPNs [142, 143]. The internal pores of silica particles were filled with PNIPAAm gel to give a thermo-responsive drug reservoir.

The coiled coil protein (See section 3.2.3.), a temperature responsive recombinant protein, was reported to be utilized as cross-linking domains in synthetic polymers [144]. This hybrid hydrogel system was assembled with poly(*N*-(2-hydroxypropyl)-methacrylamide-co-*N*',*N*'-dicarboxymethylaminopropyl)metharylamide) (poly(HPMAAm-co-DAMAAm)) and two Histine-tagged coiled coil proteins. This resulted in their metal complexation as a means of anchoring the Histine-tagged proteins. The protein-synthetic polymer hybrid hydrogels exhibited their transition temperature at 39°C. The authors proposed that hybridization of two or more of these coiled coils with synthetic polymers

could give stepwise phase transitions with each step triggered at a different temperature.

Microgels or nanogels have been investigated for biomedical applications such as drug delivery vehicles [145], and chromatographic or separation technology [148]. Micro, or nano-size hydrogel can be conventionally manufactured by emulsion *in-situ* free-radical polymerization with methylenebis(acrylamide) [23, 146]. Surfactant concentration controls the radius of these microparticles [147]. As the surfactant concentration increases, the particle radius decreases [149].

In general, nanohydrogels composed of PNIPAAm show a negative mechanism to control the drug release, that means lowering the temperature under the LCST activates the drug delivery into the medium, while the drug is held inside the gel above the LCST, due to the hardened skin layer [1, 2]. One approach to obtain positive mechanism for drug delivery was introduced by manufacturing hybrid nanogels based on interpenetrating networks of thermosensitive PNIPAAm gels and tailored nanoporous silica. A positive thermo-responsive drug release profile were observed due to the porous channels of the silica, which eliminated the skin layer effect, and allowed the drug to diffuse through the opened pores above the LCST of PNIPAAm.

The effect of incorporation of ionizable groups in micoparticles were investigated in PNIPAAm copolymer hydrogels, prepared by *N*-isopropylacrylamide (NIPAAm), *N,N'*-methylenebisacrylamide (BIS), and acrylic acid (AAc) or 1-vinylimidazole (VI) [147]. When the carboxyl or imidazolyl groups were ionized into the corresponding salt form, the dimensions of hydrogel particles containing 30 mol % of AAc or VI increased tremendously from 125 to 600 nm at 25 °C. However, sizes of uncharged gel particles

varied from 125 nm at 25 °C to 50 nm at temperatures above the LCST, 35 °C. Interestingly, almost all of the acrylic acid (AAc) groups were found in the particle's interior, which might come from the higher polymerization rate of AAc monomers than that of NIPAAm monomers. Inhomogeneities between the inside and outside of these microhydrogels were reported in free-radical polymerization of only NIPAAm with BIS [23]. Also, these structural inhomogeneities were elucidated to occur, as a result of the cross-linking monomer having a higher polymerization rate than the PNIPAM monomer, which leads to radially decreasing cross-link density in the particles.

Core-shell type microgels based on PNIPAAm were reported to have multi-responsive behaviors and multi-phase transitions [110]. Core-shell microspheres were prepared by two stage (seed and feed) polymerization [148]. In the first stage, seed microparticles were prepared via conventional free radical polymerization, and a second feed of monomers was additionally polymerized onto the seed hydrogels, resulting in core-shell type microgels. In the other study, core-shell type microgels were similarly synthesized by two stages, where the second stage was described as a shot growth process [110]. In a shot growth stage, the desired monomers (e.g. PNIPAAm) were added with initiator and cross-linker after 70 to 90 % conversion of the first polymerization step.

Recently, new routes to the preparation of hydrogel particles on a nanometer scale have been investigated by using supramolecular aggregation of two different polymer chains such as the self-assembling of two different hydrophobically modified polymers or polyelectrolyte complexes between ionically modified polymers. The former was reported as a method to produce thermoresponsive hydrogel nanoparticles [137]. In this study, a

cholesterol-bearing pullulan (CHP) was physically mixed with a copolymer of *N*-isopropylacrylamide (NIPAAm) and *N*-[4-(1-pyrenyl)butyl]-*N*-n-octadecylacrylamide] (PNIPAAm-C_{18}Py), which made physically cross-linked networks due to the aggregation of hydrophobic moieties to nanoparticle size. The structures of these hydrophobically modified copolymers are shown in Figure 1-11. Fluorescence and dynamic light scattering measurements indicated that the thermal behavior of this nanoparticle depended on the lower critical solution temperature (LCST) of PNIPAM-C_{18}Py. The radius of the nanoparticles showed a reversible change from 47 to 160 nm and visa versa, where nanoparticles extended above the LCST (32°C) and recovered their original dimension upon cooling to under the LCST.

The formation of polyelectrolyte complexes is one of the new and promising routes for the preparation of temperature responsive microgels. Ionically modified temperature responsive polymers were reported as temperature responsive polyelectrolyte complex particles [184]. PNIPAAm was ionically modified with anionic and cationic groups. Two types of copolymers based on NIPAAm monomer were respectively prepared containing sulfonate group as a strong anionic monomer and the tri-amine group as a cationic monomer. Figure 1-12 shows the structures of these ionically modified copolymers. These temperature responsive complexes showed stoichiometric complex particles on a 100 nm scale. These complex particles were also stable at nonstoichiometric mixing ratios. The swelling-deswelling process of the polyelectrolyte complex was completely reversible, where particles were highly swollen at 25°C and collapsed in a temperature range up to

50°C.

1.3.3.6. Designs of surfaces

A temperature responsive surface or interface is another route to biomedical applications such as temperature-modulated membranes [150, 151], chromatography [15, 152, 153], and cell culture dish [42]. PNIPAAm has been extensively investigated to develop temperature responsive intelligent surfaces and interfaces because of its specific advantages previously described in section 3.2.1.

Two categories can be considered for interfaces designed with immobilized temperature responsive polymers (broadly all stimuli responsive polymer); to modulate pores of a porous matrix as temperature responsive gates, and to control the wettability of nonporous matrix surfaces. For example, the modification of a membrane surface with temperature responsive polymer chains can modulate the diffusion profiles. It is well known that a PNIPAAm-grafted porous membrane shows positive control of solute diffusion, which means that the fast diffusion occurs through the opened gates at higher temperature [154], while a PNIPAAm-grafted nylon capsule exhibits negative control of solute diffusion by blocking the solutes from passing through the surface of the membrane above the LCST of the temperature responsive polymer [155].

The photoreactive phenylazido group was introduced into PNIPAAm chains to fabricate a temperature responsive porous membrane immobilized with PNIPAAm [151]. In this study, two types of azidophenyl-derivatized PNIPAAm were synthesized; 1) azophenyl group terminated PNIPAAm on its one side, and 2) azidophenyl-derivatized PNIPAAm-co-PAAc copolymer by substituting azidophenyl group on every carboxylic

group in PAAc. When a microporous membrane was filled with thick hydrogels, it showed different temperature dependences of permeation from another micoporous membrane, whose pore surfaces were covered with tethered linear chains or thin hydrogels. The latter membrane showed that the grafted chains or thin hydrogels swelled below the LCST to close the pores and deswelled above the LCST to open the pores. In contrast, the thick hydrogels filled in the former membrane swelled below the LCST to enhance the permeability and deswelled above the LCST to decrease the permeability.

Recently, the surface modification of microporous polypropylene membrane with PNIPAAm was reported by a plasma-graft-filling polymerization technique [150]. A novel mechanism for switching the permeation of hydrophobic and hydrophilic solutes by changing temperature, which could give the stepwise separation of solutes from the mixed solution, was demonstrated. Above the LCST, only hydrophilic solutes permeated the hydrophobic pore, because the hydrophobic solutes adsorbed onto the hydrophobic pore surfaces. In contrast, below the LCST, the pore surface became hydrophilic and hydrophobic solutes desorbed from the pore surface and condensed in the permeate side. Figure 1- 13 shows a schematic drawing of temperature responsive membrane and solute concentration in the permeate. Using a similar mechanism, a switchable molecular filter was fabricated by encapsulating PNIPAAm into a porous silica membrane by a sol-gel process [156, 157], whose pores became hydrophilic under the LCST to prevent water and PEG permeation and became hydrophobic above LCST to permit the flow of aqueous solutions of PEG of low molecular weight (≤5000 Da), while blocking PEGs of higher

molecular weight. The reversible on/off permeation and molecular cut-off filtration behavior of these membranes has also been described above and below the transition temperature of PNIPAAm [43]. Elastin like polypeptide (ELP) was reported to replace PNIPAAm as a protein-based molecular switch [97]. Demonstrating the same mechanism as the PNIPAAm-silica hybrid membrane, the ELP-silica hybrid membranes also were impermeable to all of the PEG solutions below the LCST, while above the LCST of ELP, they were permeable only to PEG with molecular weights less than 5000 Da.

In the case of surface modification by grafting polymer chains onto a membrane, some drawbacks have been discussed. This process changes the pore size and pore size distributions resulting in a permeability decrease and also causes different graft densities between the external surfaces and internal pores [158]. Recently, a temperature responsive microfiltration membrane was fabricated instead of modifying a porous membrane surface with a temperature responsive polymer [159]. These membranes were proposed to overcome the above-described disadvantages. In this study, the membranes were prepared from PNIPAAm-*g*-poly(vinylidene fluoride) (PVDF) copolymers by the phase inversion method, where the copolymer solution is cast onto a glass plate and immersed in a nonsolvent, such as water, after a brief evaporation of solvent in air. The PNIPAAm-*g*-PVDF was synthesized from ozone preactivated PVDF. The casting temperature was an important factor for these membranes. The membrane cast under the LCST of NIPAAm showed extensive aggregation of NIPAAm component onto the surface due to the hydrophilic interaction between NIPAAm chains and water. Therefore, the flux of water exhibited a strong and reversible dependence on permeate temperature due to

the surface property of PNIPAAm.

Switchable wettability of surface is another strategy to manufacture intelligent surfaces. Four models of graft chain conformations on the surface were suggested and their temperature responsive wettability changes were studied on the PNIPAAm-grafted surface [160, 161]. The reported four models were: 1) free end and linear grafts onto surface, 2) muli-point looped grafts onto surface, 3) free end grafts onto looped chain modified surface, and 4) thin hydrogel layer modified surface. In the case of 2), the transition temperature of surface wettability decreased to less than the LCST of PNIPAAm (32°C). When the density of PNIPAAm chains increased as in case 3), a large change of wettability was observed at the transition temperature. However, the thin hydrogel layer modified surface (case 4)) was reported to undergo less wettability change, which was explained by the restricted chain mobility caused by the cross-links.

More functional properties may be incorporated onto the PNIPAAm-grafted surface. For example, hydrophobic and ionizable hydrophilic groups were introduced in PNIPAAm chains as a random copolymer form and this copolymer was grafted onto silica beads [15]. In this study, poly(*N*-isopropylacrylamide-co-acrylic acid-co-*N*-tert-butylacrylamide) (poly(NIPAAm-co-AAc-co-tBAAm)) hydrogel was grafted onto silica beads and evaluated as a column matrix for cation-exchange thermoresponsive chromatography. In the other study, 2-carboxyisopropylacrylamide was copolymerized with PNIPAAm and this copolymer was grafted onto a polystyrene petrri dish and exhibited an intensified cell detachment over when only PNIPAAm chains were grafted on the dish under the LCST of

PNIPAAm [52].

In general, PNIPAAm has been extensively utilized to modify the surfaces that have temperature responsive wettability changes. Recently, temperature responsive ELP was also investigated as a surface modifier of solid nanoparticles [44]. ELP was adsorbed onto gold nanoparticles functionalized with a self-assembled monolayer (SAM) of mercaptoundecanoic acid. The authors reported that reversible formation of large aggregates was observed above the LCST of ELP due to interparticle hydrophobic interaction. They suggested a simple and convenient colorimetric method, colloidal surface plasmon resonance, to study the effects of environmental changes (e.g. temperature) on the properties of responsive polymers at the solid-water interface.

The dimensions of surface modification have been controlled down to micro or nano-scales. Temperature responsive nanoparticle surfaces were obtained by introducing mono-dispersed polystyrene seed particles as a shape template in the two-step swelling and polymerization method, similar to the core-shell micro-hydrogel fabrication methods described in section 3.3.5. [40]. Micropatterning with a temperature responsive polymer has been investigated, where PNIPAAm was pattern-immobilized by coupling reactions with surface-bound aminosilanes or by copolymerization of NIPAAm onto surface-bound methacrylsilane [162]. More recently, the ELP fusion protein (ELP-thioredoxin), which was recombinantly synthesized with a temperature responsive polypeptide tail (ELP), was immobilized onto a patterned hydrophobic surface [163, 164]. The ELP moiety of this fusion protein reversibly adsorbed onto a hydrophobic self-assembled monolayer (SAM) above its inverse phase transition temperature (Tc) (e.g. LCST). In these

studies, this method, where an ELP fusion protein was reversibly addressed to chemically distinct regions of a patterned surface by temperature change, was termed as thermodynamically reversible addressing of proteins (TRAP).

1.3.3.7. Designs of intelligent bioconjugates

Liposomes are composed of amphiphilic lipids such as dipalmitoylphosphtidylcholine, which forms a circular bilayer membrane capable of containing therapeutics in its inner space. Liposomes have been extensively investigated as gene delivery vehicles via pH-dependent phase transitions [172]. However it has a limitation: low intracellular transfection efficiency. To solve this drawback, conjugation of a temperature-responsive polymer to them has been suggested [48, 165]. Coating PNIPAAm onto the surface of liposome utilized octadecyl acrylate containing a long hydrophobic pendant group, which acts as an anchoring group [48]. Disintegration of the liposomes occurs above the LCST to trigger the release of the therapeutics.

Streptavidin (SA) has been known to bear a high binding affinity for biotin. This property of SA has driven extensive investigations on affinity separations, laboratory assays, and clinical diagnostics [45]. A series of reports have been published to investigate the site-specific SA conjugates that can control biotin-SA binding [45, 166-168]. When PNIPAAm was conjugated to a specific site which is located on the loop above the biotin-binding pocket of SA, the temperature responsive behavior of PNIPAAm chains controlled the reversible binding activity with biotin and triggered release of bound biotin as a “molecular gate” [45, 166]. Another temperature responsive copolymer, *N*,*N*-dimethylacrylamide (DMAAm) was selected as site specific SA conjugates [169]. In this study, 4-

phenylazophenyl acrylate was copolymerized with DMAAm to enhance the photo-responsive control of enzyme activity of biotin. The authors suggested that the conjugation site, molecular weight, and type of stimuli-responsive polymer should be considered to optimize the switching activity. The effect of the location and length of the polymer chains on the activity of binding site was investigated [168]. Through the self-assembly via hybridization of two single chain DNA sequences which were conjugated on SA and the end of a PNIPAAm chain, they controlled the location and length of the PNIPAAm chains.

A cell adhesive motif was introduced into the structure of PNIPAAm-based hydrogel beads [170]. These hydrogels were fabricated by copolymerization of NIPAAm, *N*-aminoethyl methacrylate (AEMA), and cross-linkable monomer (BIS) in the presence of calcium alginate which acts a temporal spherical mold. The conjugation of cell-adhesive motif, GRGDY (Gly-Arg-Gly-Asp-Tyr), was selectively incorporated into the surface region of these precollapsed hydrogels above the LCST. The temperature responsive conjugates were proposed as cell culture substrate for chondorcytes (See section 4.4.2.). The cell, which was attached on the bead above the LCST, was readily detached from the swollen beads below the LCST (37°C).

A substrate peptide of protein kinase A (PKA) was reported as a conjugate with PNIPAAm [171]. PKA forms one of the most important intracellular signals in cellular signal transduction. The conjugates containing the *N*-isopropylacrylamide unit and the substrate peptide unit showed an increase of its LCST from 36.7 to 40 °C in response to phosphorylation by activated PKA. This conjugate was designed to form a micellar

structure. Ethylene oxide blocks were used as the outer shell and a copolymer of NIPAAm with *N*-methyacryloyl bearing the substrate peptide sequence was designed as inner core. The alternation of the LCST of the inner core moiety by a PKA signal suggests that encapsulation of drugs into this micelle might result in an intelligent drug delivery system that communicates with an intracellular signal.

1.3.4. Recent advances in bio-related applications

1.3.4.1. Drug targeting based on local hyperthermia

Recently, temperature responsive polymers have been applied as one strategy for a gene carrier system. The recent progress and mechanisms of temperature responsive gene carriers were reviewed in comparison with viral vectors and synthetic gene carriers (e.g. cationic lipids and general polymeric gene carrier) [10, 13, 172]. In spite of its high transfection efficiency, the disadvantage of viral vectors, such as pathogenic and immunogenic problems, led to non-viral gene vectors. Even though a cationic lipid carrier could be used as a non-viral gene carrier, it was reported to have low transfection efficiency [10]. Polymeric gene carriers have had more interest due to several advantages over cationic lipid carriers. Introducing a stimuli-responsive property into a polymeric gene carrier can provide progressive advantages, such as non-pathogenic and non-immunogenic problems, high transfection efficeincy, and complex formation/dissociation with therapeutics controlled by stimuli.

The dissociation of therapeutics from polymeric carriers within cytoplasm has been proposed by introducing a temperature responsive mechanism produced by local hyperthermia. Two types of gene carriers have been developed; one is a soluble

temperature responsive polymeric carrier, which can bind anionic DNA or hydrophobic anti-cancer drugs at body temperature and dissociate them at hyperthermic temperatures [50, 173]. The other is a temperature responsive micelle or nano-hydrogel, which can contain anionic DNA or hydrophobic anti-cancer drugs in the core reservoir or the hydrogel at body temperature and release them at hyperthermic temperatures [38].

The soluble temperature responsive polymeric carrier was investigated with COS1 cells in vitro [50]. In this study, the LCST behavior of PNIPAAm was utilized as the main concept to control the dissociation of therapeutics. Along the NIPAAm segment, two more components were incorporated as a random copolymer structure; N,N'-dimethyl aminoethyl methacrylate (DMAEMA) as cationic binding units for anionic DNA, and butylmethacrylate (BMA) as a hydrophobic unit. This copolymer contained 8 mol% DMAEMA and 11 mol % BMA, whose composition made the LCST 21°C (Figure 1- 14). The copolymer was insoluble above 21°C and soluble below 21°C, so that the therapeutic/copolymer complex was stable above the same LCST (21°C) and was dissociated or weakly bound below the LCST. The copolymer was combined with plasmid DNA encoding β-galactosidase and then was incubated with COS1 cells by changing the temperature, from 37°C for 20 h to 20°C for 3 h and then returning the temperature to 37°C. The β-galactosidase activity confirmed that the dissociation of plasmid DNA in cytoplasm could be controlled by lowering the temperature to under the LCST (21°C). Hyperthermic treatments at below body temperature are limited to a site near the body surface, because of difficulty in controlling the temperature of a specific site below body temperature in vivo

(however, use of catheters could expand the range of use in the body). The reason for using the low LCST system in this study was to confirm the effect of a temperature responsive polymeric gene carrier on transfection efficiency, avoiding the possibility that the increased temperature might enhance the gene expression due to cell activation [10].

A more practical temperature responsive polymeric carrier would be designed to have its LCST above body temperature. Recently, several temperature responsive polymeric gene carrier systems were devised to have their LCST between body temperature and 42°C, at which hyperthermic treatments of cancer patients are generally performed [173]. Targeting cancer chemotherapeutics to tumors can give benefits, such as avoiding cytotoxic chemotherapeutics which also damage healthy tissues. Two different types of thermally responsive polymers were conjugated with rhodamine; a genetically engineered elastin-like polypeptide (ELP) and a copolymer of N-isopropylacrylamide (NIPAAm) and acrylamide (AAm). From in vivo fluorescence video microscopy, it was confirmed that local hyperthermia at 42°C increased the accumulation of the conjugates in the solid tumor site. At a temperature higher than the LCST of these temperature responsive polymers, precipitation of the polymer-drug conjugates took place. In summary, the first study [50] concentrated on the dissociation of the conjugates at intercellular cytoplasm, whereas the latter one [173] focused on the accumulation of the conjugates at specific sites like tumors. However, both factors should be considered to obtain a more effective gene carrier system.

The micelle structure of temperature responsive polymers has been extensively investigated as targeted drug delivery systems. Hydrophobic drugs, proteins or negatively

charged DNA can be loaded into the core of the micelles whose dimensions are usually less than 100 nm. Temperature responsive micelles have an effective advantage for targeted drug delivery over general micelle structures; they have a double targeting mechanism in both an active and passive manner [112, 173]. They also solve the problem of non-selective scavenging by the reticuloendothelial system (RES) [174]. Several methods have been reported to synthesize polymers that undergo temperature responsive micelle formation, such as terminal hydrophobization of NIPAAm, block or graft compolymeriztion of NIPAAm with hydrophobic monomers and/or hydrophilic monomers [37, 109, 111-113].

1.3.4.2. Intelligent on-off systems for separation, permeation, actuation and detachment control

Targeted proteins can be separated from aqueous solution containing undesirable impurities, by affinity binding of the targeted proteins onto a temperature responsive polymer with covalently coupled ligands specific for the target protein. Once the targeted proteins are bound onto the ligands, the proteins can be recovered from the polymer system by reversible hydrophobic/hydrophilic changes of this polymer system [6, 7]. Various ligands such as lectin [176], maltose [177], or antibodies [16] have been conjugated with stimuli-responsive polymers to separate targeted biomolecules. One strategy of protein purification is the precipitation of the temperature responsive polymer after binding the targeted proteins above the LCST [178]. By incorporating vinylimidazole (VI) moiety as metal biding site into PNIPAAm-based temperature responsive copolymer, metal-loaded copolymers were prepared as metal affinity macroligands [179]. The temperature control of this macroligands provided the effective purification of histidine-tagged single-chain

Fv-antibody fragments from the fermentation broth by metal chelate affinity precipitation. The first complexes bearing ligand-conjugated polymers and the bound proteins were precipitated at the temperature between the two different LCSTs. And the second complexes were precipitated above the higher LCST of the two. For the other approach, the ligand-conjugated polymer chains were grafted or modified on column beads and specific proteins were separated from flowing solutions. The separated proteins, which were bound by the immobilized ligands, could be reversibly recovered from the surface of columns by adjusting temperature to under the LCST [15, 16, 152]. Purification of antibodies was reported by using temperature responsive PNIPAAm and dextran derivative conjugate as a model [16]. The main idea was the combination of the temperature sensitivity of PNIPAAm and the affinity of antibodies recognizing the polysaccharide antigen, carboxymethyl dextran benzylamide sulfonate/sulfate. This conjugate was obtained by grafting amino-terminated PNIPAAm onto this dextran derivative. They confirmed that the purified antibodies and the polymer conjugates could be readily separated and recycled by a themally-dependent recovery process, which gave a rapid and sensitive procedure to separate antibodies.

Temperature responsive polymers were also reported to separate proteins by inducing the refolding process of proteins [180, 181]. Without specific affinity binding, a continuous process with facilitated polymer recycling for protein refolding was proposed by using temperature responsive polymer assistance. Protein refolding was reported by using PEO-PPO copolymer [181] and PNIPAAm [180].

A target protein, which is genetically fused to an ELP, could be easily separated

from other contaminating proteins in the cell lysate via inverse transition cycling (ITC) purification, in which the ELP fusion protein precipitates after triggering the inverse temperature phase transition of the ELP [94, 95]. The procedure is schematically illustrated in Figure 1- 15.

Stimuli responsive polymers could be utilized to manufacture microfluidic systems which can self-control microscale flow as well as separate, purify, analyze, and deliver biomolecules. A switchable protein trap was obtained with a surface coated with an end-tethered monolayer of PNIPAAm [184]. The monolayer temperature was controlled by a micro-hot plate device containing gold or platinum heater lines deposited on the thin layer. This device could adsorb and desorb the bound protein in less than 1 second due to the switchable hydrophilic/hydrophobic property of the thin layer by changing the temperature. This surprisingly rapid response time was achieved by the tenuous scale of the polymer layer, which was only 4-nanometer thick. An array of these devices could be utilized to purify the targeted protein on a large scale while preserving the rapid response time. Also this device could be applied for artificial organs, for example, artificial pancreas for controlling the release of insulin. However, external power is required for operation of this device, which can restrict their use in practical systems in vivo.

A micro-scale actuator, which can regulate flow control in response to environmental stimuli, was fabricated with stimuli responsive hydrogel valves inside microchannels [185]. Micro-scale channels, which were fabricated by lithography, were filled with a photopolymerizable liquid consisting of acrylic acid and 2-hydroxyethyl methacrylate. The hydrogels in the microchannels performed sensing and actuation function with pH

change of local flow and with rapid response times of less than 10 seconds. This device does not demand external power for operation, so that it could eliminate complex assembly, overcoming significant disadvantages of conventional microfluidic actuators. This autonomously operating device responding to environmental change could be advanced by providing the hydrogels in the microchannels with other functionality such as temperature or glucose responsive properties.

Cultivated mammalian cells can be easily recovered from substrate surfaces by introducing temperature responsive polymers into the cell culture dish. In general, mammalian cells are cultured on a hydrophobic substrate and recovered by using protease such as trypsin, which might damage the cultured cells. Without any use of such a harmful enzyme, PNIPAAm-grafted substrate surfaces have been proposed for convenient and safe culture dishes, which can change their hydrophobic surfaces above the LCST to be hydrophilic below the LCST [182, 183]. At 37 °C, cells such as lung cells [55] showed good adhesion and proliferation on this culture dish, similar to commercial polystyrene dishes. However, below the LCST, the surface became hydrophilic, which caused cell detachment from the surface. This is schematically illustrated in Figure 1- 16. This switchable property of a cell culture surface was systematically studied by monitoring blood platelet movement depending on the temperature change from 37 °C to 20 °C [56]. In a more advanced study, temperature-regulated cell detachment was reported to require cell metabolic activity requiring ATP consumption, signal transduction, and cytoskeleton reorganization [54]. The intact microglia cells harvested from this culture dish were used

for a novel cell transplantation therapy for damaged central nervous system tissue [53].

Recent progress in cell cultures is based on more effective cell culture and detachment. One approach is introducing bioconjugates of temperature responsive polymers with cell adhesive motifs [170]. The temperature responsive hydrogel beads were conjugated with cell adhesive motif only on their outer surface. These beads could more efficiently cultivate phenotypes expressing chondrocytes due to a large surface/volume ratio. The well-attached and proliferated chondrocytes were successfully detached from the culture carrier below the LCST. Carboxylic acid groups were also incorporated with a PNIPAAm-based culture dish to accelerate cell detachment below the LCST of the polymer surface [52]. However, acrylic acid introduced by copoymerization (poly(NIPAAm-AAc)) resulted in excessive surface hydration and hindered cell spreading in culture at 37 °C. To obtain two benefits (e.g. good cell adhesion and accelerated cell detachment), the authors introduced 2-carboxyisopropylacrylamide (CIPAAm) having both a similar side chain structure to NIPAAm and a functional carboxylate group. The P(NIPAAm-co-CIPAAm) showed nearly the same LCSTs and temperature sensitivity as the NIPAAm homopolymer. Also it exhibited hydrophobicity similar to homopolymer PNIPAAm-grafted surfaces at 37°C, as well as accelerated cell detachment time, which might come from its more rapid deswelling than that of PNIPAAm homopolymer due to the introduced carboxylic acid moiety. For 90% cell detachment, they observed that 120 and 60 min were required for PNIPAAm homopolymer and P(NIPAAm-co-CIPAAm) culture dishes respectively.

1.4. Conclusion

The recent advances in the stimuli responsive polymers and their bioconjugates were summarized with a view towards their fundamental molecular designs as well as their biomedical applications. The application of these “smart polymers” has undergone tremendous progress in the past few decades. Stimuli responsive behaviors of these polymers have attracted our attention as versatile bio-related intelligent systems such as gene or drug delivery, chromatography, microfiltration, actuator, sensor, injectable polymeric matrix, and artificial tissue or organs. The stimuli responsive system has broadened its usage into different physical forms such as hydrogels, micelles, surface, and bioconjugates according to their desired applications.

This review concentrates on temperature responsive polymers, because they have been the most intensively investigated in various laboratories and industries due to their relatively effective control in vivo as well as in vitro and their versatile application range. Also, some other stimuli responsive polymers were described. The molecular designs of stimuli responsive polymeric systems were discussed according to each different physical form, especially focused on recent progress. The stimuli responsive polymers should be designed at the molecular level before considering the desired applications. The LCST should be controlled to match the desired environmentally critical condition, after selecting the appropriate polymers. Rapid response to stimuli is anther important factor that can be adjusted by designing their molecular structures. Biocompatibility and biodegradability should be considered when these polymeric systems are applied into the physiological environment such as drug delivery. Incorporating a biodegradable moiety into the molecular structure of stimuli responsive polymers in different ways could control the

biodegradability, which ranges from one day to long term depending on the specific applications. Once the desirable structure is developed, it could be applied to different physical forms, also resulting in its novel utilization.

Recent progress in polymeric synthesis has led to intriguing new stimuli responsive polymer systems, resulting from novel approaches for synthesizing random, block, or graft copolymers as well efficient control of molecular weight and molecular weight distribution. Controlled/living radical polymerization, such as ATRP or RAFT, has been introduced to provide stimuli-responsive polymers with very narrow PDIs and a living nature to the polymerization. In particular, ATRP has provided a preferable solution to the synthesis of well-defined architectures of stimuli-responsive polymers, for instance, di-, tri-, gradient- or star- type block copolymers and brush type polymers.

Genetically engineered proteins have been introduced as stimuli responsive polymers and investigated in different physical forms and applications. The combination of other functionality with stimuli responsiveness could broaden and strengthen the usages of stimuli responsive polymer-based intelligent systems. Besides biodegradable moieties, ionic groups or hydrophobic groups could be incorporated to provide a binding site for therapeutics such as anionic DNA and most hydrophobic drugs. Also, the conjugation of biomolecules such as ligands and enzymes to stimuli responsive polymer could provide on/off functionality depending on the corresponding stimulus change.

Advances in bio-related applications were selectively summarized by focusing on recent interests. Drug delivery into the inside of the targeted cell (into cytoplasm of targeted cell) has been recently focused on for the needs of gene therapy and cancer treatment.

Also, bioseparation could be more conveniently performed by using this intelligent polymeric system in different forms, such as membranes and chromatographs. Protein or DNA purification via this system was introduced so that the purified protein or DNA could be easily obtained from the medium by changing on/off of the stimuli signal.

Even though the stimuli responsive polymers are attractive for their potentials, they have to overcome several barriers; rapid response, mechanical strength, reproductability, biocompatibility, biodegradability, nontoxicity and so on, according to their applications. Many trials to fulfill these requirements have been reported in recent years. Therefore we expect that our systematic review of these trials could help chemists as well as non-chemist to develop new stimuli responsive polymers or polymeric systems which could be reliably utilized in real life application.

1.5. References

[1] Okano T editor, Biorelated polymers and gels. San Diago, CA: Academic press, 1998

[2] Osada Y and Khokhlov A R editors, Polymer gels and networks. New York, NY: Marcel Dekker, 2002

[3] Gupta P, Vermani K and Garg S. Hydrogels: from controlled release to pH-responsive drug delivery. Drug discovery today 2002; 7, 569-579.

[4] Jeong B and Gutowska A. Lessons from nature: stimuli-responsive polymers and their biomedical applications. TRENDS in Biotechnology. 2002; 20, 305-311.

[5] Kikuchi A and Okano T, Intelligent thermoresponsive polymeric stationary phases for aqueous chromatography of biological compounds, Progress in Polymer Science. 2002; 27, 1165-1193.

[6] Hoffman A S et al. Really smart bioconjugates of smart polymers and receptor proteins, J Biomed Mater Res. 2000; 52, 577–586.

[7] Galaev L Y and Mattiasson B. 'Smart' polymers and what they could do in biotechnology and medicine. Trends in Biotechnology, 2000; 17, 335-340.

[8] Qiu Y and Park K. Environment-sensitive hydrogels for drug delivery. Advanced Drug Delivery Reviews. 2001; 53, 321– 339.

[9] Sershen S and West J. Implantable, polymeric systems for modulated drug delivery. Advanced Drug Delivery Reviews. 2002; 54, 1225–1235.

[10] Yokoyama M. Gene delivery using temperature-responsive polymeric carriers. Drug Discovery Today. 2002; 7, 426-432.

[11] Chilkoti A, Dreher M R, Meyer D E, and Raucher D. Targeted drug delivery by thermally responsive polymers. Advanced Drug Delivery Reviews. 2002; 54, 613–630.

[12] Bromberg L E and Ron E S. Temperature-responsive gels and thermogelling polymer matrices for protein and peptide delivery. Advanced Drug Delivery Reviews. 1998; 31, 197–221.

[13] Weidner J. Drug targeting using thermally responsive polymers and local hyperthermia. Drug discovery today. 2001; 6, 1239-1248.

[14] Sharma S, Kaur P, Jain A, Rajeswari M R, and Gupta M N. A smart bioconjugate of chymotrypsin. Biomacromolecules. 2003; 4, 330-336.

[15] Kobayashi J, Kikuchi A, Sakai K, and Okano T. Aqueous chromatography utilizing hydrophobicity-modified anionic temperature-responsive hydrogel for stationary phases. Journal of Chromatography A. 2002; 958, 109–119.

[16] Anastase-Ravion S, Ding Z, Pelle A, Hoffman A S, and Letourneur D. New antibody purification procedure using a thermally responsive poly(N-isopropylacrylamide)–dextran derivative conjugate. Journal of Chromatography B. 2001; 761, 247–254.

[17] Pinkrah V T, Snowden M J, Mitchell J C, Seidel J, Chowdhry B Z, and Fern G R. Physicochemical properties of poly(N-isopropylacrylamide-co-4-vinylpyridine) cationic polyelectrolyte colloidal microgels. Langmuir. 2003; 19, 585-590.

[18] Peng T and Cheng Y L. PNIPAAm and PMAA co-grafted porous PE membranes: living radical co-grafting mechanism and multi-stimuli responsive permeability. polymer, 2001; 41, 2091–2100.

[19] Bignotti F, Penco M, Sartore L, Peroni I, Mendichi R, Casolaro M, and D'Amore A. Synthesis, characterisation and solution behaviour of thermo- and pH-responsive polymers bearing L-leucine residues in the side chains. Polymer. 2000; 41, 8247–8256.

[20] Gan L H, Gan Y Y, and Deen G R. Poly(N-acryloyl-N'-propylpiperazine): A new stimuli-responsive polymer. Macromolecules. 2000; 33, 7893-7897.

[21] Kurisawa M and Yui N. Dual-stimuli-responsive drug release from interpenetrating polymer network-structured hydrogels of gelatin and dextran. Journal of Controlled Release. 1998; 54, 191-200.

[22] Diez-Pena E, Quijada-Garrido I, and Barrales-Rienda J M. On the water swelling behaviour of poly(N-isopropylacrylamide) [P(N-iPAAm)], poly(methacrylic acid) [P(MAA)], their random copolymers and sequential interpenetrating polymer

networks (IPNs). Polymer. 2002; 43, 4341–4348.

[23] Varga I, Gilanyi T, Meszaros R, Filipcsei G, and Zrinyi M. Effect of cross-link density on the internal structure of poly(N-isopropylacrylamide) microgels. J Phys Chem B. 2001; 105, 9071-9076.

[24] Annaka M, Tanaka C, Nakahira T, Sugiyama M, Aoyagi T, and Okano T. Fluorescence study on the swelling behavior of comb-type grafted poly(N-isopropylacrylamide) hydrogels. Macromolecules. 2002; 35, 8173-8179.

[25] Yoshida R, Uchida K, Kaneko Y, Sakai K, Kikuchi A, Sakurai Y, and Okano T. Comb-type grafted hydrogels with rapid de-swelling response to temperature changes. Nature. 1995; 374, 240-242.

[26] Nordby M H, Kjøniksen A, Nystrom B, and Roots J. Thermoreversible gelation of aqueous mixtures of pectin and chitosan. Rheology. Biomacromolecules. 2003; 4, 337-343.

[27] Chenite A, Chaput C, Wang D, Combes C, Buschmann M D, Hoemann C D, Leroux J C, Atkinson B L, Binette F, and Selmani A. Novel injectable neutral solutions of chitosan form biodegradable gels in situ. Biomaterials. 2000; 21, 2155-2161.

[28] Vercruysse K P, Li H, Luo Y, and Prestwich G D. Thermosensitive lanthanide complexes of hyaluronan. Biomacromolecules. 2002; 3, 639-643.

[29] Jeong B, Kibbey M R, Birnbaum J C, Won Y, and Gutowska A. Thermogelling biodegradable polymers with hydrophilic backbones: PEG-g-PLGA. Macromolecules. 2000; 33, 8317-8322.

[30] Jeong B, Lee K M, Gutowska A, and An Y H. Thermogelling biodegradable copolymer aqueous solutions for injectable protein delivery and tissue engineering. Biomacromolecules. 2002; 3, 865-868.

[31] Lin H and Cheng Y. In-situ thermoreversible gelation of block and star copolymers of poly(ethylene glycol) and poly(N-isopropylacrylamide) of varying architectures. Macromolecules. 2001; 34, 3710-3715.

[32] Hatefi A and Amsden B. Biodegradable injectable in situ forming drug delivery systems. Journal of Controlled Release. 2002; 80, 9–28.

[33] Jeong B. Bae Y H, Lee D S, and Kim S W. Biodegradable block copolymers as injectable drug-delivery systems. Nature. 1997; 388, 860-862.

[34] Jeong B, Bae Y H, and Kim S W. Thermoreversible gelation of PEG-PLGA-PEG triblock copolymer aqueous solutions. Macromolecules. 1999; 32, 7064-7069.

[35] Zhang R, Liu J, He J, Han B, Zhang X, Liu Z, Jiang T, and Hu G. Compressed CO2-assisted formation of reverse micelles of PEO-PPO-PEO copolymer. Macromolecules. 2002; 35, 7869-7871.

[36] Chung J E, Yokoyama M, Aoyagi T, Sakurai Y, and Okano T. Effect of molecular

architecture of hydrophobically modified poly(N-isopropylacrylamide) on the formation of thermoresponsive core-shell micellar drug carriers. Journal of Controlled Release. 1998; 53, 119–130.

[37] Neradovic D, van Nostrum C F, and Hennink W E. Thermoresponsive polymeric micelles with controlled instability based on hydrolytically sensitive N-Isopropylacrylamide copolymers. Macromolecules. 2001; 34, 7589-7591.

[38] Kohori F, Yokoyama M, Sakai K, and Okano T. Process design for efficient and controlled drug incorporation into polymeric micelle carrier systems. Journal of Controlled Release. 2002; 78, 155–163.

[39] Okabe S, Sugihara S, Aoshima S, and Shibayama M. Heat-induced self-assembling of thermosensitive block copolymer. 1. Small-angle neutron scattering Study. Macromolecules. 2002; 35, 8139-8146.

[40] Okubo M, Ahmad H, and Suzuki T. Synthesis of temperature-sensitive micron-sized monodispersed composite polymer particles and its application as a carrier for biomolecules. Colloid Polym Sci. 1998; 276, 470-475.

[41] Nakayama H, Kaetsu I, Uchida K, Sakata S, Tougou K, Hara T, and Matsubara Y. Radiation curing of intelligent coating for controlled release and permeation. Radiation Physics and Chemistry. 2002; 63, 521-523.

[42] Magoshi T, Ziani-Cherif H, Ohya S, Nakayama Y, and Matsuda T. Thermoresponsive heparin coating: Heparin conjugated with poly(N-isopropylacrylamide) at one terminus. Langmuir. 2002; 18, 4862-4872.

[43] Rama Rao G V, Krug M E, Balamurugan S, Xu H, Xu Q, and Lopez G P. Synthesis and characterization of silica-poly(N-isopropylacrylamide) hybrid membranes: switchable molecular filters. Chem Mater. 2002; 14, 5075-5080.

[44] Nath N and Chilkoti A. Interfacial Phase Transition of an environmentally responsive elastin biopolymer adsorbed on functionalized gold nanoparticles studied by colloidal surface plasmon resonance. J Am Chem Soc. 2001; 123, 8197-8202.

[45] Stayton P S, Shimoboji T, Long C, Chilkoti A, Chen G, Harris J M, and Hoffman A S. Control of protein-ligand recognition using a stimuli-responsive polymer. Nature. 1995; 378, 472–474.

[46] Ohya S, Nakayama Y, and Matsuda T. Thermoresponsive artificial extracellular matrix for tissue engineering: Hyaluronic acid bioconjugated with poly(N-isopropylacrylamide) grafts. Biomacromolecules. 2001; 2, 856-863.

[47] Lackey C A, Murthy N, Press O W, Tirrell D A, Hoffman A S, and Stayton P S. Hemolytic activity of pH-responsive polymer-streptavidin bioconjugates. Bioconjugate Chem. 1999; 10, 401-405.

[48] Hayashi H, Kono K, and Takagishi T. Temperature-dependent associating property of liposomes modified with a thermosensitive polymer. Bioconjugate Chem. 1998; 9,

382-389.

[49] Leroux J, Roux E, Garrec D L, Hong K, and Drummond D C. N-isopropylacrylamide copolymers for the preparation of pH-sensitive liposomes and polymeric micelles. Journal of Controlled Release. 2001; 72, 71–84.

[50] Kurisawa M, Yokoyama M, and Okano T. Gene expression control by temperature with thermo-responsive polymeric gene carriers. Journal of Controlled Release. 2000; 69, 127–13.

[51] Benns J M, Choi J, Mahato R I, Park J, and Kim S W. pH-sensitive cationic polymer gene delivery vehicle: N-Ac-poly(L-histidine)-graft-poly(L-lysine) comb shaped polymer. Bioconjugate Chem. 2000; 11, 637-645.

[52] Ebara M, Yamato M, Hirose M, Aoyagi T, Kikuchi A, Sakai K, and Okano T. Copolymerization of 2-carboxyisopropylacrylamide with N-isopropylacrylamide accelerates cell detachment from grafted surfaces by reducing temperature. Biomacromolecules. 2003; 4, 344-349.

[53] NakajimaK, Honda S, Nakamura Y, Redondo F L H, Kohsaka S, Yamato M, Kikuchi A, and Okano T. Intact microglia are cultured and non-invasively harvested without pathological activation using a novel cultured cell recovery method. Biomaterials. 2001; 22, 1213-1223.

[54] Yamato M, Konno C, Kushida A, Hirose M, Utsumi M, Kikuchi A, and Okano T. Release of adsorbed fibronectin from temperature-responsive culture surfaces requires cellular activity. Biomaterials. 2000; 21, 981-986.

[55] Nandkumar M A, Yamato M, Kushida A, Konno C, Hirose M, Kikuchi A, and Okano T. Two-dimensional cell sheet manipulation of heterotypically co-cultured lung cells utilizing temperature-responsive culture dishes results in long-term maintenance of di differentiated epithelial cell functions. Biomaterials. 2002; 23, 1121 –1130.

[56] Uchida K, Sakai K, Ito E, Kwon O H, Kikuchi A, Yamato M, and Okano T. Temperature-dependent modulation of blood platelet movement and morphology on poly(N-isopropylacrylamide)-grafted surfaces. Biomaterials. 2000; 21, 923-929.

[57] Meyer D E, Kong G A, Dewhirst M W, Zalutsky M R, and Chilkoti A. Targeting a genetically engineered elastin-like polypeptide to solid tumors by local hyperthermia. Cancer Res. 2001; 61, 1548–1554.

[58] Fujishige S and Kubota K. I. Ando, Phase transition of aqueous solutions of poly(N-isopropylacrylamide) and poly(N-isopropylmethacrylamide). J Phys Chem. 1989; 93, 3311–3313.

[59] Schild H G. Poly(N-isopropylacrylamide): Experiment, theory and application. Prog Polym Sci. 1992; 17, 163–249.

[60] Guenet J M Editor. Thermoreversible Gelation of Polymers and Biopolymers, London, Academic Press, 1992.

[61] Soutar I, Swanson L, Thorpe F G, and Zhu C. Fluorescence studies of the dynamic behavior of poly(dimethylacrylamide) and its complex with poly(methacrylic acid) in dilute solution. Macromolecules. 1996; 29, 918-924.

[62] Garay M T, Llamas M C, and Iglesias E. Study of polymer-polymer complexes and blends of poly(N-isopropylacrylamide) with poly(carboxylic acid): 1. Poly(acrylic acid) and poly(methacrylic acid). Polymer. 1997; 38, 5091-5096.

[63] Brown W, et al. Triblock copolymers in aqueous solution studies by static and dynamic light scattering and oscillatory shear measurements. Influence of relative block sizes. J Phys Chem. 1992; 96, 6038–6044.

[64] Aoyagi T, Ebara M, Sakai K, Sakurai Y, and Okano T. Novel bifunctional polymer with reactivity and temperature sensitivity, J. Biomater Sci, Polym Ed., 2000; 1, 101-110.

[65] Ebara M, Aoyagi T, Sakai K, and Okano T. Introducing reactive carboxyl side chains retains phase transition temperature Sensitivity in N-isopropylacrylamide copolymer gels. Macromolecules. 2000, 33, 8312-8316.

[66] Aoki T, Muramatsu M, Torii T, Sanui K, and Ogata N. Thermosensitive phase transition of an optically active polymer in aqueous milieu. Macromolecules. 2001; 34, 3118-3119.

[67] Gan L H, Roshan Deen G, Loh X J, and Gan Y Y. New stimuli-responsive copolymers of N-acryloyl-N'-alkyl piperazine and methyl methacrylate and their hydrogels. 2001; Polymer. 42, 65–69.

[68] Suwa K, Yamamoto K, Akashi M, Takano K, Tanaka N, and Kunugi S. Effects of salt on the temperature and pressure responsive properties of poly(N-vinylisobutyramide) aqueous solutions. Colloid Polym Sci. 1998; 276, 529-533.

[69] Maeda Y. IR spectroscopic study on the hydration and the phase transition of poly(vinyl methyl ether) in water. Langmuir. 2001; 17, 1737-1742.

[70] Inoue T et al. Temperature sensitivity of a hydrogel network containing different LCST oligomers grafted to the hydrogel backbone. Polym Gels Networks. 1997; 5, 561–575.

[71] Malmsten M and Lindman B. Self-assembly in aqueous block copolymer solution. Macromolecules. 1992; 25, 5446–5450.

[72] Zhang Z and Khan A. Phase behavior of poly(ethyleneoxide)–poly(propylene oxide)–poly(ethylene oxide) triblock copolymers in water. Macromolecules. 1995; 28, 3807–3812.

[73] Mortensen K and Perdersen S. Structural study on micelle formation of poly(ethylene oxide)-poly(propylene oxide)-poly(ethylene oxide) triblock copolymer in aqueous solution. Macromolecules. 1993; 26, 805–812.

[74] Alexandridis P, Holzwarth J F, and Hatton T A. Micellization of poly(ethylene oxide)–

poly(propylene oxide)–poly-(ethylene oxide) triblock copolymers in aqueous solutions: Thermodynamics of copolymer association. Macromolecules. 27, 6046–6054.

[75] Glatter O et al. Characterization of a poly(ethylene oxide)-poly(propylene oxide) triblock copolymer (EO27-PO39-EO27) in aqueous solution. Macromolecules. 1994; 27, 6046–6054.

[76] Li H, Yu G, Price C. Booth C, Hecht E, and Hoffmann H, Concentrated aqueous micellar solutions of diblock copoly(oxyethylene/oxybutylene) E41B8: A Study of Phase Behavior. Macromolecules. 1997; 30, 1347-1354.

[77] Yu G E, Yang Y W, Yang Z, Attwood D, Booth C, and Nace V M. Association of diblock and triblock copolymers of ethylene oxide and butylene oxide in aqueous solution. Langmuir. 1996; 12, 3404-3412.

[78] Lee S B, Song S, Jin J, and Sohn Y S. A New Class of biodegradable thermosensitive polymers. 2. Hydrolytic properties and salt effect on the lower critical solution temperature of poly(organophosphazenes) with methoxypoly(ethylene glycol) and amino acid esters as side groups. Macromolecules. 1999; 32, 7820-7827.

[79] Song S, Lee S B, Jin J, and Sohn Y S. A new class of biodegradable thermosensitive polymers. I. Synthesis and characterization of poly(organophosphazenes) with methoxy-poly(ethylene glycol) and amino acid esters as side groups. Macromolecules. 1999; 32, 2188-2193.

[80] B.H. Lee B H, Y. M. Lee Y M, Y. S. Sohn Y S, and S. Song S. A thermosensitive poly(organophosphazene) gel. Macromolecules. 2002; 35, 3876-3879.

[81] Lee S B, Song S, Jin J, and Sohn Y S. Structural and thermosensitive properties of cyclotriphosphazenes with poly(ethylene glycol) and amino acid esters as side groups. Macromolecules. 2001; 34, 7565-7569.

[82] Lee S B, Song S, Jin J , and Sohn Y S. Thermosensitive cyclotriphosphazenes. J Am Chem Soc. 2000; 122, 8315-8316.

[83] Kuijpers A J, Engbers G H M, Feijen J, De Smedt S C, Meyvis T K L, Demeester J, Krijgsveld J, Zaat S A J, and Dankert J. Characterization of the network structure of carbodiimide cross-linked gelatin gels. Macromolecules. 1999; 32, 3325-3333.

[84] Ramzi M, Rochas C, and Guenet J. Structure-properties relation for agarose thermoreversible gels in binary solvents. Macromolecules. 1998; 31, 6106-6111.

[85] Dentini M, Desideri P, Crescenzi V, Yuguchi Y, Urakawa H, and Kajiwara K. Solution and gelling properties of gellan benzyl esters. Macromolecules. 1999; 32, 7109-7115.

[86] Chen T, Embree H D, Wu L, and Payne G F. In vitro protein-polysaccharide conjugation: Tyrosinase-catalyzed conjugation of gelatin and chitosan. Biopolymers. 2002; 64, 292-302.

[87] Isogai N, Gong J P, and Osada Y. Thermosensitive polymer gel by reversible surfactant binding. Macromolecules. 1996; 29, 6803-6806.

[88] Wei Y C and Hudson S M. The interactions of polyelectrolytes and surfactants of opposite charge: A review of the literature. J of Macromol Sci Reviews. 1995; C35, 15-45.

[89] Wei Y C and Hudson S M. Binding of sodium dodecyl sulfate to a polyelectrolyte based on chitosan. Macromolecules. 1993; 26, 4151-4154.

[90] Deming T J. Facile synthesis of block copolypeptides of defined architecture. Nature. 1997; 390, 386-389.

[91] Nowak A P, Breedveld V, Pakstls L, Ozbas B, Plne D J, Pochan D, and Deming T J. Rapid recovering hydrogel scaffolds from self-assembling diblock copolypeptide amphiphiles. Nature. 2002; 417, 424-428.

[92] Kopecek J, Polymer chemistry: Swell gels. Nature. 2002; 417, 388-391.

[93] Petka W A, Harden J L, McGrath K P, Wirtz D, and Tirrell D A. Reversible hydrogels from self-assembling artifcial proteins. Science. 1998; 281, 389-392.

[94] Meyer D E and Chilkoti A. Purification of recombinant proteins by fusion with thermally-responsive polypeptides. Nature biotechnology. 1999; 17, 1112-1115.

[95] Meyer D E, Trabbic-Carlson K, and Chilkoti A. Protein purification by fusion with an environmentally responsive elastin-like polypeptide: Effect of polypeptide length on the purification of thioredoxin. Biotechnol Prog. 2001; 17, 720-728.

[96] Cappello J, Crissman J W, Crissman M, Ferrari F A, Textor G, Wallis O, Whitledge J R, Zhou X, Burman D, Aukerman L, and Stedronsky E R. In-situ self-assembling protein polymer gel systems for administration, delivery, and release of drugs. Journal of Controlled Release. 1998; 53, 105–117.

[97] Rama Rao G V, Balamurugan S, Meyer D E, Chilkoti A, and Lopez G P. Hybrid bioinorganic smart membranes that incorporate protein-based molecular switches. Langmuir. 2002; 18, 1819-1824.

[98] Wu A S, A.S. Hoffman A S, Yager P J. Synthesis and characterization of thermally reversible macroporous poly(N-isopropylacrylamide) hydrogels. J Polym Sci, Polym Chem. 1992; 30, 2121-2129.

[99] Kishi R, Hirasa O, and Ichijo H. Fast responsive poly(N-isopropylacrylamide) hydrogels prepared by γ-ray irradiation. Gels Networks. 1997; 5, 145.

[100] Kaneko Y, Nakamura S, Sakai K, Aoyagi T, Kikuchi A, Sakurai Y, and Okano T. Rapid deswelling response of poly(N-isopropylacrylamide) hydrogels by the formation of water release channels using poly(ethylene oxide) graft chains. Macromolecules. 1998; 31, 6099-6105.

[101] Annaka M, Sugiyama M, Kasai M, Nakahira T, Matsuura T, Seki H, Aoyagi T, and

Okano T. Transport properties of comb-type grafted and normal-type N-isopropylacrylamide hydrogel. Langmuir. 2002; 18, 7377-7383.

[102] Matsukata M, Aoki T, Sanui K, Ogata N, Kikuchi A, Sakurai Y, Okano T. Effect of molecular architecture of poly(N-isopropylacrylamide)–trypsin conjugates on their solution and enzymatic properties. Bioconjugate Chem. 1996; 7, 96–101.

[103] Takei Y G, Aoki T, Sanui K, Ogata N, Sakurai Y, and Okano T. Dynamic contact angle measurement of temperature-responsive surface properties for poly(N-isopropylacrylamide) grafted surfaces. Macromolecules. 1994; 27, 6163–6166.

[104] Zhang X, Yang Y, Wang F, and Chung T. Thermosensitive poly(N-isopropylacrylamide-co-acrylic acid) hydrogels with expanded network structures and improved oscillating swelling-deswelling properties. Langmuir. 2002; 18, 2013-2018.

[105] Shibayama M and Tanaka T. Volume phase transition and related phenomena of polymer gels. Adv Polym Sci. 1993; 109, 1–62.

[106] Chen G and Hoffman A S. Graft copolymers that exhibit temperature-induced phase transition over a wide range of pH. Nature. 1995; 373, 49–52.

[107] Neradovic D, Hinrichs W L J, Kettenes-van den Bosch J J, and Hennink W E. Poly(N-isopropylacrylamide) with hydrolyzable lactic acid ester side groups. A new type of thermosensitive polymer. Macromol Rapid Commun. 1999; 20, 577-581.

[108] Sukuki A and Tanaka T. Phase transition in polymer gels induced by visible light. Nature. 1990; 346, 345-347.

[109] Topp M D C, Dijkstra P J, Talsma H, and Feijen J. Thermosensitive micelle-forming block copolymers of poly(ethylene glycol) and poly(N-isopropylacrylamide). Macromolecules. 1997; 30, 8518-8520.

[110] Duracher D, Elaıssari A, Mallet F, and Pichot C. Adsorption of modified HIV-1 capsid p24 protein onto thermosensitive and cationic core-shell poly(styrene)-poly(N-isopropylacrylamide) particles. Langmuir. 2000; 16, 9002-9008.

[111] Virtanen J, Holappa S, Lemmetyinen H, and Tenhu H. Aggregation in aqueous poly(N-isopropylacrylamide)-block-poly(ethylene oxide) solutions studied by fluorescence spectroscopy and light scattering. Macromolecules. 2002; 35, 4763-4769.

[112] Kohori F, Sakai K, Aoyagi T, Yokoyama M, Sakurai Y, and Okano T. Preparation and characterization of thermally responsive block copolymer micelles comprising poly(N-isopropylacrylamide-b-DL-lactide). Journal of Controlled Release. 1998; 55, 87–98.

[113] Chung J E, Yokoyama M, and Okano T. Inner core segment design for drug delivery control of thermo-responsive polymeric micelles. Journal of Controlled Release. 2000; 65, 93–103.

[114] Su Y, Wang J, Liu H. FTIR Spectroscopic Investigation of effects of temperature and concentration on PEO-PPO-PEO block copolymer properties in aqueous solutions. Macromolecules. 2002; 35, 6426-6431.

[115] Wang Y D, Gan Q, Shi C Y, Zheng X L, Yang S H, Li Z M, Dai Y Y. Separation of phenol from aqueous solutions by polymeric reversed micelle extraction. Chemical Engineering Journal. 2002; 88, 95-101.

[116] Liaw J, Chang S, Hsiao F. In vivo gene delivery into ocular tissues by eye drops of poly(ethylene oxide)-poly(propylene oxide)-poly(ethylene oxide) (PEO-PPO-PEO) polymeric micelles. Gene Therapy. 2001; 8, 999-1004.

[117] Gladysheva L P, Polekhina O V, Karmakova T A, Nemtsova E R, Yakubovskaya R I, Shen W, Kennedy A R, and Larionova N I. Potential of block copolymer- and immuno-conjugates for tumor-targeted delivery of Bowman-Birk soybean proteinase inhibitor. Journal of Controlled Release. 2001; 74(1-3), 303-308.

[118] Katakam M, Ravis W R, and Banga A K. Controlled release of human growth hormone in rats following parenteral administration of poloxamer gels. Journal of Controlled Release. 1997; 49, 21–26.

[119] Bromberg L. Polyether-modified poly(acrylic acid): Synthesis and applications. Ind Eng Chem Res. 1998; 37, 4267–4274.

[120] Bromberg L. Novel family of thermogelling materials via C–C bonding between poly(acrylic acid) and poly(ethylene oxide)-b-poly(propylene oxide)-b-poly(ethylene oxide). J Phys Chem B. 1998; 102, 1956–1963.

[121] Bromberg L. Properties of aqueous solutions and gels of poly(ethylene oxide)-b-poly(propylene oxide)-b-poly(ethylene oxide)-g-poly(acrylic acid). J Phys Chem B. 1998; 102, 10736–10744.

[122] Miyazaki S, Ohkawa Y, Takada M, and Attwood D. Pharmaceutical application of biomedical polymers. XXXII. Antitumor effect of Pluronic F-127 gel containing mitomycin C on sarcoma-180 ascites tumor in mice. Chem Pharm Bull. 1992; 40, 2224-2226.

[123] Bhardwaj R and Blanchard J. Controlled-release delivery system for the -MSH analog Melanotan-I using poloxamer 407. J Pharm Sci. 1996; 85, 915-919.

[124] Jeong B et al. Biodegradable thermoreversible gelling PLGA-g-PEG copolymer. Chem Commun. 2001; 16, 1516–1517.

[125] Behravesh E, Shung A K, Jo S, and Mikos A G. synthesis and characterization of triblock copolymers of methoxy poly(ethylene glycol) and poly(propylene fumarate). Biomacromolecules. 2002; 3, 153-158.

[126] Pruitt J D, Husseini G, Rapoport N, and Pitt W G. Stabilization of Pluronic P-105 micelles with an interpenetrating network of N,N-diethylacrylamide. Macromolecules. 2000; 33, 9306-9309.

[127] Cammas-Marion S, Okano T, and Kataoka K. Functional and site-specific macromolecular micelles as high potential drug carriers. Colloids Surf, B:Biointerface. 1999; 16, 207-215.

[128] Kim I S, Jeong Y I, Cho C S, and Kim S H. Thermo-responsive self-assembled polymeric micelles for drug delivery in vitro. Int J Pharm. 2000; 205, 165-172.

[129] Konak C, Oupicky D, Chytry V, and Ulbrich K. Thermally controlled association in aqueous solutions of diblock copolymers of poly[N-(2-hydroxypropyl)methacrylamide] and Poly(N-isopropylacrylamide). Macromolecules. 2000; 33, 5318-5320.

[130] Topp M C D, Leunen I H, Dijkstra P J, Tauer K, Schellenberg C, and Feijen J. Quasi-living polymerization of N-isopropylacrylamide onto poly(ethylene glycol). Macromolecules. 2000; 33, 4986-4988.

[131] Konak C, Reschel T, Oupicky D, and Ulbrich K. Thermally controlled association in aqueous solutions of poly(L-lysine) grafted with poly(N-isopropylacrylamide). Langmuir. 2002; 18, 8217-8222.

[132] Chung J E, Yokoyama M, Suzuki K, Aoyagi T, Sakurai Y, and Okano T. Reversibly thermoresponsive alkyl-terminated poly(N-isopropylacrylamide) core-shell micellar structures. Colloids Surfaces B: Biointerfaces. 1997; 9, 37–48.

[133] Whichterle O and Lim D. Hydrophilic gels for biological uses. Nature. 1960; 185, 117-118.

[134] Voldrich Z, Tomanek Z, Valik J, and Kopecek J. Long-term experience with poly(glycol monomethacrylate) gel in plastc operation of the nose. J Biomed Mater Res. 1975; 9, 675-685.

[135] Stile R A, Burghardt W R, and Healy K E. Synthesis and characterization of injectable poly(N-isopropylacrylamide)-based hydrogels that support tissue formation in Vitro. Macromolecules. 1999; 32, 7370-7379.

[136] Haraguchi K, Takehisa T, and Fan S. Effects of Clay content on the properties of nanocomposite hydrogels vomposed of poly(N-isopropylacrylamide) and clay. Macromolecules. 2002; 35, 10162-10171.

[137] Akiyoshi K, Kang E, Kurumada S, Sunamoto J, Principi T and Winnik F M. Controlled association of amphiphilic polymers in water: Thermosensitive nanoparticles formed by self-assembly of hydrophobically modified pullulans and poly(N-isopropylacrylamides). Macromolecules. 2000; 33, 3244-3249.

[138] Dıez-Pena E, Quijada-Garrido I, Frutos P, and Barrales-Rienda J M. Thermal properties of cross-linked poly(N-isopropylacrylamide) [P(N-iPAAm)], poly(methacrylic acid) [P(MAA)], their random copolymers [P(N-iPAAm-co-MAA)], and sequential interpenetrating polymer networks (IPNs). Macromolecules. 2002; 35, 2667-2675.

[139] Ju H K, Kim S Y, and Lee Y M. pH/Temperature responsive behaviors of semi-IPN and comb-type graft hydrogels composed of alginate and poly(N-isopropylacrylamide). Polymer. 2001; 42, 6851.

[140] Bromberg L. Zein-poly(N-isopropylacrylamide) conjugates. J Phys Chem B. 1997; 101, 504-507.

[141] Dhara D, Rathna G V N, and Chatterji P R. Volume phase transition in interpenetrating networks of poly(N-isopropylacrylamide) with gelatin. Langmuir. 2000; 16, 2424-2429.

[142] Suzuki K, Yumura T, Tanaka Y, Serizawa T, and Akashi M, Interpenetrating inorganic–organic hybrid gels: preparation of hybrid and replica gels. Chem Lett. 2000; 12, 1380–1381.

[143] Suzuki K, Yumura T, Tanaka Y, and Akashi M. Thermo-responsive release from interpenetrating porous silica–poly(N-isopropylacrylamide) hybrid gels. Journal of Controlled Release. 2001; 75, 183–189.

[144] Wang C, Stewart R J and Kopecek J. Hybrid hydrogles assembled from synthetic polymers and coiled-coil protein domains. Nature. 1999; 397, 417-420.

[145] Ramkissoon-Ganorkar C, Liu F, Baudys M and Kim S W. Modulating insulin-release profile from pH/thermosensitive polymeric beads through polymer molecular weight. Journal of Controlled Release. 1999; 59 287–298.

[146] Benee L S, Snowden M J, and Chowdhry B Z. Novel gelling behavior of poly(N-isopropylacrylamide-co-vinyl laurate) microgel dispersions. Langmuir. 2002; 18, 6025-6030.

[147] Ito S, Ogawa K, Suzuki H, Wang B, Yoshida R, and Kokufuta E. Preparation of thermosensitive submicrometer gel particles with anionic and cationic charges. Langmuir. 1999; 15, 4289-4294.

[148] Gan D and Lyon L A. Synthesis and protein adsorption resistance of PEG-modified Poly(N-isopropylacrylamide) Core/Shell Microgels. Macromolecules. 2002; 35, 9634-9639.

[149] Ordian G. Principles of polymerization, third edition. Staten island, NY; Wiley-Interscience Publication, 1991. p. 347-348,

[150] Choi Y, Yamaguchi T, and Nakao S. A novel separation system using porous thermosensitive membranes. Ind Eng Chem Res. 2000; 39, 2491-2495.

[151] Park Y S, Ito Y, and Imansish Y. Permeation control through porous membranes immobilized with thermosensitive polymer. Langmuir. 1998; 14, 910-914.

[152] Hosoya K, Kubo T, Tanaka N, and Haginaka J. A possible purification method of DNAs' fragments from humic matters in soil extracts using novel stimulus responsive polymer adsorbent. Journal of Pharmaceutical and Biomedical Analysis.

2003; 30, 1919-1922.

[153] Ma C S, Zhang W, and Ciszkowska M. Transport of ions and electrostatic interactions in thermoresponsive poly(N-isopropylacrylamide-co-acrylic acid) hydrogels: Electroanalytical studies. J Phys Chem B. 2001; 105, 10446-10452.

[154] Iwata H, Oodate M, Uyama Y, Amemiya H, and Ikada Y. Preparation of temperaturesensitive membranes by graft polymerization onto a porous membrane. J Membr Sci. 1991; 55, 119-130.

[155] Okahata Y, Noguchi H, and Seki T. Thermoselective permeation from a polymer-graftedcapsule membrane. Macromolecules. 1986; 19, 493-494.

[156] Rama Rao G V and López G P. Encapsulation of poly(N-Isopropyl acrylamide) in silica: A stimuli-responsive porous hybrid material that incorporates molecular nano-valves. Advanced Material. 2000; 12, 1692-1695.

[157] Lu Y, Cao G, Kale R P, Prabakar S, López G P, and Brinker C J. Microporous silica prepared by organic templating: Relationship between the molecular template and pore structure. Chem Mater. 1999; 11, 1223-1229.

[158] Hester J H, Banerjee P, and Mayes A M. Preparation of protein-resistant surfaces on poly(vinylidene fluoride) membranes via durface degregation. Macromolecules. 1999; 32, 1643-1650.

[159] Ying L, Kang E T, and Neoh K G. Synthesis and vharacterization of poly(N-isopropylacrylamide)-graft-poly(vinylidene fluoride) copolymers and temperature-sensitive membranes. Langmuir. 2002; 18, 6416-6423.

[160] Uakushiji T, Sakai K, Kikuchi A, Aoyagi T, Sakurai Y, and Okano T. Graft architectural effects on thermo-responsive wettability changes of poly(N-isopropylacrylamide)-modified surfaces. Langmuir. 1998; 14, 4657-62.

[161] Yakushiji T, Sakai K, Kikuchi A, Aoyagi T, Sakurai Y, and Okano T. Effects of cross-linked structure on temperature-responsive hydrophobic interaction of PIPAAm hydrogel modifed surfaces with steroids. Anal Chem. 1997; 71, 1125-1130.

[162] Bohanon T, Elender G, Knoll W, Koberle P, Lee J S, Offenhausser A, Ringsdorf H, Sackmann E, Simon J, Tovar G, and Winnik F M. Neural pattern formation on glass and oxidized silicon surfaces modifed with poly(N-isopropylacrylamide). J Biomater Sci Polym Ed. 1996; 8, 19-39.

[163] Frey W, Meyer D E, Chilkoti A. Dynamic addressing of a surface pattern by a stimuli-responsive fusion protein. Advanced materials. 2003; 15, 248-251.

[164] Frey W, Meyer D E, Chilkoti A. Thermodynamically reversible addressing of a stimuli responsive fusion protein onto a patterned surface template. Langmuir. 2003; 19, 1641-1653.

[165] Kim J C, Bae S K, and Kim J D. Temperature-sensitivity of liposomal lipid bilayers mixed with poly(N- isopropylacrylamide). J Biochem. 1997; 121,

15–19.

[166] Ding Z, Long C J, Hayashi Y, Bulmus E V, Hoffman A S, and Stayton P S. Temperature control of biotin binding and release with a streptavidin-polyNIPAAm site-specific conjugate. Bioconjugate Chem. 1999; 10, 395–400.

[167] Bulmus E V, Ding Z, Long C J, Stayton P S, and Hoffman A S. synthesis and site-specific conjugation of a pH- and temperature-sensitive polymer to streptavidin for pH-controlled binding and triggered release of biotin. Bioconjugate Chem. 1999; 11, 78–83.

[168] Fong R B, Ding Z, Long C J, Hoffman A S, and Stayton P S. Thermo-precipitation of streptavidin via oligonucleotide-mediated self-assembly with Poly(NIPAAm). Bioconjugate Chem. 1999; 10, 720–725.

[169] Shimoboji T, Ding Z, Stayton P S, and Hoffman A S. Mechanistic investigation of smart polymer-protein conjugates. Bioconjugate Chem. 2001; 12, 314 –319.

[170] Kim M R, Jeong J H, and Park T G. Swelling Induced detachment of Chondrocytes using RGD-modified poly(N-isopropylacrylamide) hydrogel beads. Biotechnol Prog. 2002; 18, 495-500.

[171] Katayama Y, Sonoda T, and Maeda M. A polymer micelle responding to the protein kinase A signal. Macromolecules. 2001; 34, 8569-8573.

[172] Verma I et al. Gene therapy - promises, problems and prospects. Nature. 1997; 389, 239–242.

[173] Meyer D E, Shin B C, Kong G A, Dewhirst M W, and Chilkoti A. Drug targeting using thermally responsive polymers and local hyperthermia. Journal of Controlled Release. 2001; 74, 213–224.

[174] Yang H M, Reisfeld R. Doxorubicin conjugated with a monoclonal antibody directed to a human melanoma-associated proteoglycan suppresses the growth of established tumor xenografts in nude mice. Proc Natl Acad Sci USA. 1998; 85, 1189–1193.

[175] Thedrez P, Saccavini J C, Nolibe D, Simoen J P, Guerreau D, Gestin J F, Kremer M, Chatal J F. Biodistribution of indium-111-labeled OC 125 monoclonal antibody after intraperitoneal injection in nude mice intraperitoneally grafted with ovarian carcinoma. Cancer Res. 1989; 49, 3081–3086.

[176] Pan L, Chien C. A novel application of thermo-responsive polymer to affinity precipitation of polysaccharide. Journal of Biochemical and Biophysical Methods. 2003; 55, 87-94.

[177] Hoshino K, Taniguchi M, Kitao T, Morohashi S, Sasakura T. Preparation of a new thermo-responsive adsorbent with maltose as a ligand and its application to affinity precipitation. Biotechnology and Bioengineering. 1998; 60, 568-579.

[178] Chen J P and Hoffman A S. Polymer-protein conjugates. II. Affinity precipitation separation of human immunogammaglobulin by a poly(N-isopropylacrylamide)-

protein A conjugate. Biomaterials. 1990; 11, 631–634.

[179] Kumar A, Wahlund PO, Kepka C, Galaev IY, Mattiasson B. Purification of histidine-tagged single-chain Fv-antibody fragments by metal chelate affinity precipitation using thermoresponsive copolymers. Biotech and Bioeng 2003; 84: 494-503.

[180] Chen Y, Huang L, Chiu H, and Lin S. Temperature-responsive polymer-assisted protein refolding. Enzyme and Microbial Technology. 2003; 32, 120–130,

[181] Kuboi R, Morita S, Ota H, and Umakoshi H. Protein refolding using stimuli-responsive polymer-modified aqueous two-phase systems. Journal of Chromatography B. 2000; 743, 215–223.

[182] Okano T et al. Mechanism of cell detachment from temperature-modulated, hydrophilic-hydrophobic polymer surfaces. Biomaterials. 1995; 16, 297–303.

[183] Okano T, Kikuchi A, Sakurai Y, Takei Y and Ogata N. Temperature-responsive poly (N-isopropylacrylamide) as a modulator for alteration of hydrophilic/hydrophobic surface properties to control activation/inactivation of platelets. Journal of Controlled Release. 1995; 36, 125–133.

[184] Huber D L, Manginell R P, Samara M A, Kim B and Bunker B C. Programmed adsorption and release of proteins in a microfluidic device, Science, 2003; 301, 352–354.

[185] Beebe D J, Moore J S, Bauer J M, Qing Yu Q, Robin H, Liu R H, Chelladurai Devadoss C and Jo B, Functional hydrogel structures for autonomous flow control inside microfluidic channels, Nature 404 (2000), pp. 588–590.

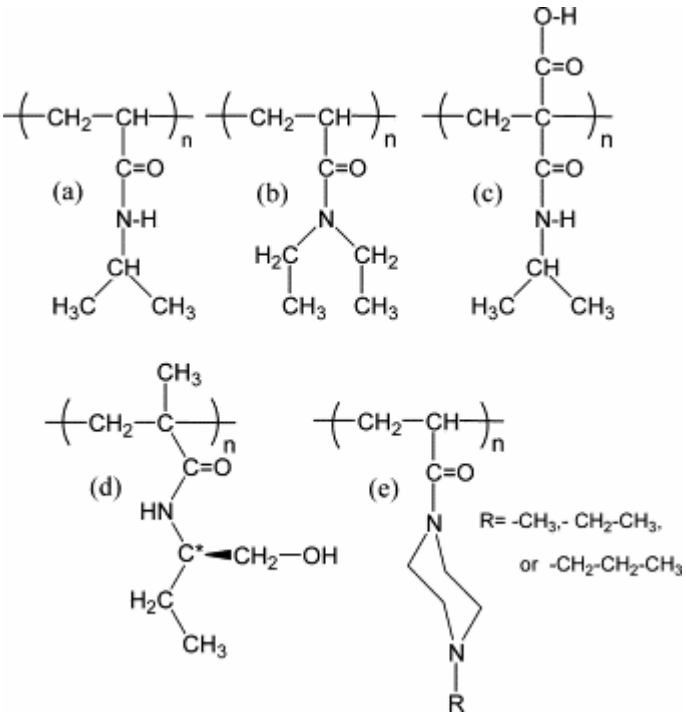

Figure 1- 1 Poly(N-substituted acrylamide) showing a LCST

(a) Poly(N-isopropylacrylamide) (PNIPAAm)

(b) Poly(N,N'-diethylacrylamide) (PDEAAm)

(c) Poly(2-carboxyisopropylacrylamide) (PCIPAAm)

(d) Poly(N-(L)-(1-hydroxymethyl) propylmethacrylamide (P(L-HMPMAAm))

(e) Poly(N-acryloyl-N'-alkylpiperazine)

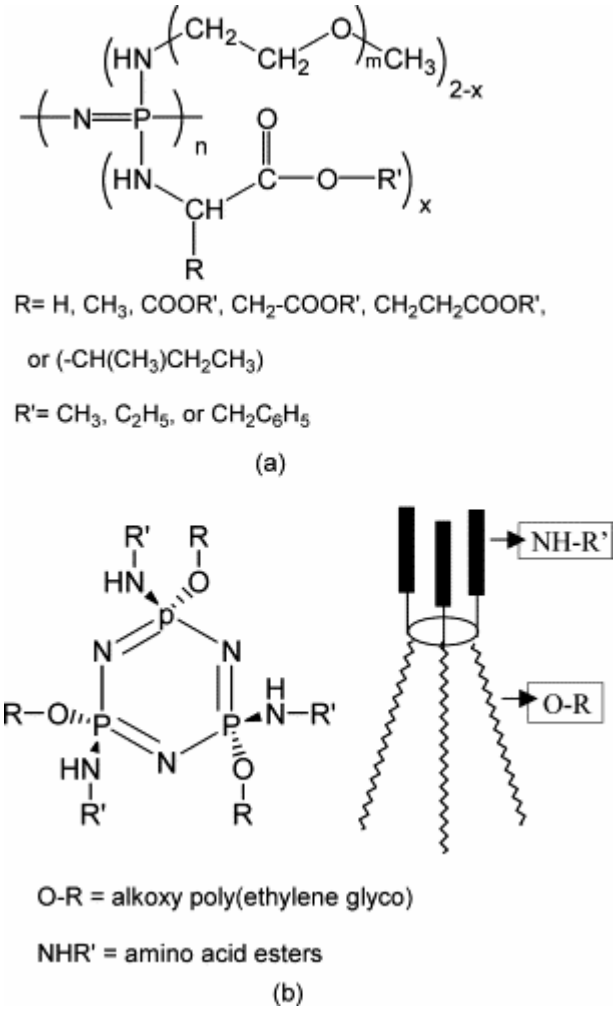

Figure 1- 2 (a) Poly(organophosphazene) [78]

(b) Cyclotriphosphazenes with poly(ethyleneglycol) and amino acid esters [81, 82]

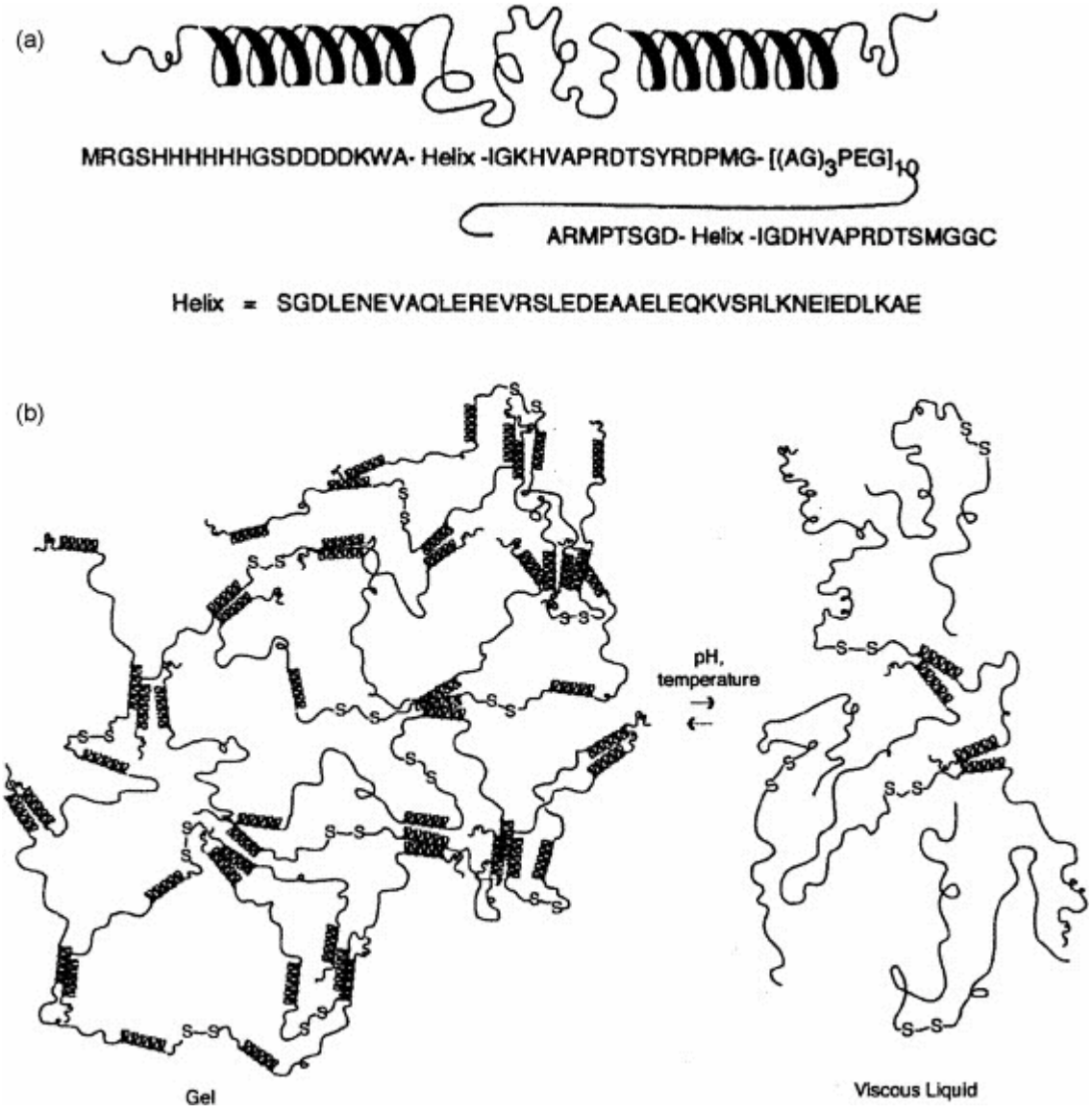

Figure 1- 3 (a) Tri-block copolymer consists of 230 amino acids, 84 of which make up the Helix repeat and 90 of which make up the alanyl glycine rich repeat. Single-letter abbreviations for the amino acid residues are as follows: A, Ala; C, Cys; D, Asp; E Glu; F Phe; G, Gly; H, His; I Ile; K, Lys; L, Leu; M, Met; N, Asn; P, Pro; Q, Gln; R, Arg; S, Ser; T, Thr; V, Val; and W, Trp. (b) Proposed physical gelation of monodisperse tri-block copolymer. [93] Reprinted from Science. 1998; 281, 389-392.

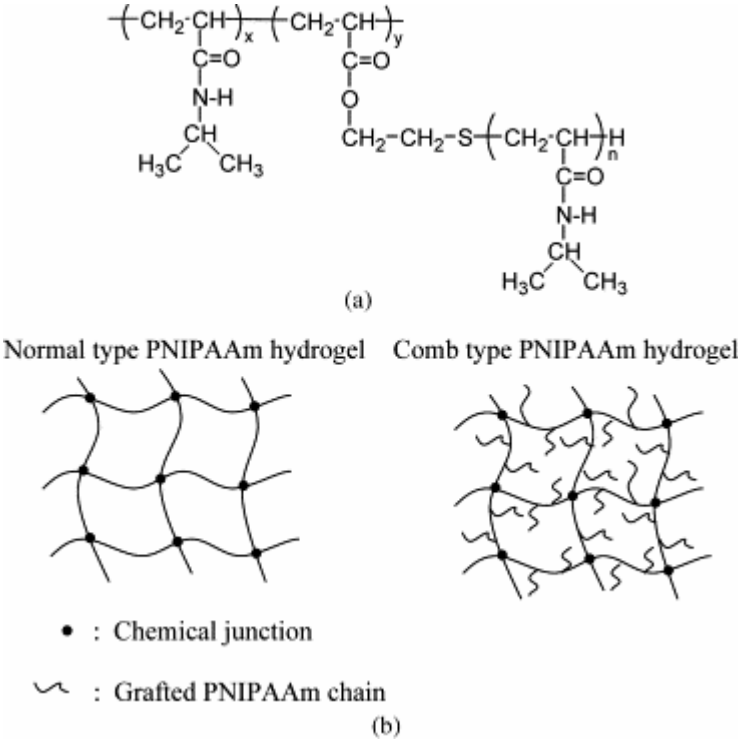

Figure 1- 4 Comb type poly(N-isopropylacrylamide) [100] (a) Chemical structure (b) Schematic forms of normal type and comb type hydrogels

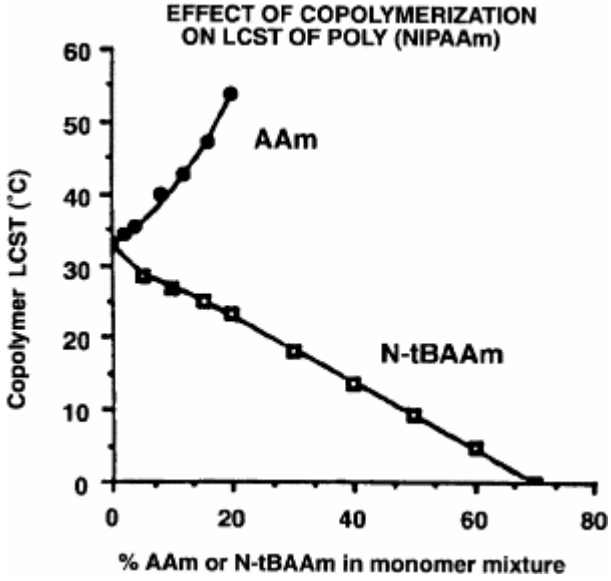

Figure 1- 5 Effect of copolymerization of poly(N-isopropylacrylamide) with acryl amide (more hydrophilic comonomer) and N-test butyl-acrylamide (more hydrophobic comonomer) on the LCST. [6] Reprinted from J Biomed Mater Res. 2000; 52, 577–586.

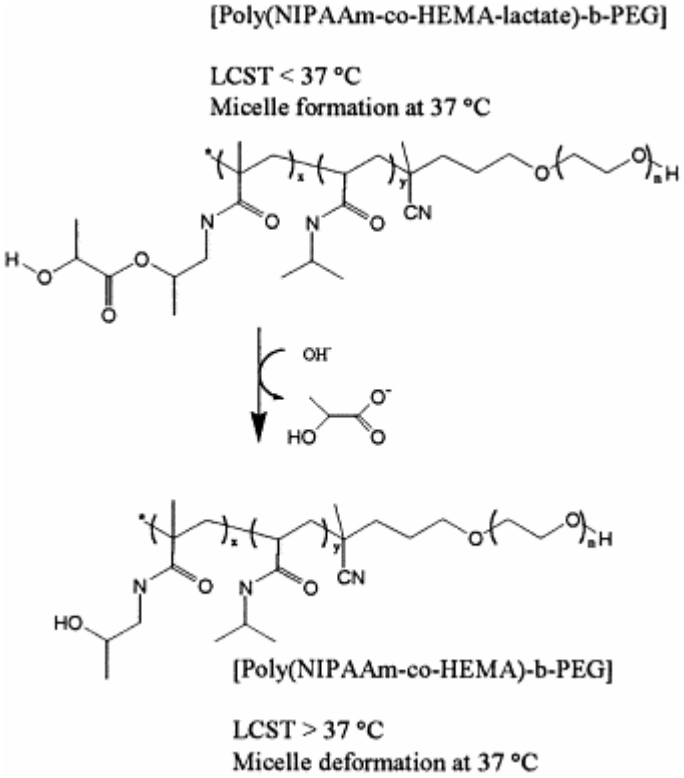

Figure 1- 6　Hydrolytically sensitive micelle formation based on the LCST control [37]

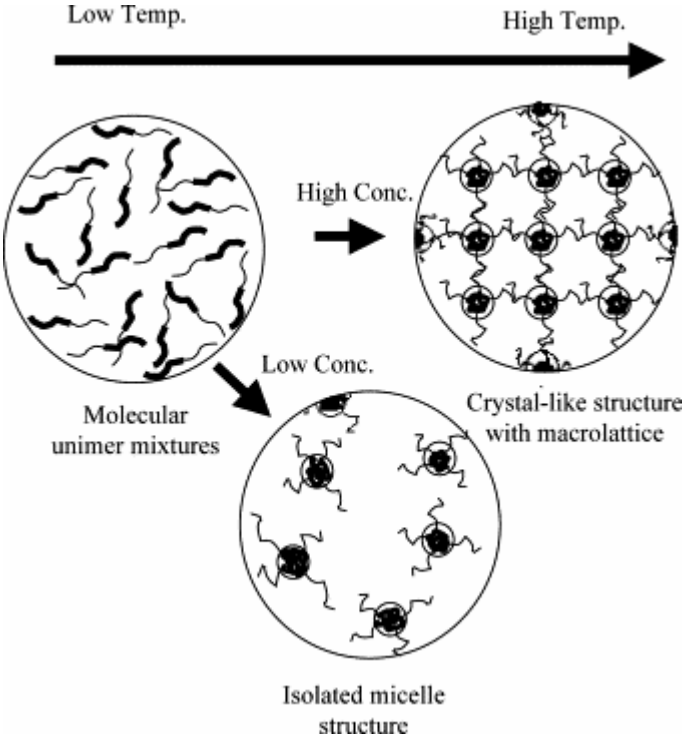

Figure 1- 7 Two transitions of molecular unimer mixtures consisting of amphibilic block copolymers to isolated micelle structure and crystal-like structure with macrolattice by stacking micelles [39]

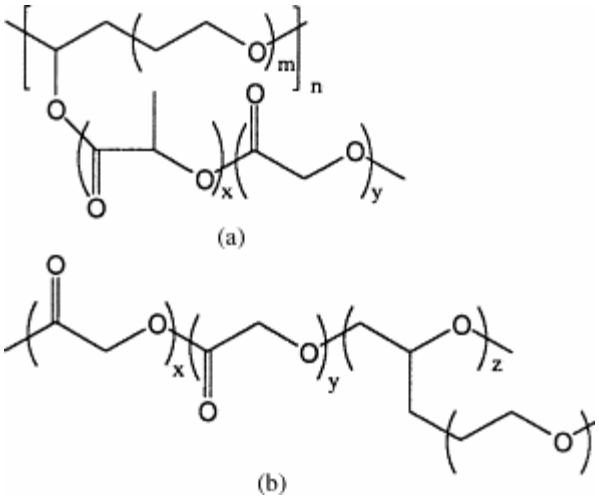

Figure 1- 8 (a) PEG-g-PLGA (PEG backbone) and (b) PLGA-g-PEG (PLGA backbone) [29]

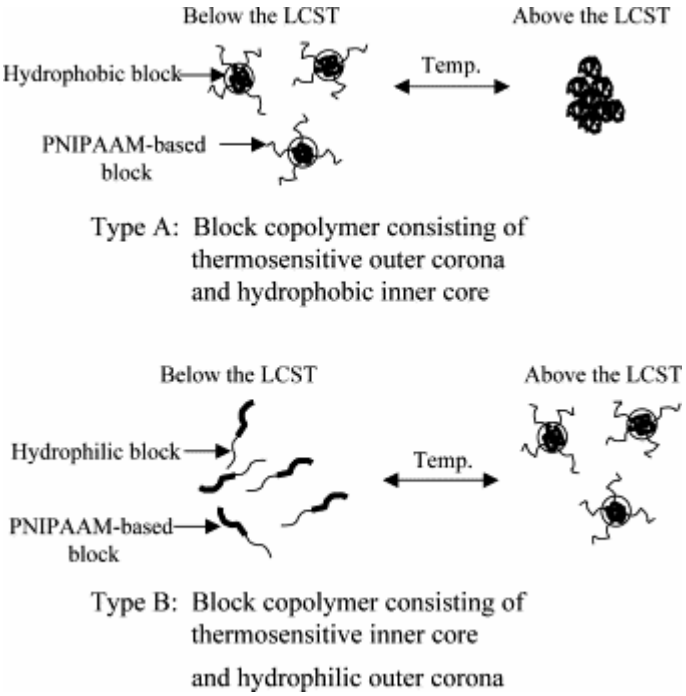

Figure 1- 9 Two types of the micellar structure of a block copolymer containing a temperature responsive polymer segment

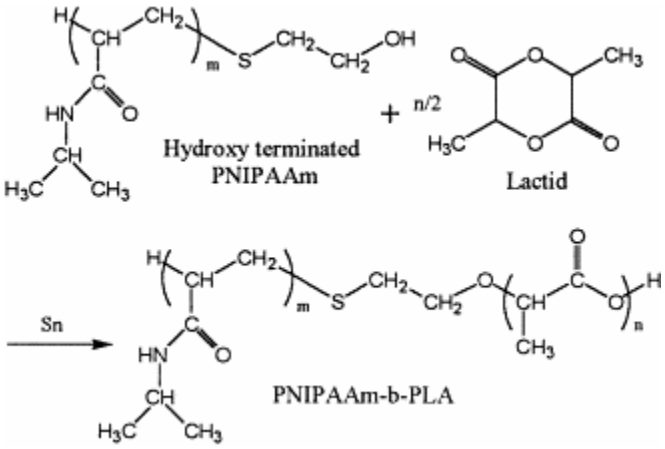

Figure 1- 10 Synthesis of poly(N-isopropylacrylamide-block-DL latide) [112]

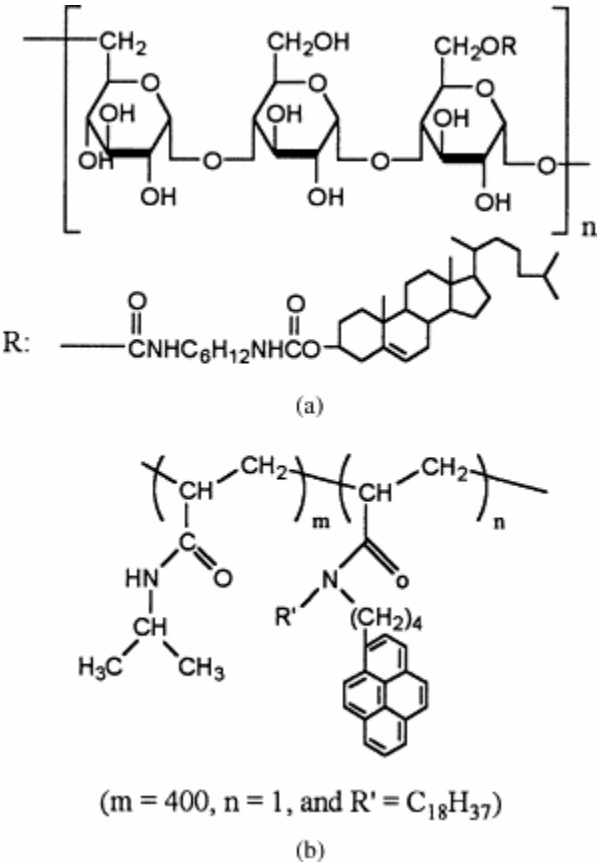

Figure 1- 11 Cholesterol-bearing pullulan and N-[4-(1-pyrenyl)butyl]-N-n-octadecyl acrylamide (PNIPAAm-C18Py) [137]

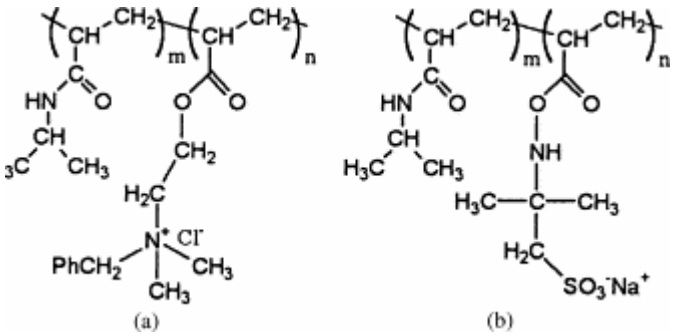

Figure 1- 12 (a) Poly(N-isopropylacrylamide)-co-acrylamido-2methylpropane- sulfonate (b) poly(N-isopropylacrylamide)-co-N,N,N',N'-tetrakis(2-hydroxypropyl) propyl-enediamine [184]

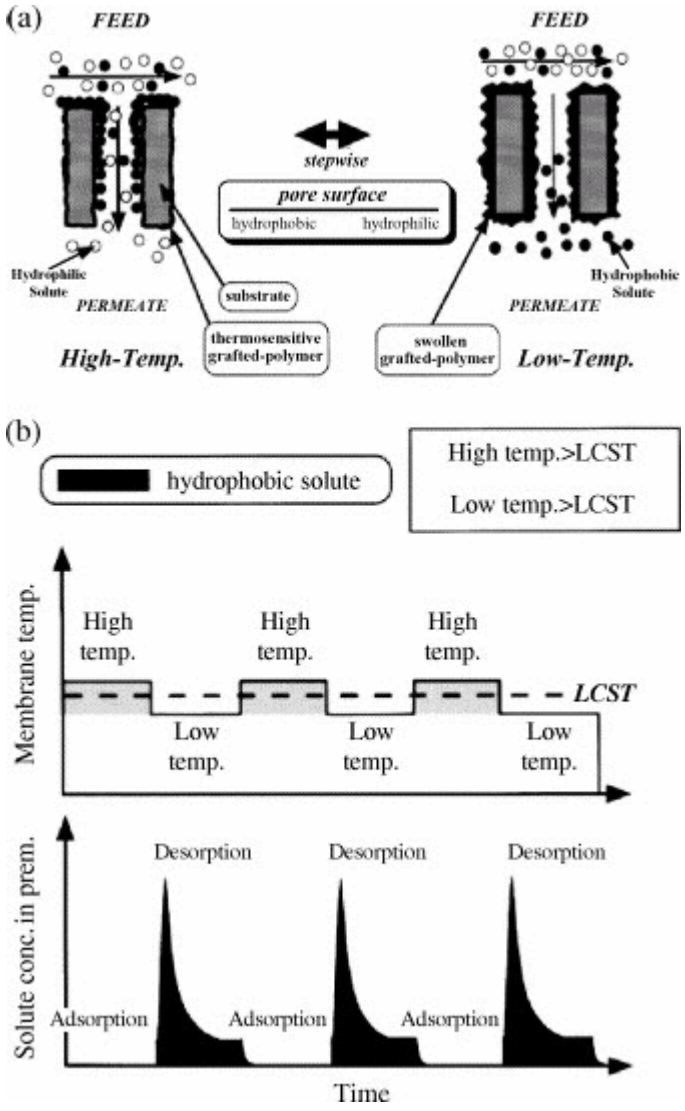

Figure 1- 13 (a) The schematic drawing of separation system of temperature responsive membrane (b) Solute concentration in the permeate. [150] Reprinted from Ind Eng Chem Res. 2000; 39, 2491-2495.

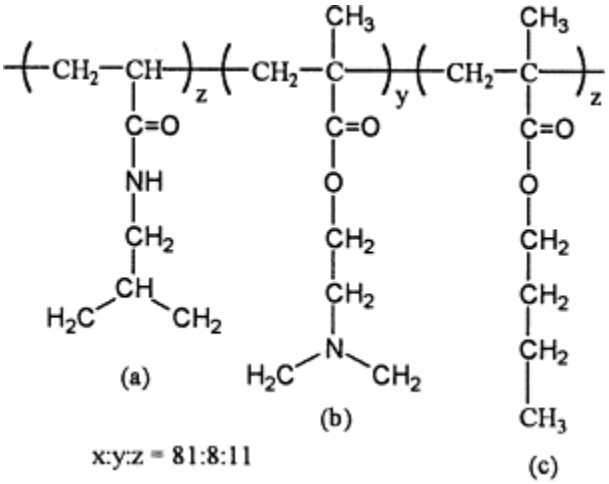

Figure 1- 14 The chemical structure of temperature responsive copolymer for gene carrier. The LCST is 21 °C. [50] (a) N-isopropylacrylamide (NIPAAm): Temperature responsive moiety (b) N,N'-dimethyl aminoethyl methacrylate (DMAEMA): Cationic amines bind an anionic DNA (c) butylmethacrylate (BMA): Hydrophobic moiety.

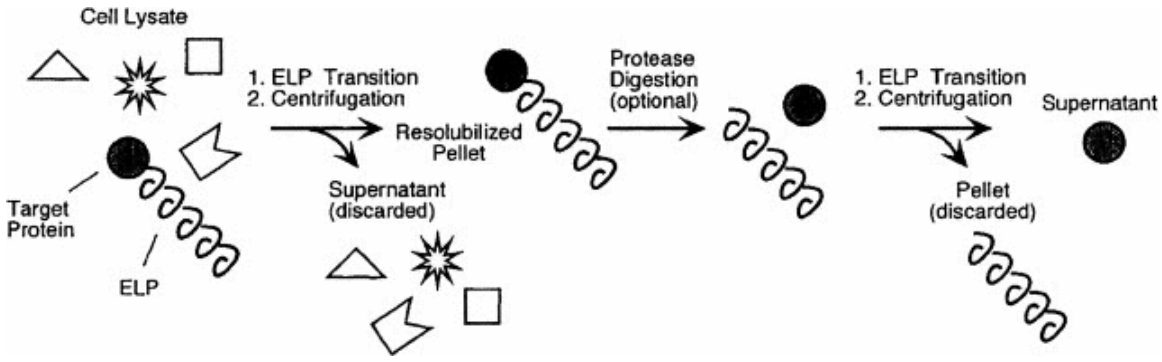

Figure 1- 15 Schematic illustration of inverse transition cycling (ITC) purification scheme. The aggregated ELP fusion protein above the Tt is separated by centrifugation. After discarding supernatant, the pellet is resolubilized by cooling to below its Tt. The fused ELP tag can be removed by cleavage at a specific protease recognition site engineered between the ELP tag and the target protein. The purification of the cleaved ELP follows another round of ITC. The purified target protein is obtained in the supernatant above Tt. [95] Reprinted from Biotechnol Prog. 2001; 17, 720-728.

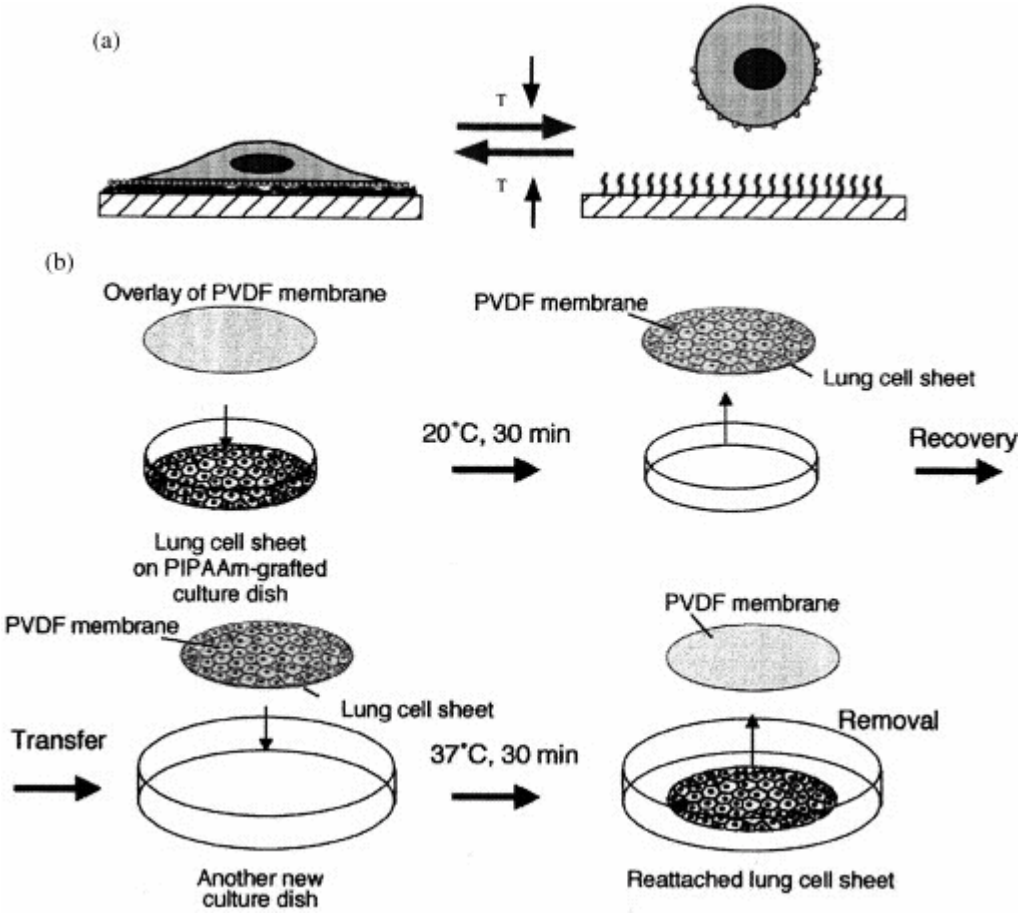

Figure 1- 16 Schematic illustration of temperature responsive poly(N-isopropylacrylamide)-grafted cell culture dish (a) The cells began to detach from the hydrophilic and expanded poly(N-isopropylacrylamide) surface below 32 °C (right in (a)). Small spheres on the cell surfaces depict extracellular matrix proteins mediating cell adhesion to the surfaces. [53] Reprinted from Biomaterials. 2001; 22, 1213-1223. (b) Schematic representation of lung cell sheet transfer from poly(N-isopropylacrylamide) grafted dish to virgin dish. [55] Reprinted from Biomaterials. 2002; 23, 1121 – 1130.

2. Gelatin/Silk Fibroin Protein-based Hydrogels Utilizing β-Sheet Conformation as Cross-Links:

2.1. Characterization of Thermal, Rheological Properties and Temperature Responsive Reversible IPNs/semi-IPNs Transitions

Abstract

Novel protein-based complex hydrogels were prepared by blending gelatin (Gel) with Bombyx mori silk fibroin (SF) and introducing β-sheet conformation of SF in their complex networks. The influence of solvent-induced SF crystallization on the properties and structure of these binary protein complexes was determined as functions of blend composition and preparation history. Rheological tests confirmed that the fine β-sheet crystalline structure successfully governed the Gel/SF complex networks, increasing their viscoelastic properties and sustaining their physical form as hydrogels even at body temperature. The helix-coil transition of gelatin in the Gel/SF complex hydrogels was determined by DSC and rheological tests to be reversible between ambient and body temperatures, so that these hydrogels exhibit reversible IPNs/semi-IPNs transition. This reversible temperature-responsive conformational change of gelatin molecules in Gel/SF complex hydrogels could promote an abrupt swelling increase and a temperature-triggered protein release from the networks at body temperature, which would be utilized for a targeted drug delivery. It is anticipated that these blends in the form of binary protein hydrogels will be useful for smart drug-delivery devices and bioadhesive films for wound tissue, such as for drug release within wound care systems. Also, β-sheet crystalline

networks of SF could be utilized to develop biocompatible IPNs or semi-IPNs with other functional synthetic polymers as well as biopolymers.

2.1.1. Introduction

Hydrogels are formed by three-dimensional networks of polymer chains, where some parts are solvated by water molecules, while other parts are chemically or physically linked with each other. This structure gives an interesting property that they swell, but do not dissolve in an aqueous environment. Hydrogel applications have been explored for biomedical materials, such as contact lenses [1], scaffolds for tissue engineering [2], controlled release of drug [3], actuators [4], and chromatography [5]. However, many bio-related applications in hydrogel forms are demanding more biocompatibility and biodegradability.

Protein based hydrogels have advantages not only in the food and cosmetic industry [6, 7], but also in biomedical applications such as drug delivery systems [8], sealant for vascular prostheses [9] or artificial tissue matrix [10, 11] due to its biocompatibility, biodegradability and nonimmunogenic properties.

Gelatin is a protein that is obtained by breaking the triple-helix structure of collagen into single-strand molecules. The gelation of gelatin originates from its tendency to reform the triple-helix structure of collagen. Gelatin is a thermally reversible hydrogel, which means that it forms gels in aqueous solution by cooling below around 30°C as the chains transform their conformations from random coil to helix, during which aggregation is promoted and a physical network occurs [12].

However, as the physical network breaks down at higher temperature, gelatin hydrogels have weak thermal and mechanical stability over different temperature ranges (e.g. body temperature 37°C). To overcome this problem, many studies have concentrated on chemical cross-linking by introducing small chemical agents such as glutaraldehyde [13], or by modifying gelatin with polymerizable monomers such as methacrylamide [14], but the toxicity of these cross-linking chemicals still remains as a problem.

Silk fibroin (SF) is an excellent candidate as a biomedical material, because it has good mechanical strength in the wet state [15], biocompatibility for the growth of cells [16], high dissolved-oxygen and water-vapor permeability [17] and resistance against enzymatic degradation [18]. From these benefits, the applications for biomedical fields has been suggested for surgical sutures [19], cosmetics [20], enzyme immobilization [21], wound covering materials [22], substrate for cell culture [16], controlled drug-delivery carriers [23], and scaffolds for tissue engineering. [15]

Recently, our laboratory discovered a novel salt system composed of calcium nitrate and methanol as a solvent of silk fibroin [24, 25]. When as-cast SF film is immersed in an organic solvent such as methanol, the effect of crystallization of SF was investigated by observing the change from random coil to β-sheet conformation (silk II) [25]. The silk II crystalline structure grows by treatment with a solvent having a dehydration action.

In this study, these two proteins were blended at different ratios and their as-cast films were prepared. Aqueous methanol mixtures were used for inducing β-sheet conformation of SF as permanent physical cross-links in the Gel/SF complex networks. The conformational

and thermal studies of the complex films were investigated to elucidate the structure and property of the Gel/SF complex networks. Thermoreversible thermal and rheological properties of the complex hydrogels, which would be caused by conformational changes of gelatin in Gel/SF complex hydrogels, were examined before and after inducing β-sheet conformation. The temperature responsive IPNs (Interpenetrating polymer networks)/semi-IPNs transition in the developed Gel/SF complex hydrogels could lead to smart materials for drug delivery and as bioadhesive film.

2.1.2. Experiments

2.1.2.1 Materials

Grade 5A raw silk with an average denier of 20.86 produced in Brazil by the Fiaçào de Seda Bratac S.S. was used. Gelatin (Type A from porcine skin, 175 bloom) was purchased from Sigma. All other chemicals used were purchased from Fisher or Aldrich, and used directly without further purification.

2.1.2.2 SF solution preparation

SF solution was prepared by following a previously published method [25]. The dried *Bombyx mori* silk was degummed with 0.25 % w/v sodium lauryl sulfate and 0.25% w/v sodium carbonate in boiling water, bath ratio of 1:10(w/v), for 1 h. The remaining silk fibroin was then removed from the boiling water and thoroughly washed in deionized water. The serine fraction was calculated as 0.229. The dried SF (10 wt %) was dissolved in $Ca(NO_3)_2$-$4H_2O$/MeOH 75/25 w/w solution. The SF solution was dialyzed with cellulose membrane tube (MWCO 6,000-8,000) for 4 days by changing the deionized water daily.

The concentrations of the dialyzed silk fibroin solutions were around 4.2 w/w %. The concentration was controlled as 4 w/w % by adding deionized water into the dialyzed SF solution.

2.1.2.3 Blending and film preparation

The dried gelatin was suspended in deionized water (4 w/w %) and the suspension was dissolved by heating it at 40°C with stirring. The composition of Gelatin and SF were controlled by mixing the SF solution and the gelatin solution, and the prepared samples are listed in Table 1. All films were prepared by solvent casting on polystyrene pettri dish at 10 °C and stored over one week in desiccators under vacuum before use. Clear, colorless and flexible films (0.2 mm thickness) were obtained.

Table 2-1 Preparation of gelatin and silk fibroin blends

	Weight fraction	
	Gelatin[1]	Silk Fibroin[2]
Gel	1.0	0.0
Gel/SF 9/1	0.9	0.1
Gel/SF 3/1	0.75	0.25
Gel/SF 3/2	0.6	0.4
Gel/SF 1/1	0.5	0.5
Gel/SF 2/3	0.4	0.6
Gel/SF 1/3	0.25	0.75
SF	0.0	0.0

1: Gelatin 4 w/w % aqueous soltution
2: SF 4 w/w % aqueous soltution

2.1.2.4 Treatment of films in methanol/water system

SF film and Gel/SF blend films were treated with methanol and methanol/water mixtures at 20 °C to induce β-sheet conformation of SF in the presence of the triple-helix structure

of gelatin. The films were immerged in methanol/water mixture (methanol/water weight ratios: 100/0 (Me100), 75/25 (Me75), 50/50 (Me50), 25/75 (Me25), 10/90 (Me10)) for 5 min to 600 min at 20 °C. If there is no described condition, the films were treated in Me75 at 20 °C for 2 hours.

2.1.2.5 X-ray studies

The Wide Angle X-ray Diffraction (WAXD) curves of the untreated and treated Gel, SF, and Gel/SF films were obtained with a Seimens type F X-ray diffractometer. Ni-filtered Cu Kα radiation was used for the X-ray source with 35 kV voltage and 25 mA current. All scans were performed from 5 ° to 40 ° (2θ) at a speed of 1.0°/min.

2.1.2.6. FTIR studies

FTIR spectra of all samples were obtained using Nicolet 510P FT-IR Spectrometer with OMIIC software. Attenuated Total Reflectance (ATR) accessory was used for the spectra of as-cast films and methanol/water treated films. All scans were performed with an average of 32 repeated scans and 4 cm^{-1} scan resolution.

2.1.2.7 Differential scanning calorimetry

Calorimetric thermograms were obtained using the Perkin Elmer Diamond DSC equipped with Perkin Elmer intercooler 2P. Before all measurements, temperature and enthalpy were calibrated with indium (T_m = 156.60 °C and delta ΔH = 28.45 J/g). The thermograms of air-dried films were scanned from 25 °C to 150 °C at a rate of 20 °C/min. The DSC traces of the swollen hydrogels were obtained as follows; the complex films were swollen in deionized water at 5 °C for 1 day and were wiped with tissue paper. After 5 min

holding time at 5 °C, the samples were heated to 60 °C, and cooled to 0 °C at a rate of 5 °C/min.

2.1.2.8 Thermogravimetric Analysis

Thermal degradation measurements were performed using a Perkin Elmer TGA Pyris 1^{TM}. As-cast films and treated films in Me75 for 2 hours of ca. 3-4mg were cut and mounted onto the sample holder. All samples were heated at the rate of 50°C/min under N_2 purging until the TGA curves reach a plateau region, where the absorbed water should be thoroughly evaporated, and then weighed as their initial weights. Then, all samples were heated up to 600ºC at the rate of 50ºC/min under nitrogen atmosphere.

2.1.2.9 Rheological Measurements

The viscoelastic properties were investigated by dynamic shear oscillation measurements at small constant shear strain. These measurements were carried out with a REOLOGICA rheometer (REOLOGICA Instruments AB), using parallel plates of 25 mm diameter. The rheological data of the untreated Gel/SF complex gels (10 w/v %) and the treated Gel/SF gels are measured by increasing and then decreasing temperature at the rate of 2.0 °C/min with temperature ranges from 5 °C to 50°C and from 50°C to 5°C, respectively, at constant frequency of 1 Hz and constant shear strain of 1.0×10^{-3}. The series of Gel/SF blend solutions (10 w/v %) are mounted between parallel plates with 0.5 mm gap at 40 °C and cooled to 5 °C. With cooling, the solutions became gels. After holding samples at 5 °C for 5 min, the rheological tests of the untreated complex gels were performed. The treated Gel/SF films were swollen at 5 °C for 1 day, wiped with tissue paper and mounted between

parallel plates at 5 °C. After a 5 min holding time, the rheological data of the treated gels were obtained. The normal force loaded onto the treated hydrogels was automatically adjusted to 2.0 N.

2.1.3. Results and Discussion

2.1.3.1 Induced β-sheet crystalline networks of SF in Gel/SF blends

The conformational change of regenerated SF films from random coil conformation into β-sheet structure has been reported after treatment with organic solvents such as methanol, ethanol, and isopropanol [25]. The conformational change might come from a dehydration action of methanol upon the random coil SF molecules, resulting in reorganization of SF conformations to induce intra- or intermolecular secondary bonds. Here, it is intriguing to investigate the possibility of solvent-induced SF crystallization in Gel/SF blends, because the topological constraints by entanglements could block the conformational change of SF molecules. The WAXD curves of SF, Gel, and Gel/SF 2/3 are shown in Figure 2-1-1 and compared between before and after treatment. The dried as-cast films were treated in Me75 for 2 hours. A broad peak at 2θ = 20° in regenerated SF was reported as a typical characteristic pattern of an amorphous structure. A major peak at 2θ = 21° and two minor peaks at 2θ = 9° and 24° are shown in a methanol treated SF, assigned as characteristic peaks of a β-sheet crystalline structure [25]. In our WAXD curves, the treated SF shows a strong peak at 2θ = 21° and small peaks at 9 ° and 24 °, indicating the induced β-sheet conformation of SF, but untreated SF exhibits a pronounced amorphous curve. By contrast,

the treated gelatin film shows an unchanged WAXD curve, which means that the collagen-like structure of gelatin is not affected by methanol treatment. The untreated Gel/SF 3/2 and 2/3 do not have characteristic peaks for SF crystalline structure, but show a peak at 2θ = 7.8°, indicating that the gelatin component in Gel/SF 3/2 and 2/3 adopts a triple helix structure as pure gelatin film [26]. After Gel/SF 3/2 and 2/3 films are treated in Me75, their WAXD curves exhibit peaks at 2θ = 21° and 24°. This result indicates that β-sheet crystalline structure of SF is successfully introduced in gelatin networks, and that the gelatin triple-helix structure does not constrain the conformational change of SF.

2.1.3.2. Effect of treatment conditions on Gel/SF structure

To investigate the effect of treatment time on inducing β-sheet crystalline structure of SF in Gel/SF blends, the FTIR spectra of Gel/SF blends are obtained according to treatment time from 5 min to 600 min, and compared with those of Pure SF. Figure 2-1-2-a) shows FTIR spectra of SF as-cast film and treated SF films for different periods of time in Me75. The FTIR spectrum of SF fiber (spectrum (7)) exhibited evidence of β-sheet conformation at each amide peak. The amide I peak, the amide II peak, the amide-III peak were observed at 1625 cm^{-1}, 1520 cm^{-1}, 1265 cm^{-1} respectively. The SF fiber obtained after removing the outer sericins part of silk worm fiber has been reported to consist of silk II structure, which contains β-sheet crystal [27]. The FTIR bands of SF fiber support the existence of their Silk II structure. The amide I peak, which is related to the stretching of C=O groups in SF back bone, was shifted from 1655 cm^{-1} to 1625 cm^{-1}, and the amide II peak, which originates from the N-H deformation in SF amide groups, shifted from 1545 cm^{-1} to 1520 cm^{-1} at all

treatment times. Also, in all spectra for the treated SF films, a new amide-III peak for the vibration involving O-C-O and N-H was observed at 1265 cm^{-1} with the same intensity. The regenerated SF film did not show any evidence of β-sheet crystalline structure in its FTIR spectrum, while all films treated in Me75 during all tested time periods exhibited the absorption bands related to β-sheet structure at 1625 cm^{-1} (amide I), 1520 cm^{-1} (amide II) and 1265 cm^{-1} (amide III) [24]. Figure 2-1-2-a) indicates that most of the β-sheet formation occurs during the first 5 minutes of treatment. By contrast, gelatin films showed no peak shift in the FTIR spectrum after treatment in Me75 for 2 hr (Figure 2-1-2-b)). The FTIR spectrum of gelatin exhibits the peaks at 1645 cm^{-1} and 1555 cm^{-1} attributed to amide-I and amide-II peaks, respectively.

In Figure 2-1-2-c), FTIR spectra were obtained to investigate the effect of treatment time period for inducing β-sheet conformation of SF molecules in Gel/SF 3/2 complex film. Spectrum (1) confirms that the Gel/SF 3/2 complex structure bears the random coil structure of SF molecules, since amide I and amide II peaks were observed at 1650 cm^{-1} and 1550 cm^{-1} and amide-III peak at around 1270 cm^{-1} was not seen. Here, it is notable that amide-I (1650 cm^{-1}) and amide-II (1550 cm^{-1}) peaks of Gel/SF 3/2 are shown between those of the as-cast SF (1655 cm^{-1} and 1545 cm^{-1}) and those of the as-cast gelatin (1645 cm^{-1} and 1555 cm^{-1}). When blended polymers are compatible, intermolecular interactions occur, resulting in FTIR spectra of the blends different from those of the pure polymers. This result implies that the two protein, gelatin and SF, show good compatibility. In spectrum (2) to (6), all films (Gel/SF 3/2) treated in Me75 for different time periods showed the

absorption bands related to β-sheet structure at 1628 cm^{-1} (amide I), 1530 cm^{-1} (amide II) and 1267 cm^{-1} (amide III). These results show the same tendency as the pure SF films treated in methanol/water (75/25 w/w) in Figure 2-1- 2-a).

Besides treatment time, methanol/water ratio in the treatment bath was reported to affect the conformational change of pure SF film [28]. This led to an investigation of the conformational change of SF in Gel/SF blends with treatments in different methanol/water ratios. Figure 2-1-3 shows FTIR spectra of Gel/SF 1/1 complex films which were treated with different ratios of methanol/water. The shift of amide I and II peaks is observed and a new peak of amide III appears with the treatment as shown in Figure 2-1-2. This indicates that the structure of SF in Gel/SF complex films is changed from random coil conformation to β-sheet conformation when the Gel/SF complex films are treated with methanol and various ratios of methanol/water mixtures. Interestingly, Me75 and Me50 induces a more prominent shift of the amide I and amide II peak from random coil (1655 cm^{-1} and 1545 cm^{-1}) to β-sheet conformation (1625 cm^{-1} and 1530 cm^{-1}) rather than pure methanol does. The amide III peak of the β-sheet conformation is also stronger at 1267 cm^{-1}, when the films are treated in Me75 and M50. These results are coincident with a previous report for pure SF films, where it was found that a methanol/water mixture is more effective in inducing β-sheet conformation of regenerated SF film than pure methanol [18]. These FTIR spectra indicate that the treatment in methanol/water mixture rather than in pure methanol is more effective to induce β-sheet conformation of SF in the Gel/SF complex films as in SF film. However, the effect of methanol/water mixture on inducing β-sheet conformation

decreases as water content increased higher than 50 wt %. In the cases of Me25 and Me10, the random SF conformation is still predominant, as observed in FTIR spectra (5) and (6). Therefore, the effect of water content in the treatment bath on inducing β-sheet conformation of SF in Gel/SF complex should show a maximum at around 25 wt %, and decrease with higher water content. In both cases of pure SF and Gel/SF, small water content could make the networks swollen and give free space for SF chains easily to rotate, so that the methanol might easily diffuse and induce the conformational change of SF molecules. However, the dehydration action by methanol should not be as effective, when the water content in the methanol/water mixture is too high.

2.1.3.3. DSC studies of Gel/SF complex films

The thermal properties of proteins such as SF and gelatin have been reported to be very sensitive to moisture content, which acts as a plasticizer to decrease their thermal transition temperatures. Agarwal N. et al reported that T_g of regenerated SF films were shifted from 178°C for dry SF to 39°C for an 18 wt % moisture content [29]. The glass temperature of gelatin was also reported to decrease approximately from 217°C for dry gelatin to 0°C for 25 wt % of moisture [30].

All Gel/SF complex films actually contain some extent of moisture at atmosphere conditions, at which these materials would be used. Figures 4 display DSC heating curves of air-dried SF, Gel and Gel/SF complex as-cast films (Figure 2-1-4-a)), and their treated films (Figure 2-1-4-b)), which contain approximately 10 wt% moisture. The respective moisture contents of the samples were measured by TGA and listed in the caption of Figure

2-1-4. The glass transition temperature (T_g) and the crystallization temperature (T_c) of air-dried SF as-cast film were at 78°C and at 120°C, respectively. These values are respectively 83°C and 85°C lower than those of dried SF as-cast film, whose T_g and T_c were 181°C and 227°C in our previous report [25].

The air-dried gelatin containing 13.4 wt % of water shows its helix-coil transition temperature (T_d) at 103°C. Water acts as plasticizer in various hydrophilic polymers such as poly(vinyl alcohol), poly(vinyl pyrrolidone), polyacrylamide and gelatin as well [31-34]. In these reports, water did not crystallize below a critical weight fraction (C*) of water and the non-crystalline water acted as plasticizer to decrease the glass transition temperature. In fact, gelatin molecules need water molecules to form triple-helix crystals (gelatin-water mixed crystal) and shows a eutectic melting temperature with the bound water, even though the difference between melting points of pure gelatin and pure water is as large as 230°C [34].

In Gel/SF complex films, water also acts as a plasticizer to shift all transition peaks to lower temperatures, corresponding to the shifts of transition peaks in pure SF and gelatin films. The more gelatin content the complex films have, the more water content they contain. This suggests that gelatin is more hydrophilic than SF. SF-rich complex as-cast film (Gel/SF 1/3) exhibits not only T_g and T_c of SF content, but also T_d of gelatin. However, the early range of the exothermic peak (T_c) of SF for crystallization is merged into the end range of the endothermic peak of gelatin (T_d). The T_c of SF is shown at 118.5°C and the T_d of gelatin is displayed at 114.2°C, representing a 4.3°C difference between two peaks.

Actually, in the DSC thermograms of dried pure SF and gelatin films, both exothermic and endothermic peaks of respective pure SF and gelatin have been found within a close range near around 220~230°C [25, 34]. Therefore, partial merging of the two peaks is an expected result.

In the case of gelatin-rich complex film (Gel/SF 3/1), the exothermic peak of SF (T_c) is not detectable. The endothermic peak of gelatin could be recognized in SF-rich complex film, but the exothermic peak of SF could not be detected in gelatin-rich complex film, since the merged exothermic peak of SF is considerably smaller than the exothermic peak of gelatin. The T_g of SF could not be detected, either.

The treated Gel/SF complex films show only the endothermic peaks for gelatin helix-coil transition without the transition peaks shown by the thermal transition behaviors related to SF bearing the random coil structure and a small amount of α-form crystals. These DSC data indicate that the methanol/water mixture promotes β-sheet conformation of SF not only in pure regenerated SF but also in gelatin-SF complex blends.

2.1.3.4. Improved thermal stability of Gel/SF with β-sheet structure of SF

TGA thermographs of as-cast Gel/SF blend samples and the treated Gel/SF blend samples are shown in Figure 2-1-5 and the related analysis corresponding to these TGA curves are listed in Table 2-2. TGA curve of gelatin was not shown in Figure 2-1-5, but the analyzed data are listed in Table 2-2. The first degradation region (around 300°C ~ 420°C) should be related to the decomposition of side chain groups of both proteins, while the second degradation region (around 420°C ~ 600°C) should be governed by the

decomposition of the main backbone of the protein polymers.

In the case of the residue at 550°C, at which most side groups should be degraded, the untreated SF exhibits 44 % of residue and the treated SF showed 45.3 % of residue, while gelatin showed 31.4 %. These results are interpreted by considering the different composition of amino acids in both proteins. SF is mainly composed of the amino acid units bearing short side chain groups such as Glycine and Alanine, which contains H- and CH_3- groups in their side chains [35]. On the other hand, gelatin is composed of the amino acids bearing relatively longer and heavy side chains such as proline and hydroxyproline [36]. The Gel/SF complex films exhibit the middle weight % of residue at 550°C.

Table 2-2 TGA data of Silk Fibroin, Gelatin and their complex films.

	Onset Temp. (°C)	Temp. at max. rate (°C)	Maximum rate (%/°C)	Residue at 380 °C (%)	Residue at 550 °C (%)
SF	323	377	0.39	74.8	44.0
SF Treated[1]	337	392	0.47	78.5	45.3
Gel/SF 1/3	334	373	0.43	74.0	39.0
Gel/SF 1/3 Treated	342	388	0.59	76.8	39.7
Gel/SF 3/1	331	379	0.50	70.3	31.6
Gel/SF 3/1 Treated	348	391	0.60	75.1	34.4
Gelatin	340	378	0.52	73.4	31.4

1: treatment condition; in Me75, at 20 °C, for 2 hours.

The Gel/SF complex films show the middle weight % of residue also at 380°C, at which

the degradation of samples proceeds with approximately maximum rates. The treated SF and the treated Gel/SF complex films show higher weight % of residue than the untreated as-cast samples at 380°C as well as 550°C, which means that the thermal stability of SF and Gel/SF complex films increased surely due to their conformational changes from random coil to β-form. The residue differences at 380°C are more remarkable than at 550°C. This indicates that the conformational change of SF affects the thermal stability in the first degradation region, where the side groups of proteins are rapidly degraded. However, after most side chain groups of SF are degraded, the secondary structure of SF might be a less significant factor to the thermal stability of SF and Gel/SF complex films.

Onset temperature, maximum degradation rate and the temperature at maximum rate are related to the first degradation region. The onset temperature of as-cast SF is shifted from 323°C to 337°C after the treatment. When the SF molecules form β-sheet structure, the intermolecular secondary bonds (parallel hydrogen bonding, and vertical Van der Waals force) should increase the activation energy needed to break the covalent bonds in side chain groups of SF. It is also noted that the onset temperature of gelatin (340°C) is closer to that of the treated SF (337°C) than that of the untreated SF (323°C). Gelatin forms a triple-helix structure based on hydrogen bonding among three gelatin molecular chains and water molecules, and the rod-like structures with triple-helix conformation aggregate and form a crystalline structure [36]. Therefore, the onset temperature of gelatin might be higher than that of the untreated SF bearing random coil amorphous structure.

Maximum degradation rate (Max. rate) and temperature at maximum degradation rate

(Temp. at max. rate) are other thermal characteristics influenced by the conformational structure of protein molecules. If Max. rate (negative value) and Temp. at max. rate are elevated, it means that the degradation mechanism occurs more sharply at higher temperature and that the resistance against the breaking force induced by thermal energy becomes higher. After treatment of SF and Gel/SF, all samples exhibited increased Max. rate (higher as much as 0.18 %/°C for SF, 0.16%/°C for Gel/SF 1/3, 0.10%/°C for Gel/SF 3/1) and the increased Temp. at max. rate (higher as much as 15°C for SF, 15°C for Gel/SF 1/3, 12°C for Gel/SF 3/1). These results indicate that the more crystalline structure the protein has, the higher Max. rate and Temp. at max. rate the protein samples show, since secondary bonds like hydrogen bonding or Van der Waals force should increase the thermal stability of these proteins. Interestingly, the treated Gel/SF complex samples shows higher onset temperatures and Max. rates than those of both the treated SF and gelatin samples. The SF β-form crystalline networks restrict the gelatin triple helix crystalline network or visa versa so that this restriction force could act against thermal breaking forces. However, the SF crystalline networks should restrict the gelatin networks more than the gelatin does, because the gelatin rich-composition complex (Gel/SF 3/1) showed higher onset temperature and Max. rate than the SF rich-composition complex (Gel/SF 1/3).

2.1.3.5. DSC studies of Gel/SF complex hydrogels

Figure 2-1-6 shows DSC heating curves of Gelatin and Gel/SF complex hydrogels. All Gel/SF complex as-cast films were treated in Me75 for 2 hours to induce non-reversible networks of SF molecules as β-form crystals. The treated Gel/SF complex films and the

dried gelatin film were immersed in deionized water at 5 °C for 24 hours to be swollen. These swollen hydrogels exhibited endothermic peaks, which are associated with the helix-coil transition (or gel-sol transition) of gelatin. Here helix-coil transition can be associated with gel-sol transition, because gel-sol transition is a macroscopical nomenclature and helix-coil transition is a microscopical one. The data for these endothermic peaks are listed in Table 2-3.

Interestingly, Gel/SF 1/3 and 2/3 complex hydrogels exhibit different transition behaviors, compared with gelatin and gelatin-rich complex hydrogels. Gelatin, Gel/SF 9/1, Gel/SF 3/1, and Gel/SF 3/2 hydrogels show their onset temperatures at around 28~29°C and their peak temperatures at around 33~35°C, while Gel/SF 2/3 shows its onset temperature at 32.3 °C and its peak temperature at 45.9 °C.

Table 2-3 DSC heating data of Gelatin and Gel/SF complex hydrogels.

	Onset	Peak	$^{1}\Delta H_d$	$^{2}\Delta H_d^*$
	(°C)	(°C)	(J/g)	(J/g)
Gelatin	28.4	34.8	15.8	15.8
Gel/SF 9/1	28.5	33.0	13.7	15.2
Gel/SF 3/1	29.4	35.0	11.5	15.3
Gel/SF 3/2	28.1	33.1	10.1	16.8
Gel/SF 2/3	32.3	45.9	9.1	22.8

1: heat of denaturation of Gel/SF complex hydrogels

2: real heat of denaturation of gelatin portion in Gel /SF complex hydrogels. $\Delta H_d^* = \Delta H_d/$(gelatin weight ratio in complex films)

The gelatin hydrogel, whose network was chemically cross-linked, had a helix-coil transition peak shifted up to 74°C and a decreased endothermic heat change, depending on the degree of chemical cross-links [37]. In this report, they explained that the shifting of

helix-coil transition to higher temperature and the decreased endothermic heat change might originate from a reduction of bound water and the presence of covalent crosslinks.

Because there are no introduced covalent crosslinks in Gel/SF complex networks, the shift of helix-coil transition temperature might be induced by a reduction of bound water due to the restriction of tight SF β-sheet networks. This result would be in agreement with the role of water associated with the protein in the conformational transition temperature range. In the DSC trace of Gel/SF 1/3 hydrogel, the endothermic peak for triple helix-coil transition of gelatin was undetectable.

The real heat of denaturation of the gelatin portion in gelatin/SF hydrogels (ΔH_d^*) could be calculated by dividing the area of the endothermic peak by the weight ratio of gelatin in the gelatin/SF complex. In gelatin-rich hydrogels, the heat of denaturation of the gelatin portion (ΔH_d^*) of the gelatin/SF complex hydrogels does not exhibit variations in comparison with the ΔH_d of pure gelatin hydrogel. However, Gel/SF 2/3 complex hydrogel showed a higher ΔH_d^*.

In Figure 2-1-7, the DSC cooling curve of Gel is compared with that of Gel/SF 3/1 complex hydrogels to investigate the possibility of reversible coil-helix transition (or sol-gel transition) of gelatin molecules in Gel/SF complex hydrogels. After the hydrogels were heated to 60°C, their cooling thermograms were observed down to 0°C. When the Gel/SF complex hydrogels are heated above the gel-sol transition of gelatin, they are not liquidized (This will be discussed along with rheological tests in the next chapter). The β-form crystalline networks of SF should sustain the physical form of hydrogels. Therefore, it is a

remarkable result that the Gelatin/SF complex hydrogel showed coil-helix transition peak in cooling trace. The gelatin molecules bearing random coil conformation should be encapsulated in the temperature-irreversible SF β-sheet networks and show reversible IPN/semi-IPN transition, even though the weight ratio of SF is smaller than that of gelatin in their complex networks.

The data for these exothermic peaks are listed in Table 2-4. The onset temperature of Gel/SF 3/1 hydrogel was observed at 26.2°C, which was 3.5°C higher than the value of gelatin (22.7°C). The shift of peak temperature was more pronounced than that of the onset temperature. The Gel/SF 3/1 hydrogel peak temperature (19.2°C) was shifted 6.3°C higher, compared with the value of gelatin (13.9°C). The recrystallization of gelatin from random coil to helix occurs earlier and faster during cooling. The real heat of recrystallization of the gelatin portion (ΔH_{rc}^{*}) in Gel/SF 3/1 complex hydrogel does not show appreciable variations in comparison with the ΔH_{rc} of gelatin. Therefore, the SF β-form networks do not disturb the coil-helix transition behavior of the encapsulated gelatin molecules in gelatin-rich Gel/SF complex networks.

Table 2-4 DSC cooling data of Gelatin and Gel/SF complex hydrogels.

	Onset	Peak	[a]ΔH_{rc}	[b]ΔH_{rc}^{*}
	(°C)	(°C)	(J/g)	(J/g)
Gelatin	22.7	13.9	7.9	7.9
Gel/SF 3/1	26.2	19.2	6.3	8.4

a: heat of recrystiallization of Gel/SF complex hydrogels
b: real heat of recrystiallization of gelatin portion in Gel/SF complex hydrogels. ΔHrc*= ΔHrc/(gelatin weight ratio in complex films)

2.1.3.6 Rheological studies of Gel/SF complex hydrogels

Figure 2-1-8 shows the heating traces of the dynamic rhoelogical properties of Gel/SF gels without treatment. The blend aqueous solutions of 10 w/v % were mounted between parallel plates and cooled down to 5 °C, forming gel. The gelation of these solutions implies the formation of physical networks composed of gelatin triple helix structure. Figure 2-1-8-a) represents the comparison for the G' and G'' of gelatin and Gel/SF 1/1 gels. To avoid visible complexity, only G' and G'' of Gel/SF 1/1 gel are compared with those of gelatin gel in Figure 2-1-8-a). The G's of all Gel/SF gels are plotted in Figure 2-1-8-b). Gelatin gel exhibits considerably higher G' than G'' at lower temperature, but over 25~35 °C, the G' and G'' dramatically drop and their values cross over. At the crossover temperature (G'/G'' = 1), the gel network of gelatin is considered to meet a transition to a solution (e.g. gel-sol transition). All Gel/SF gels show rapid drops of their G' and G'' and the curves of G' and G'' cross over as shown in gelatin gel. The gel-sol transition temperatures (G'/G'' =1) gradually decrease with increasing content of SF in the blend solution. The density of triple helix networks should affect the gel-sol transition temperature of the gels. The G' and G'' of gelatin and Gel/SF blend gels at specific temperatures are compared according to the SF weight fraction in Figure 2-1-9-a) (at 20 °C) and b) (at 40 °C). At 20 °C, G' and G'' decrease with more SF content, exhibiting typical S-type curves. At 40 °C, the curves look like noise, but all G'' are higher than G', implying dissolution of the Gel/SF gels like gelatin gel. From the viscoelastic properties of the Gel/SF gels, it can be noted that only gelatin networks form in these Gel/SF system.

The rheological properties for the treated Gel/SF complex hydrogels we investigated and compared with the untreated Gel/SF blend gels to observe the effect of the induced SF β-sheet crystalline networks in the Gel/SF complex hydrogels. Figure 2-1-10-a) shows the heating traces of the dynamic rheological properties, comparing the treated Gel/SF complex hydrogels with the treated gelatin hydrogel. The treated gelatin and Gel/SF films were immersed in pure water at 5 °C for 24 hr and the swollen hydrogels were mounted on the rheometer. The treated gelatin hydrogels shows the crossover of G' amd G'' curves at the same temperature as untreated gelatin gel shown in Figure 2-1-8, indicating the treatment does not affect the breakdown of gel networks in pure gelatin gel. In the treated Gel/SF 9/1 hydrogels, only 10 wt % SF content prevented the crossover of G' and G'' curves, indicating the preservation of gel property even at higher temperature. With G' higher than G'', the treated Gel/SF 9/1 shows the decreasing ramps of G' and G'' curves at the gel-sol transition temperature of gelatin. Moreover, the G' and G'' of the treated Gel/SF 9/1 hydrogels are higher than those of gelatin. For the comparison of rheological properties of the treated Gel/SF hydrogels according to SF weight fraction, the G' of the treated Gel/SF hydrogels are plotted in Figure 2-1-10-b). Here, only the G' curves are plotted and compared for the sake of clarity. The G' of the treated Gel/SF hydrogels increases with more SF content, and keeps higher than the G'' throughout the measured temperature range. The dropping ramp at the gelatin gel-sol temperature upon heating is shown in the treated Gel/SF 9/1, 3/1, and 6/4 complex hydrogels, but disappears with higher content of SF. The temperatures showing the dropping ramps of G' are overlapped with DSC thermograms of

the same samples. This means that the drop of G' is due to the conformational change of gelatin molecules in the complex hydrogels from helix to coil structure, which causes the gel-sol transition of gelatin.

G' and G'' of the treated Gel/SF complex hydrogels at specific temperatures are plotted in Figure 2-1-11-a) (at 20 °C) and b) (at 40 °C). At both temperatures, the G' and G'' increase with more SF content, exhibiting typical S-type curves. This implies that the treated complex hydrogels have structures different from the untreated Gel/SF gels. The treated Gel/SF hydrogels have the induced SF β-sheet crystalline structure in their gel networks. At ambient temperatures below the gelatin gel-sol transition temperature, the treated complex gels have two 3-dimensional physical networks: triple helix networks of gelatin and β-sheet networks of SF. β-sheet networks show stronger visocelastic properties than gelatin, resulting in increased G' and G'' of the treated complex hydrogels with higher SF content. However, above the gel-sol transition temperature of gelatin, only SF β-sheet crystalline networks maintain the gel network structure due to the conformational change of gelatin from triple helix to random coil structure.

Figure 2-1-12 shows the cooling traces of dynamic rheological properties for Gel/SF 9/1 and Gel/SF 3/1. The curves of G' show the increasing ramps at 25 ~ 20 °C, below which the G's of the complex hydrogels return to the previous G' before heating the hydrogels. Therefore, the helix-coil transition behavior of gelatin in the Gel/SF complex networks is reversible, so that they could be utilized in a temperature-fluctuating situation (e.g. between ambient temperature and body temperature). Usually, chemical cross-linking with small

chemical reagents has been reported to make the transition behavior of gelatin networks irreversible [38]. In these reports, once the triple helix structure of the chemically cross-linked gelatin was denatured at a higher temperature, the random coil structure of gelatin did not return back to a triple helix structure at a lower temperature due to the restriction of mobility.

However, in our system, the denatured random coil molecules of gelatin retain the mobility to return to triple helix structure at lower temperature, because there were no chemical changes to restrict the individual gelatin molecules.

It is notable that the G' curve of Gel/SF 3/1 show its ramp at higher temperature than that of Gel/SF 9/1, which means that the conformational change of gelatin in 25 % SF networks occurs at higher temperature than in 10 wt % SF networks. This result is in agreement with the DSC cooling trace (Figure 2-1-7). The coil-to-helix transition of gelatin molecules in SF networks is accelerated by the restriction imposed by the SF.

From the rheological and DSC tests, we can conclude the following:

1) SF content with random coil structure decreases the viscoelastic property of Gel/SF gels
2) SF content with β-sheet crystalline structure increases the viscoelastic property of Gel/SF gels
3) The SF β-sheet networks maintain the gel form of the complex hydrogels at higher temperature
4) The conformational change of gelatin molecules is reversible in SF networks,

representing an IPNs/semi-IPNs transition (see Scheme 2-1).

Figure 2-1-13 shows the effect of treatment condition (methanol/water ratio) on the viscoelastic properties of the complex films. The heating traces of dynamic rheological properties of the Gel/SF 3/1 hydrogels in all treatment condition were obtained from 10 to 45 °C. The measured G' at 20 and 40 °C was representatively chosen to investigate the effect of methanol/water ratio in treatment bath on the rheological property. The Gel/SF 3/1 treated in Me75 show a maximum. The Gel/SF 3/1 hydrogels treated in Me100 and Me25 exhibit lower G' than those treated in Me75 and Me50. This result can be explained with the FTIR data shown in Figure 2-1-3. The β-sheet conformation of SF in the Gel/SF complex hydrogels was more predominantly developed in Me75 and Me50 than in M100 and Me25.

2.1.4. Conclusions

Protein-based complex hydrogels have been obtained by blending gelatin with silk fibroin and inducing β-sheet conformation of SF in their complex networks. The methanol/water mixture with small ratio of water was more effective to induce β-sheet conformation of SF in the blend system. The induced SF β-sheet structure increased thermal stability and viscoelastic property of the Gel/SF complex hydrogels.

The experimental results demonstrated that the helix-coil transition of gelatin in the Gel/SF complex hydrogels was reversible between ambient and body temperatures. Therefore, the Gel/SF complex hydrogels showing a temperature responsive IPNs/semi-IPNs transition can be considered potentially a very good biomaterial for bioadhesive

hydrogels showing temperature targeted drug delivery.

2.1.5. References

[1] Kim S H, Opdahl A, Marmo C, Somorjai G A. AFM and SFG studies of pHEMA-based hydrogel contact lens surfaces in saline solution: adhesion, friction, and the presence of non-crosslinked polymer chains at the surface. Biomaterials. 2002, 23, 1657-1666.

[2] Nowak A P, Breedveld V, Pakstls L, Ozbas B, Plne D J, Pochan D, and Deming T J. Rapid recovering hydrogel scaffolds from self-assembling diblock copolypeptide amphiphiles. Nature. 2002, 417, 424-428.

[3] Qiu Y and Park K. Environment-sensitive hydrogels for drug delivery. Advanced Drug Delivery Reviews. 2001, 53, 321–339.

[4] Beebe D J, Moore J S, Bauer J M, Qing Yu Q, Robin H. Liu R H, Chelladurai Devadoss C, and Jo B. Functional hydrogel structures for autonomous flow control inside microfluidic channels, Nature, 2000, 404, 588-590.

[5] Kobayashi J, Kikuchi A, Sakai K, and Okano T. Aqueous chromatography utilizing hydrophobicity-modified anionic temperature-responsive hydrogel for stationary phases. Journal of Chromatography A. 2002, 958, 109–119.

[6] Mao R, Tang J, Swanson B G. Relaxation time spectrum of hydrogels by CONTIN analysis. Journal of food science, 2000, 65, 374-381.

[7] Peppas N A, Huang Y, Torres-Lugo M, Ward J H, and Zhang J. Physicochemical foundations and structural design of hydrogels in medicine and biology. Annu. Rev. Biomed. Eng. 2000, 2, 9–29.

[8] Einerson N J, Stevens K R, and Kao W Y J. Synthesis and physicochemical analysis of gelatin-based hydrogels for drug carrier matrices. Biomaterials 2003, 24, 509-523.

[9] Laemmel E, Penhoat J, Warocquier-Clerout R, and Sigot-Luizard M. Heparin immobilized on proteins usable for arterial prosthesis coating: Growth inhibition of smooth-muscle cells. J. Biomed. Mater. Res. 1998, 39, 446-452.

[10] Halstenberg, S.; Panitch, A.; Rizzi, S.; Hall, H.; Hubbell, J. A. Biologically engineered protein-graft-poly(ethylene glycol) hydrogels: A cell adhesive and plasma in-degradable biosynthetic material for tissue repair. Biomacromolecules 2002, 3, 710-723.

[11] Girotti A, Reguera J, Rodriguez-Cabello J C, Jose C, Arias F J, Alonso M, and Testera A M. Design and bioproduction of a recombinant multi(bio) functional elastin-like protein polymer containing cell adhesion sequences for tissue engineering purposes. J. Mater. Sci. Mater. Med. 2004, 15, 479-484.

[12] Joly-Duhamel C, Hellio D, and Djabourov M. All Gelatin Networks: 1. Biodiversity

and Physical Chemistry. Langmuir 2002, 18, 7208-7217.

[13] Matsuda S, Iwata H, Se N, and Ikada Y. Bioadhesion of gelatin films crosslinked with glutaraldehyde. J. Biomed. Mater. Res. 1999, 45, 20-27.

[14] Van den Bulcke A I, Bogdanov B, De Rooze N, and Schacht E H. Cornelissen, M.; Berghmans, H. Structural and rheological properties of methacrylamide modified gelatin hydrogels. Biomacromolecules 2000, 1, 31-38.

[15] Nazarov R, Jin H, and Kaplan D. Porous 3-D Scaffolds from Regenerated Silk Fibroin. Biomacromolecules, 2004, 5, 718-726

[16] Gotoh Y, Tsukada M, Minoura N, and Imai Y. Synthesis of poly(ethylene glycol)-silk fibroin conjugates and surface interaction between L-929 cells and the conjugates. Biomaterials, 1997, 18, 267-271.

[17] Minoura N, Tsukada M, Nagura M. Fine structure and oxygen permeability of silk fibroin membrane treated with methanol. Polymer, 1990, 31, 265-269.

[18] Gu J, Yang X, and Zhu H. Surface sulfonation of silk fibroin film by plasma treatment and in vitro antithrombogenicity study. Materials Science and Engineering: C, 2002, 20, 199-202.

[19] Vonfraunhofer J A, and Sichina W J. Characterization of surgical suture materials using dynamic mechanical analysis. Biomaterials, 1992, 13, 715-720

[20] Padamwar M N, and Pawar A P. Silk sericin and its applications: A review, Journal of scientific and industrial research, 2004, 63, 323-329

[21] Zhang Y Q. Natural silk fibroin as a support for enzyme immobilization. Biotechnology advances, 1998, 16, 961-971.

[22] Santin M, Motta A, Freddi G, and Cannas M. In vitro evaluation of the inflammatory potential of the silk fibroin. Journal of biomedical materials research, 1999, 46, 382-389.

[23] Rujiravanit R, Kruaykitanon S, Jamieson A M, Tokura S. Preparation of crosslinked chitosan/silk fibroin blend films for drug delivery system. Macromolecular bioscience 2003, 3, 604-611.

[24] Mathur A B, Tonelli A and Hudson S. The Dissolution and Characterization of Bombyx Mori Silk in Calcium Nitrate/Methanol Solution and Regeneration and Characterization of Thin Films. Biopolymers, 1997, 42, 61-74.

[25] Ha S, Park Y H., Hudson M S. Dissolution of Bombyx mori Silk Fibroin in the Calcium Nitrate Tetrahydrate-Methanol System and Aspects of Wet Spinning of Fibroin Solution. Biomacromolecules, 2003, 4, 488-496.

[26] Bigi A, Panzavolta S, Rubini K. Relationship between triple-helix content and mechanical properties of gelatin films. Biomaterials, 2004, 25, 5675-5680.

[27] Vieny, C. From Natural Silks to New Polymer Fibers, J. Text. Inst. 2000,

93, 2-23.

[28] Tsukada M, Gotoh Y, Nagura M, Minoura N, and Kasai N, Freddi G. Structural-changes of silk fibroin membranes induced by immersion in methanol aqueous-solution. Journal of polymer science part B-polymer physics, 1994, 32, 961-968.

[29] Agarwal, N.; Hoagland, D. A.; Farris R. J. Effect of moisture absorption on the thermal properties of *Bombyx mori* silk fibroin films. J. Appl. Polym. Sci. 1997, 63, 401-410.

[30] Rose, P I. In The theory of the photographic process, James, T. H Ed, 4th de. New York: MacMillan, 1977, p. 67.

[31] Rault, J, Gref R, Ping Z H; Nguyen Q T, and Neel J. Glass transition temperature regulation effect in a poly(vinyl alcohol)-water system. Polymer, 1995, 36, 1655-1661.

[32] Rault J, Gref R, Ping Z H, and Nguyen Q T. The T_g regulation effect in hydrophilic polymers. Non-Cryst. Solids, 1994, 172, 733-736.

[33] Ponomariova T, Melnichenko Y, Albouy P A, and Rault J. Influence of the crosslinks density on the crystallization of water in PAA gels. Polymer, 1997, 38, 3561-3564.

[34] Patil R D, Mark J E, Apostolov A, Vassileva E, and Fakirov S. Crystallization of water in some crosslinked gelatins. Eur. Polym. J. 2000, 36, 1055-1061.

[35] Suzuki Y, Gage L P, and Brown D D. The genes for silk fibroin in *Bombyx mori*. J. Mol. Bio. 1972, 70, 637-649.

[36] Nijenhuis K. Thermoreversible networks: Viscoelastic properties and structure of gels. Berlin; New York: Springer, 1997,160-193

[37] Bigi A, Cojazzi G, Panzavolta S, Rubini K, and Roveri N. Mechanical and thermal properties of gelatin films at different degrees of glutaraldehyde crosslinking. Biomaterials, 2001, 22, 763-768.

[38] Kuijpers A J, Engbers G H M, Feijen J, De Smedt S C, Meyvis T K L, Demeester J, Krijgsveld J, Zaat S A J, and Dankert J. Characterization of the network structure of carbodiimide cross-linked gelatin gels. Macromolecules, 1999; 32, 3325-3333.

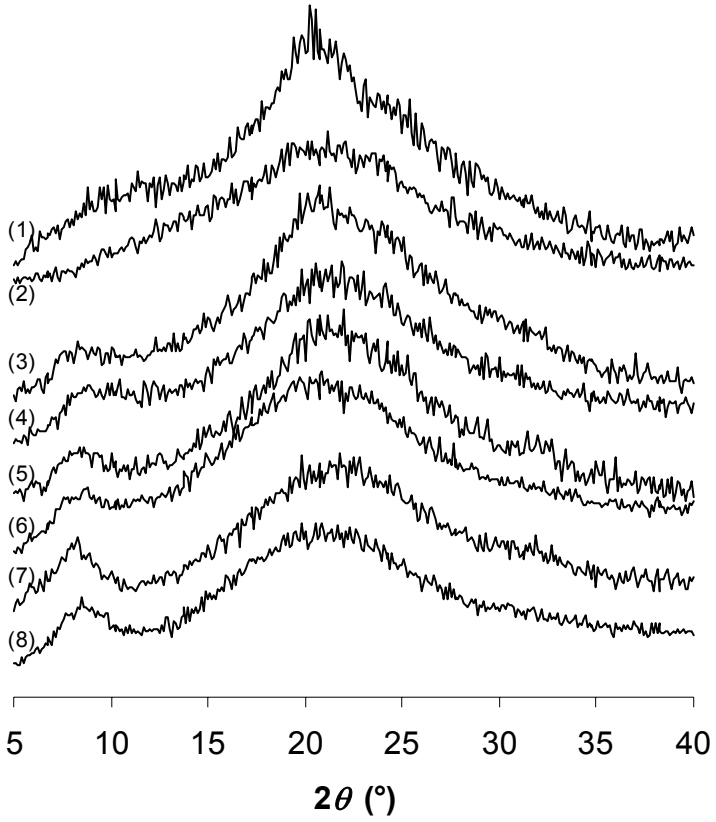

Figure 2-1-1 WAXD curves of untreated and treated SF, Gel, and Gel/SF 3/2, and Gel/SF 2/3 films. (1) Treated SF, (2) Untreated SF, (3) Treated Gel/SF 2/3, (4) Untreated Gel/SF 2/3, (5) Treated Gel/SF 3/2, (6) Untreated Gel/SF 3/2, (7) Treated Gel, (8) Treated Gel

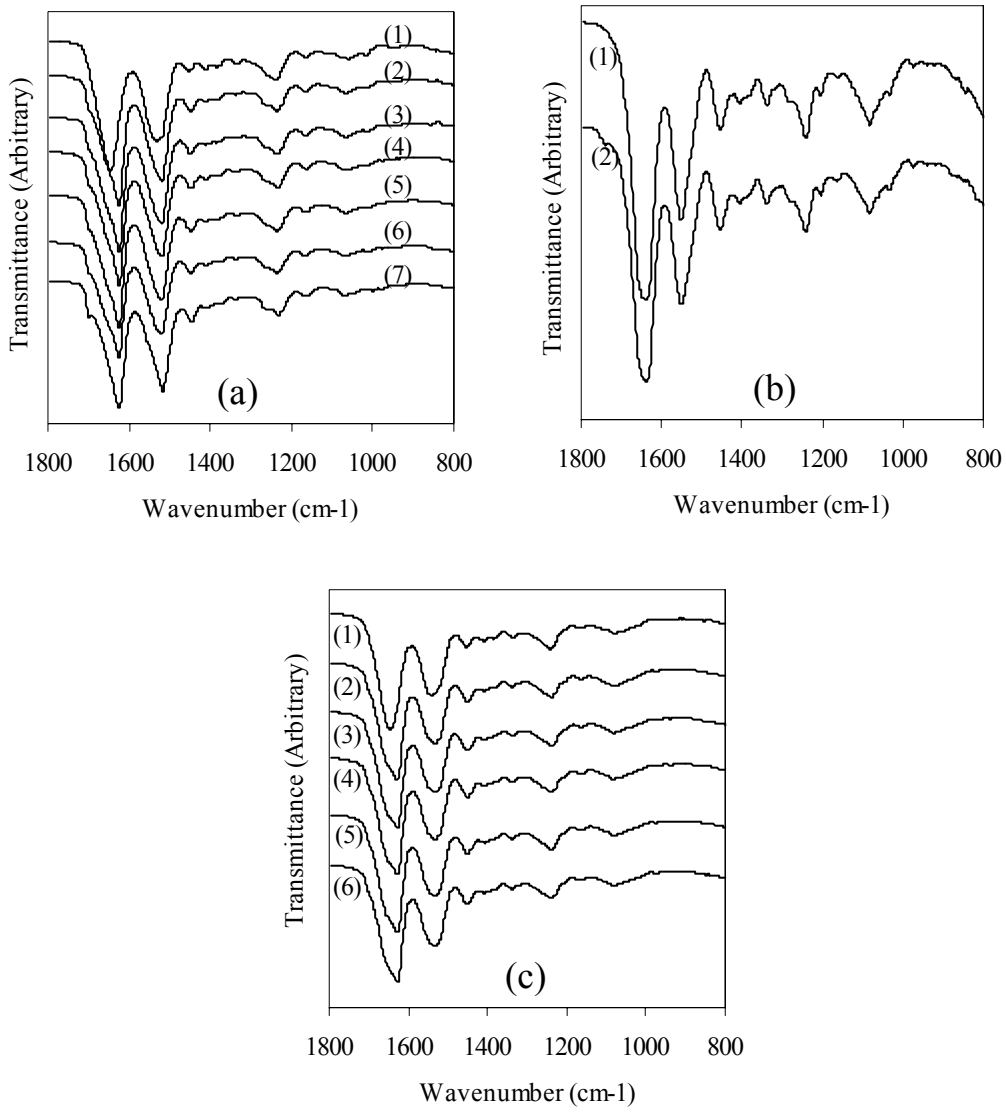

Figure 2-1-2 **a)** FTIR spectra of SF films treated in Me75 for different times: (1) SF as-cast film, (2) for 5 min, (3) for 20 min., (4) for 60 min., (5) for 120 min., (6) for 600 min., (7) SF fiber

b) FTIR spectra of Gel films (1) as-cast film (2) treated in Me75 for 120 min

c) FTIR spectra of Gel/SF 3/2 films treated for different treatment times: (1) as-cast film, (2) for 5 min, (3) for 20 min., (4) for 60 min., (5) for 120 min., (6) for 600 min.

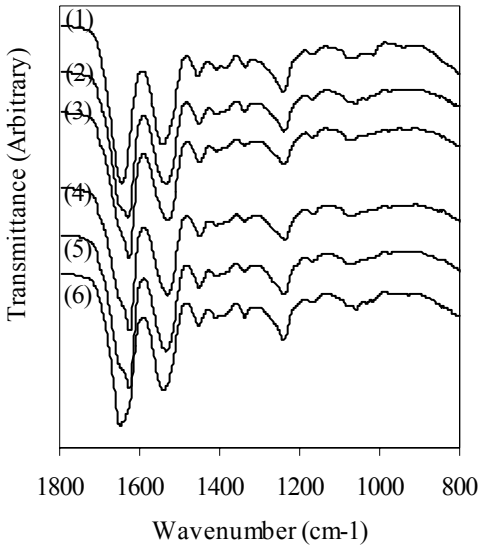

Figure 2-1-3 FTIR spectra of Gel/SF 1/1 films treated at different ratios of methanol/water for 2 hours at 20 °C (1): as-cast film, (2): in Me100, (3): in Me75, (4) in Me50, (5) in Me25, (6) in Me10

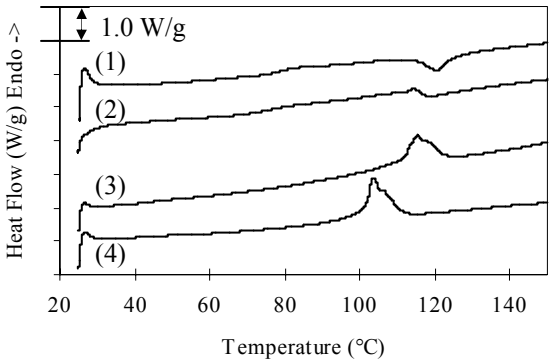

(a)

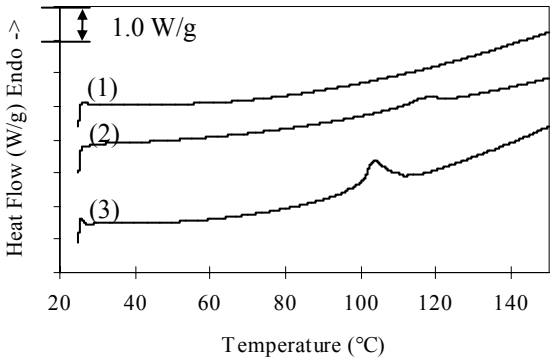

(b)

Figure 2-1-4 DSC heating curves Gelatin and Gel/SF complex: a) as-cast films and b) treated films, which were dried in air. The films were treated in Me75 for 2 hours at 20 ºC. Samples were heated at the rate of 20 ºC/min under N_2 purging. (1): Silk Fibroin, (2): Gel/SF 1/3, (3): Gel/SF 3/1, (4): Gelatin.

Water content; SF-as cast: 8.2 %, Gel/SF 1/3-as cast: 9.1 %, Gel/SF 3/1-as cast: 10.4 %, Gel-as cast: 13.4 %, SF-treated: 5.6 %, Gel/SF 1/3- treated: 8.3 %, Gel/SF 3/1- treated: 12.3 %.

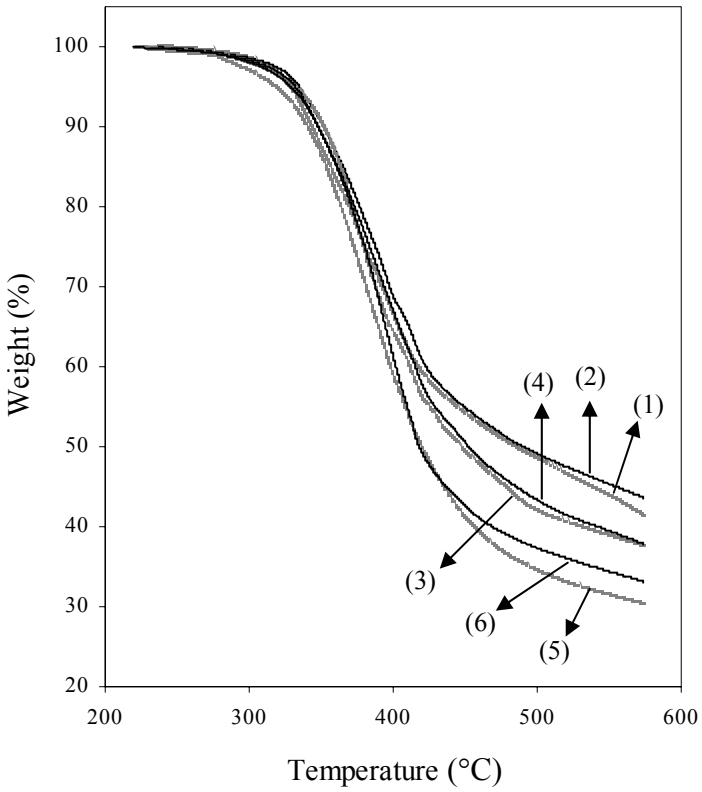

Figure 2-1-5 TGA thermographs of Gel/SF complex films: 1) SF as-cast film, 2) SF treated film, 3) Gel/SF 1/3 as-cast film, 4) Gel/SF 1/3 treated film, 5) Gel/SF 3/1 as-cast film, 6) Gel/SF 3/1 treated film. The films were treated in Me75 for 2 hours at 20 ºC. Samples were heated at the rate of 50 ºC/min under N2 purging.

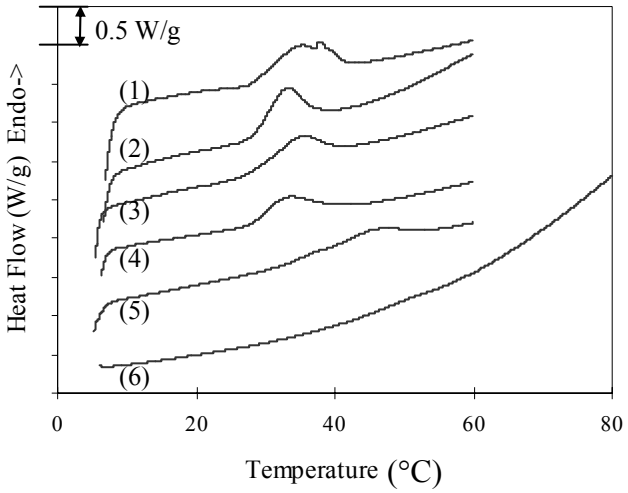

Figure 2-1-6 DSC heating curves of Gelatin and Gel/SF complex hydrogels. Samples were heated at the rate of 5 ºC/min under N2 purging. The films were treated in Me75 for 2 hours at 20 ºC. (1): Gelatin, (2):Gel/SF 9/1, (3):Gel/SF 3/1, (4): Gel/SF 3/2, (5): Gel/SF 2/3 (6): Gel/SF 1/3

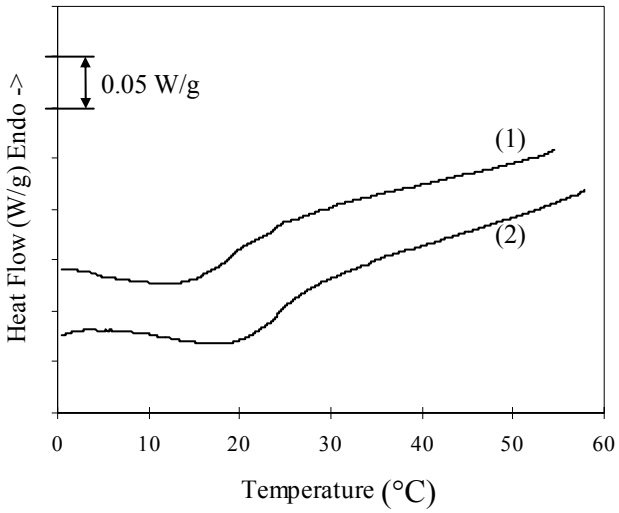

Figure 2-1-7 DSC cooling curves of Gelatin and Gel/SF complex hydrogels. Samples were cooled at the rate of 5 ºC/min under N_2 purging. The films were treated in Me75 for 2 hours at 20 ºC. (1): Gelatin, (2): Gel/SF 3/1

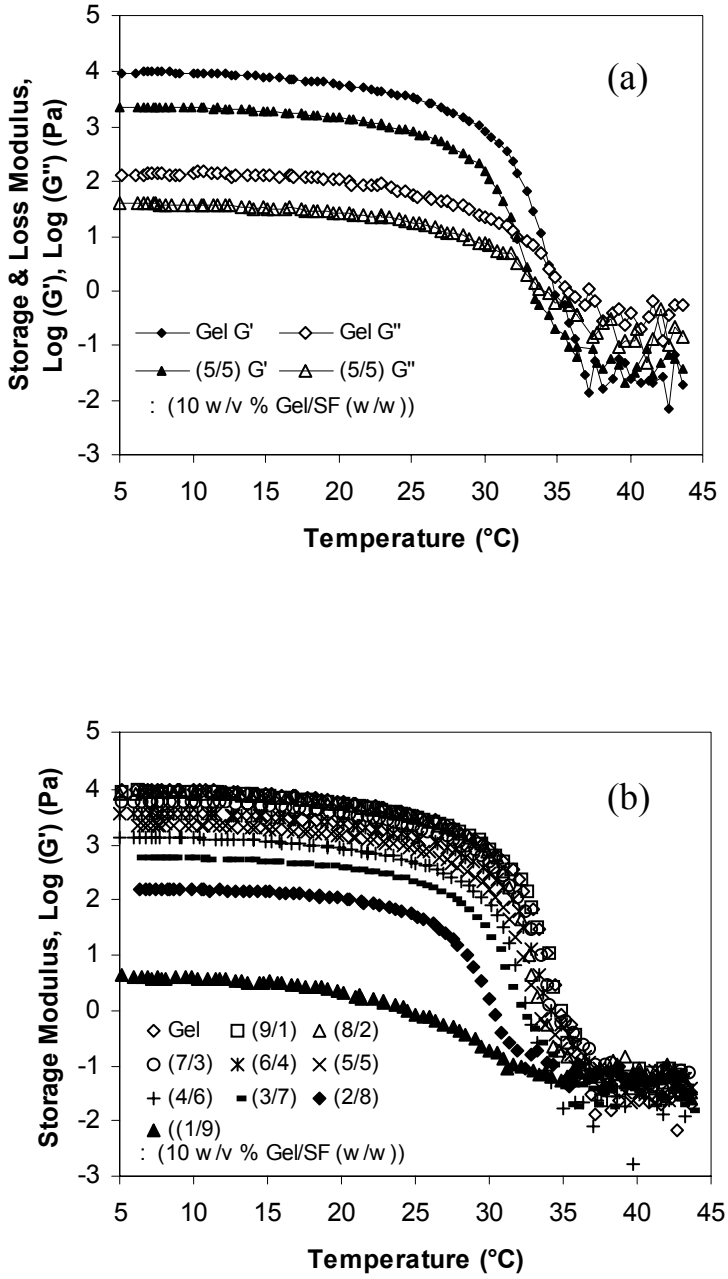

Figure 2-1-8 Heating traces of the dynamic rhoelogical properties of Gel/SF gels (10 w/v %) without treatment. a) G' and G'' of gelatin and Gel/SF 1/1 gels, b) G's of gelatin and all Gel/SF gels

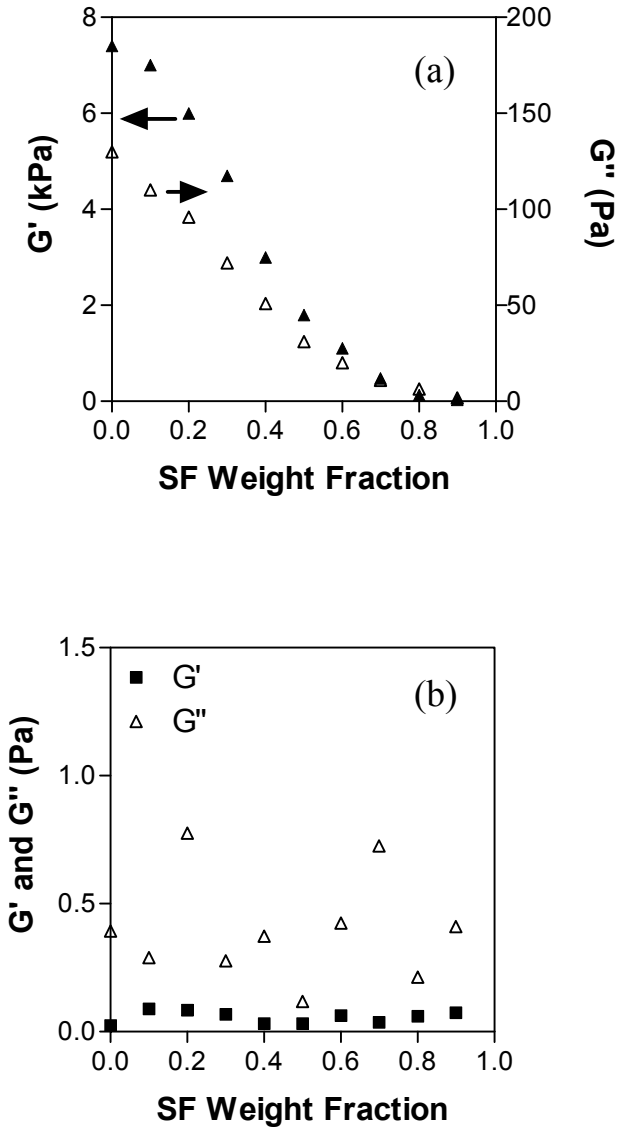

Figure 2-1-9　G’ and G’’ of gelatin and Gel/SF blend gels: a) at 20 °C and b) at 40 °C

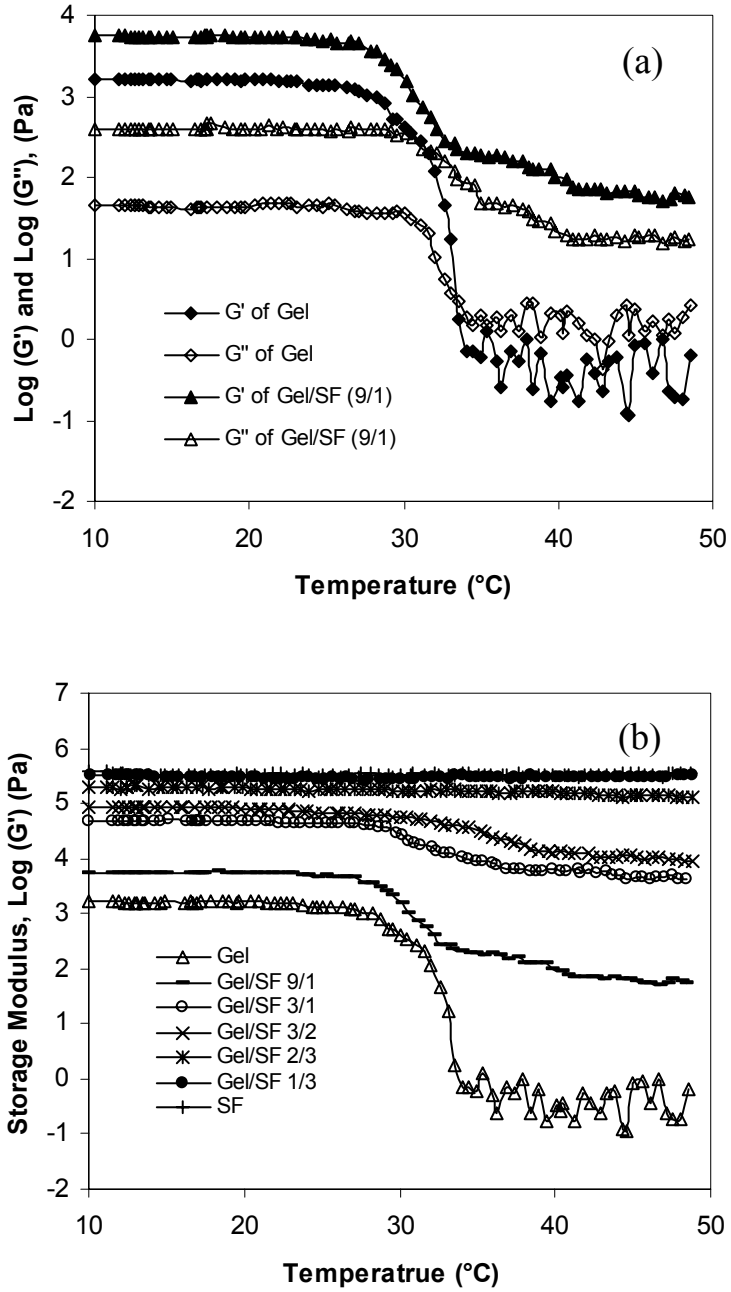

Figure 2-1-10 Heating traces of the dynamic rhoelogical properties of the treated Gel/SF hydrogels. The treated Gel/SF films were swollen at 5 °C for 24 hours before measurement. a) G' and G'' of gelatin and Gel/SF 9/1 hydrogels, b) G's of gelatin and all treated Gel/SF hydrogels

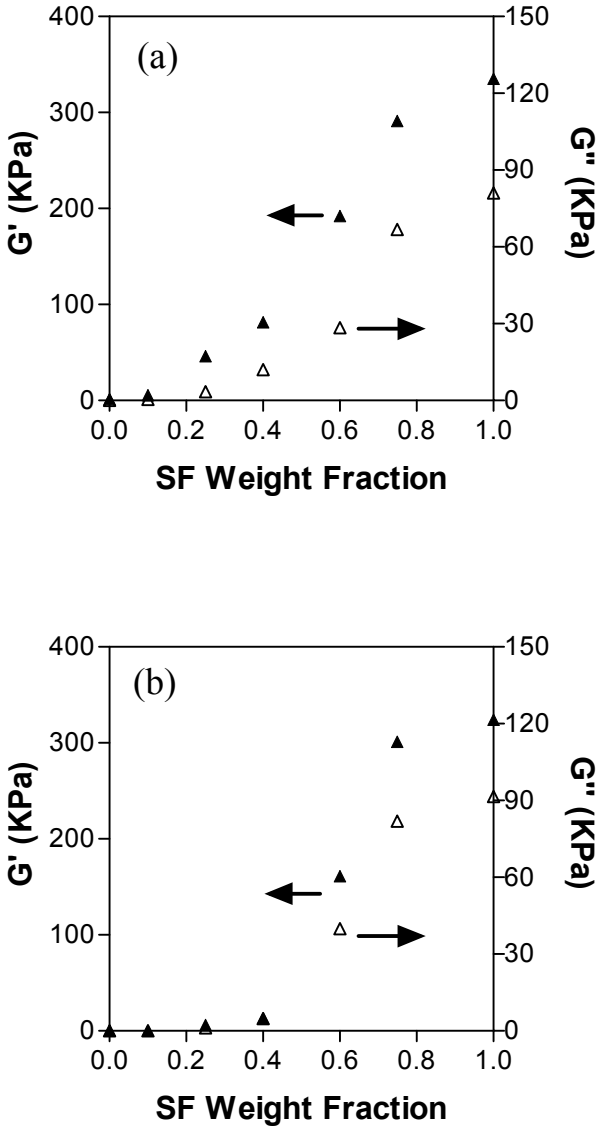

Figure 2-1-11 G' and G'' of gelatin and Gel/SF hydrogels treated in Me75: a) at 20 °C and b) at 40 °C. The treated Gel/SF films were swollen at 5 °C for 24 hours before measurement.

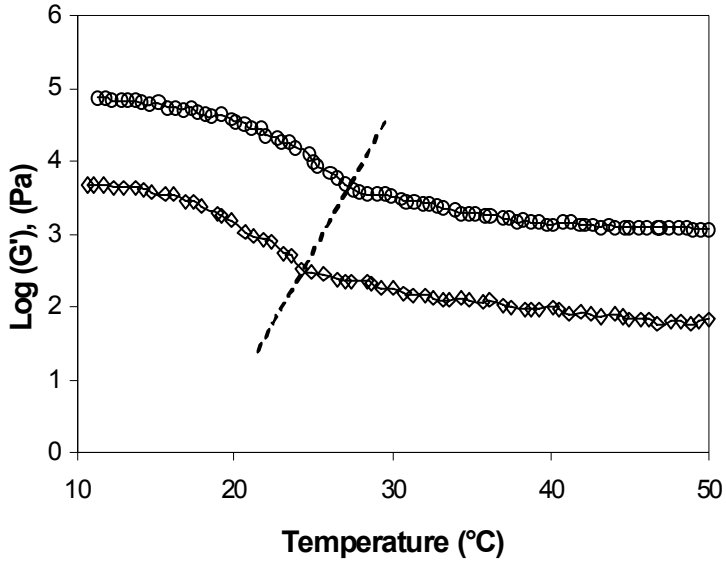

Figure 2-1-12 Cooling traces of dynamic rheological properties for Gel/SF 9/1 and Gel/SF 3/1. The treated Gel/SF films were swollen at 5 °C for 24 hours before measurement.

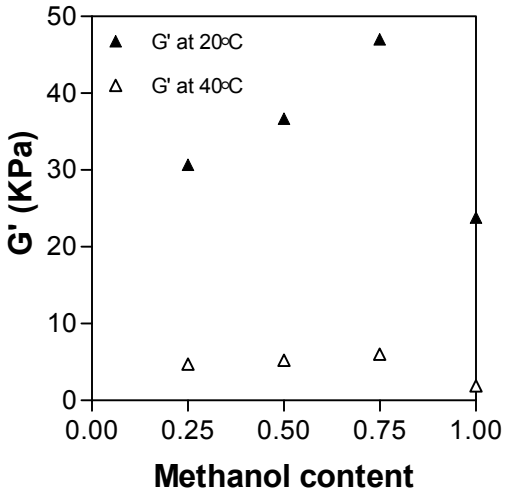

Figure 2-1-13 G's of Gel/SF 3/1 hydrogels treated in different methanol/water ratios at °20 °C and at 40 °C. The treated Gel/SF films were swollen at 5 °C for 24 hours before measurement.

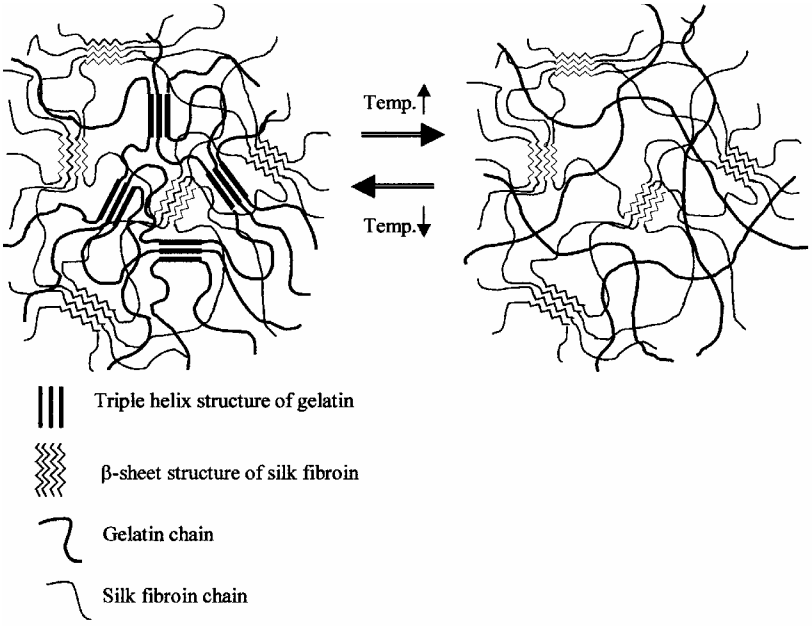

Scheme 2-1-1 Schematic illustration of gelatin and silk fibroin complex structure responding to environmental temperature change in water medium. Triple helix structures of gelatin are broken at body temperature, leading to the increased release of loaded drugs as well as gelatin while sustaining its hydrogel network due to irreversible β-sheet structure of silk fibroin.

2.2. Swelling Properties and Temperature Responsive Protein Release

Abstract

Protein-based complex hydrogels were manufactured by blending gelatin (Gel) with *Bombyx mori* silk fibroin (SF) and introducing β-sheet conformation of SF molecules in their complex networks. These hydrogels show a temperature-responsive gelatin release profile: at 20°C they exhibited no gelatin release and maintained their hydrogel dimension, but at 37°C they showed time-dependent gelatin release and their hydrogel dimension decreased. Once the triple-helix conformation of gelatin in Gel/SF complex hydrogels is broken at body temperature, an abrupt increase in swelling and gelatin release occur. Also, the swelling properties of the hydrogels are elucidated according to treatment condition.

2.2.1. Introduction

In the previous chapter, we described the fabrication and characterization of the Gel/SF complex films and hydrogels and showed the thermally induced IPN/semi-IPN transition in their networks. The purpose of this work was to fabricate the pure protein-based hydrogels without any addition of chemicals and to show the possibility for temperature responsive drug release controlled by diffusion and erosion of the gelatin molecules from the complex hydrogels. From the good biological properties of gelatin and silk fibroin, respectively, the combination of these two proteins should lead to more desirable benefits and broad applications. In the present study, we have evaluated the complex hydrogels for swelling properties according to the treatment conditions. Also, we have investigated the gelatin release profiles coresponding to temperature changes. The results suggest that gelatin/silk

fibroin blends can be useful for the temperature responsive drug release as hydrogel forms.

2.2.2. Experiments

2.2.2.1. Materials

Grade 5A raw silk with an average denier of 20.86 produced in Brazil by the Fiaçào de Seda Bratac S.S. was used. Gelatin (Type A from porcine skin, 175 bloom) was purchased from Sigma. All other chemicals used were purchased from Fisher or Aldrich, and used directly without further purification.

2.2.2.2. SF solution preparation

SF solution of 4 w/w % was prepared by following the method of 2.1.2.2.

2.2.2.3. Blending and preparing films

All blending solution and films (Gel, Gel/SF 9/1, Gel/SF 3/1, Gel/SF 3/2, Gel/SF 2/3, Gel/SF 1/3, and SF) were prepared by following the method of 2.1.2.3. Clear, colorless and flexible films (0.2 mm thickness) were obtained.

2.2.2.4. Treatment of films in methanol/water system

The films were treated, as described in the method of 2.1.2.4. Briefly, the films were treated in methanol/water mixture (methanol/water weight ratios: 100/0 (Me100), 75/25 (Me75), 50/50 (Me50), 25/75 (Me25), 10/90 (Me10)) for 5 min to 600 min at 20 °C. If there is no described condition, the films were treated in Me75 for 2 hours.

2.2.2.5. Swelling test

All films of 1×1cm were dried under vacuum for 1 day and weighed. The films were immersed in Phosphate-buffered saline solution (PBS; pH7.4) at 20 °C or 37 °C. The

weights of swollen films were measured and the swollen films were air-dried and then dried under vacuum for 1 day and weighed.

Weight ratio of the swollen hydrogels to initial dried films was used to investigate the weight change of hydrogels caused by gelatin diffusion. Weight ratios were calculated by the following equation.

$$\text{Weight ratio (WR)} = (W_s - W_{d1})/W_{d1}$$

where W_s and W_{d1} are the weight of swollen films and the weight of initial dried film before swelling test. Here, only W_s is a parameter to govern Weight ratio.

Swelling ratio is conventionally used to investigate the property of hydrogels. Swelling ratios were calculated by the following equation.

$$\text{Swelling ratio (SW)} = (W_s - W_{d2})/W_{d2}$$

where W_s and W_{d2} are the weight of swollen films and the weight of dried film after swelling test. Here, W_s and W_{d2} are parameters to govern Swelling ratio.

If there is no weight loss from the hydrogels, the swelling ratio is same as the weight ratio because $W_{d1} = W_{d2}$.

The experimental plots were averages of three samples with standard deviation (S.D.) error bars.

2.2.2.6. Release of protein

A Gel/SF complex film of 20 mg was immersed in PBS (pH 7.4) of 6 ml at 20 °C and 37 °C. The release solution of 200 μl was collected at regular intervals and PBS of 200 μl was refilled to the sample solution. The concentration of the released protein was calculated by

colorimetric assay by a bicinchoninic acid protein assay kit (Sigma Chemical Co., St. Louis) [1]. The collected release solution (200 μl) was mixed with assay solution of 2 ml. The solutions were incubated in ambient temperature for 24 hours. The absorbance at 562 nm was measured and used for the calculation of protein release at each interval. The calibration curve was obtained from 5 series of different protein concentration solutions by diluting the gelatin stock solutions, where the dried gelatin film of 20 mg was dissolved in PBS of 6 ml.

2.2.3. Results and discussion

2.2.3.1 Effect of treatment condition on the swelling property

Figure 2-2-1 shows the effect of treatment time period on the swelling ratios of Gel/SF complex films at 20°C. The swelling ratios of the complex films do not seem to be different over the full range of treatment time (5 min ~ 1200 min). This feature suggests that most of the β-sheet conformational change is induced within a period as short as 5 min in accordance with FTIR data shown in previous chapter Figure 2-1-2. However, the swelling ratios of pure SF film and SF-rich complex films still decreased within 20~60 min treatment before reaching steady values. The swelling ratio of pure SF film dropped from 0.33 for 5 min to 0.26 for 20 min and 0.25 for 60 min. Also, the swelling ratio of Gel/SF 1/3 film shows 0.65 for 5 min, 0.58 for 20 min and 0.55 for 60 min. That of Gel/SF 2/3 decreases from 0.80 for 5 min to 0.67 for 20 min and then reaches a steady value.

On the other hand, the swelling ratios of gelatin-rich complex films seem to reach steady values within 5 min. Gelatin-rich complex films seem to have quicker conformational

changes of SF molecules from random coil to β-sheet conformation than pure SF films and SF-rich complex films. The methanol molecules are likely to more easily access SF in gelatin-rich complex networks, than in pure SF films and SF-rich complex networks, because the methanol molecules should more slowly diffuse through the hardened surface of mostly β-sheet crystalline SF structure into the core of pure SF film and SF-rich complex films.

Figure 2-2-2 shows the effect of treatment condition by evaluating the effect of methanol/water ratios on the swelling ratios of Gel/SF complex films at both 20 °C and 37°C. Gel/SF 3/1 films were treated in Me100 ~ Me10 for 2 hours at 20 C. The treated Gel/SF 3/1 films were immersed in PBS (pH 7.4) for 2 days to reach equilibrium swelling state. When the Gel/SF 3/1 films were treated in Me75, the swelling ratio exhibits a minimum. The hydrogels treated in M100 and M10 show relatively higher swelling ratio in 20 °C and 37 °C, respectively. The swelling ratios of the complex films treated in methanol/water mixture with different water content are strongly related to the FTIR spectra results (previous chapter, Figure 2-1-3), which show that the treatment in methanol/water mixture with around 25-50 wt % water content is more effective to induce β-sheet conformation of SF in Gel/SF complex. Therefore, the swelling ratios of the complex film should be governed by the β-form crystalline network properties of SF in the Gel/SF complex networks.

It is important to see that the swelling ratios are related to the conformation of gelatin. The increased swelling ratio at 37 °C should come from the broken triple helix networks of

gelatin in the complex networks.

2.2.3.2 Weight change of hydrogels

Figure 2-2-3 displays the weight ratios of Gel/SF complex hydrogels according to soaking times in PBS (pH 7.4) at 20 °C. Gelatin film begins to be swollen and quickly gains weight within 1 day. After 1 day, the gelatin film shows slow increase of weight ratio. Similarly, the Gel/SF 9/1 exhibits a fast increase of weight ratio within 8 hour and shows still slow increase of weight ratio like gelatin hydrogel. The slow increase of weight ratio indicates that the physical networks should become loose and bear more space that could accommodate surrounding water molecules as time increases. SF and Gel/SF 3/2 and 3/1 show quick swelling and reached steady state within 1 hour. After that time, these hydrogels do not display weight increase. After the swelling process is equilibrated, SF β-form networks containing more than 25 wt% of SF in the complex networks should restrict the gelatin triple-helix networks from absorbing environmental water molecules. This indicates that the Gel/SF complex hydrogels maintain their stable complex networks at 20 °C.

In Figure 2-2-4, the weight ratios of Gel/SF complex hydrogels are represented according to soaking times in PBS (pH 7.4) at 37 °C. The hydrogels are quickly swollen within 1 hour and show maximum weight ratios at 1 hour. The weight ratios of all samples at 2 hours stand near the values at 1hour and sharply decrease within 8 hours. This indicates that the diffusion of water molecules into the complex hydrogels dominates within 1 hour, leading to fast swelling, and competes with the weight decrease of hydrogels within 2 hours. After 2 hours, the weight decrease of hydrogels dominates over the swelling process and the

swollen complex hydrogels lose their weight. This decrease of weight ratio at 37 °C was not observed at 20 °C (in Figure 2-2-3). To observe the weight change of the hydrogels, the data of weight ratios in Figure 2-2-4 were converted to % change of weight by considering the gel weight of all samples at 1 hour as an initial gel weight (See Figure 2-2-5). The complex hydrogels exhibit more weight decrease with more gelatin content, while SF kept the weight at a steady state. There are two possibilities for the decrease of hydrogel weight: one is the shrinkage of the complex networks while expelling water and the other is the release of protein molecules from the complex hydrogels with a dimensional decrease. However, the former might not happen, because the swelling ratios were higher at 37 °C than at 20 °C, indicating that the hydrogels contain more water at 37 °C.

To prove the reason for weight change of hydrogels at 37 °C, the swelling ratios and weight ratios of the hydrogels after 6 days at 37 °C are compared with those at 20 °C and represented in Figure 2-2-6. At 20 °C, the swelling ratios almost overlap over the weight ratios in all Gel/SF complex hydrogels. By definition, weight ratio of hydrogels equals to swelling ratio if there is no release of protein from the matrix.

In contrast, after soaking the complex hydrogels for 6 days at 37 °C, the swelling ratios become higher and the weight ratios move lower, compared with those at 20 °C. This means that the hydrogels gain more water and lose more weight at 37 °C than at 20 °C. Therefore, the decrease of hydrogel dimension should occur through protein release at 37 °C.

The released proteins from the matrix at 37 C might be gelatin molecules rather than SF

molecules, because SF does not show weight change even at 37 °C and the Gel/SF complex hydrogels containing more gelatin content show more % change of weight at 37 °C. More precise data could be obtained by measuring the protein concentration in the release solution, which will be discussed in section 2.2.3.3.

2.2.3.3. Release of protein

Figure 2-2-7 displays the protein release profiles from the Gel/SF complex hydrogels at 20 °C (Figure 2-2-7-a)) and at 37 °C (Figure 2-2-7-b)). In Figure 2-2-7-a), the Gel/SF complex hydrogels show no release of protein after they are swollen at 20 °C. However, in Figure 2-2-7-b), the Gel/SF complex hydrogels exhibit the release of protein even after they are swollen at 37 °C. The Gel/SF consist of complex networks with two different types of physical cross-links: β-sheet structure for SF and triple-helix structure for gelatin at ambient temperature. However, the interpenetrating polymer networks (IPNs) at ambient temperature changes to semi-IPNs due to the break of triple helix networks of gelatin at body temperature. Therefore, the protein release from Gel/SF complex hydrogels at 37 °C is due to the diffusion of the random coil gelatin molecules from SF β-sheet networks.

In the case of pure SF hydrigels, there a negligible release of protein at 37 °C as well as at 20 °C. SF are reported to consist of the fibroin heavy chain (ca 350 kDa), which might potentially induce β-sheet conformation, and fibroin light chain (ca. 25 kDa), which might form a globular structure and represent an amorphous region [2]. In these data, the fibroin light chains, which consist of approximately half mole ratio in total SF, were not released from the SF β-form networks. This indicates that the Cys residues in N-terminal and C-

terminus of the fibroin heavy chains induce disulfide bonds with the fibroin light chains, resulting in covalent connection between the fibroin light and heavy chains [2].

2.2.4. Conclusion

We described the swelling properties and temperature-responsive gelatin release properties of the Gel/SF complex hydrgels. Swelling studies demonstrated that the swelling ratio was affected by the methanol/water ratios in treatment bath, but not considerably affected by the treatment time above 5 min. The swelling ratio of Gel/SF hydrogels was higher at 37 °C than at 20 °C, indicating the broken triple helix structure of gelatin in the complex networks leads to more water absorbtion.

Also, the experimental results showed that at 20 °C the complex hydrogels exhibited no gelatin release without dimensional change, but at 37 °C they showed gelatin release with their dimensional decrease.

As seen in scheme 2-2-1, triple helix and β-sheet networks coexist in Gel/SF complex networks as two different types of physical cross links at 20 °C. However, the triple helix structure was broken and non-reversible β-sheet structure sustained the dimensional form of the hydrogels at 37 °C. The broken triple helix networks, which were one of two physical networks in the Gel/SF complex hydrogels at 20 °C, induced the dimensional decrease of the hydrogels at 37 °C by the release of the denatured gelatin molecules from the SF β-sheet networks.

2.2.5. References

[1] Bigi A, Cojazzi G, Panzavolta S, Roveri N, and Rubini K. Stabilization of gelatin films by crosslinking with genipin. Biomaterials, 2002, 23, 4827-4832.

[2] Zhou C Z, Confalonieri F, Medina N, Zivanovic Y, Esnault C, Yang T, Jacquet M, Janin J, Duguet M, Perasso R, and Li Z G. Fine organization of Bombyx mori fibroin heavy chain gene, Nucleic Acids Res. 2000, 28, 2413-2419.

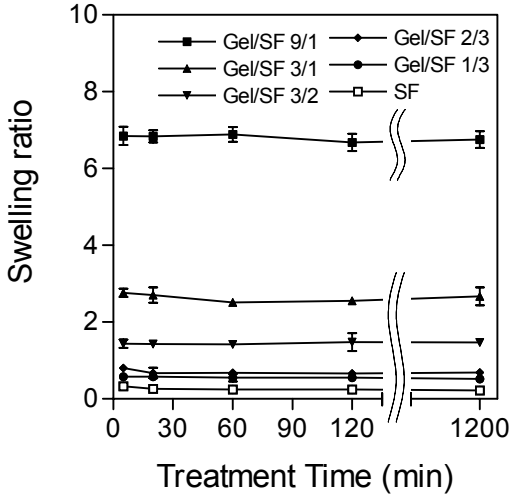

Figure 2-2-1 Effect of treatment time period on the swelling ratios of Gel/SF complex films at 20°C

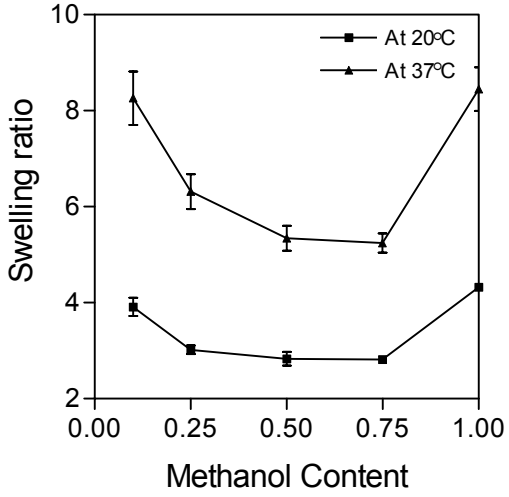

Figure 2-2-2 Effect of methanol/water ratios on the swelling ratios of Gel/SF complex films at both 20 °C and 37°C.

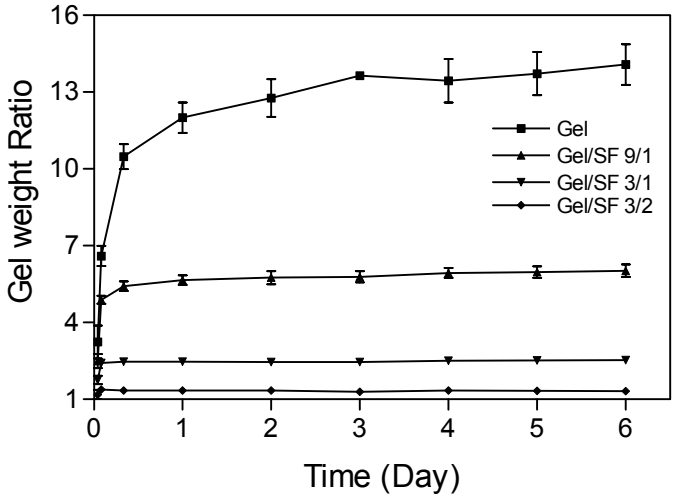

Figure 2-2-3 Weight ratios of Gel/SF complex hydrogels according to soaking times in PBS (pH 7.4) at 20 °C.

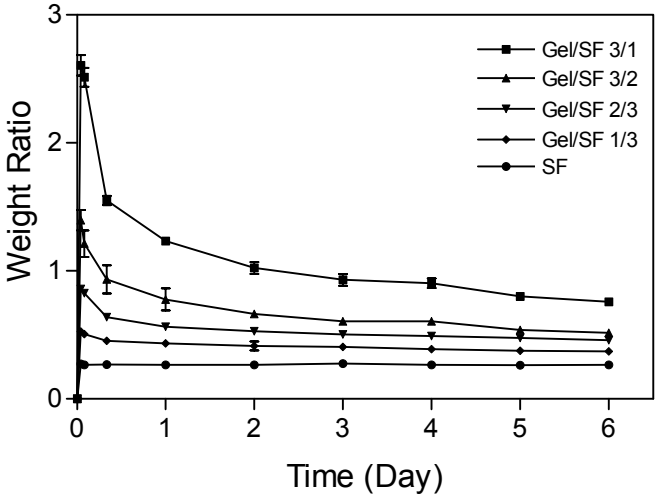

Figure 2-2-4 Weight ratios of Gel/SF complex hydrogels according to soaking times in PBS (pH 7.4) at 37 °C

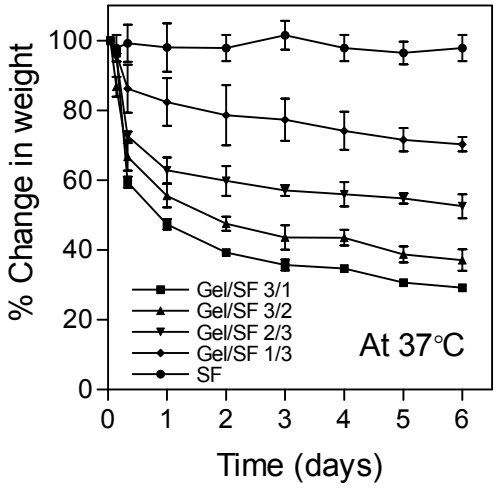

Figure 2-2-5 % change of weight of Gel/SF complex hydrogels according to soaking times. The gel weight of all samples at 1 hour was used as an initial gel weight.

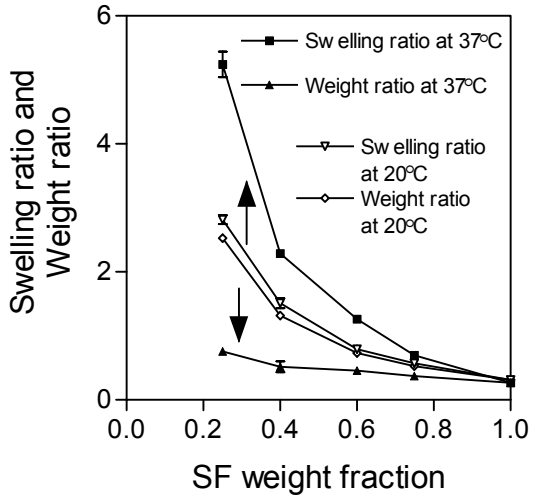

Figure 2-2-6 Swelling ratios and weight ratios of the hydrogels after 6 days at 20 °C and at 37 °C.

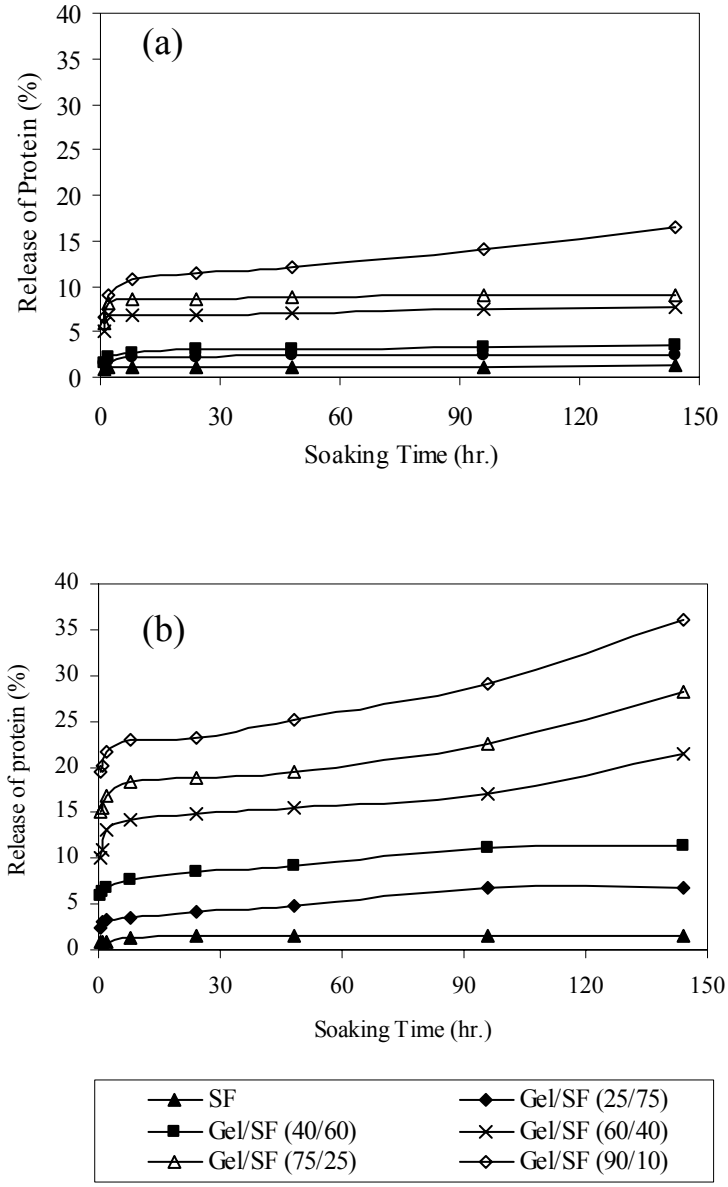

Figure 2-2-7 Protein release from the Gel/SF complex hydrogels a) at 20 °C and b) at 37 °C.

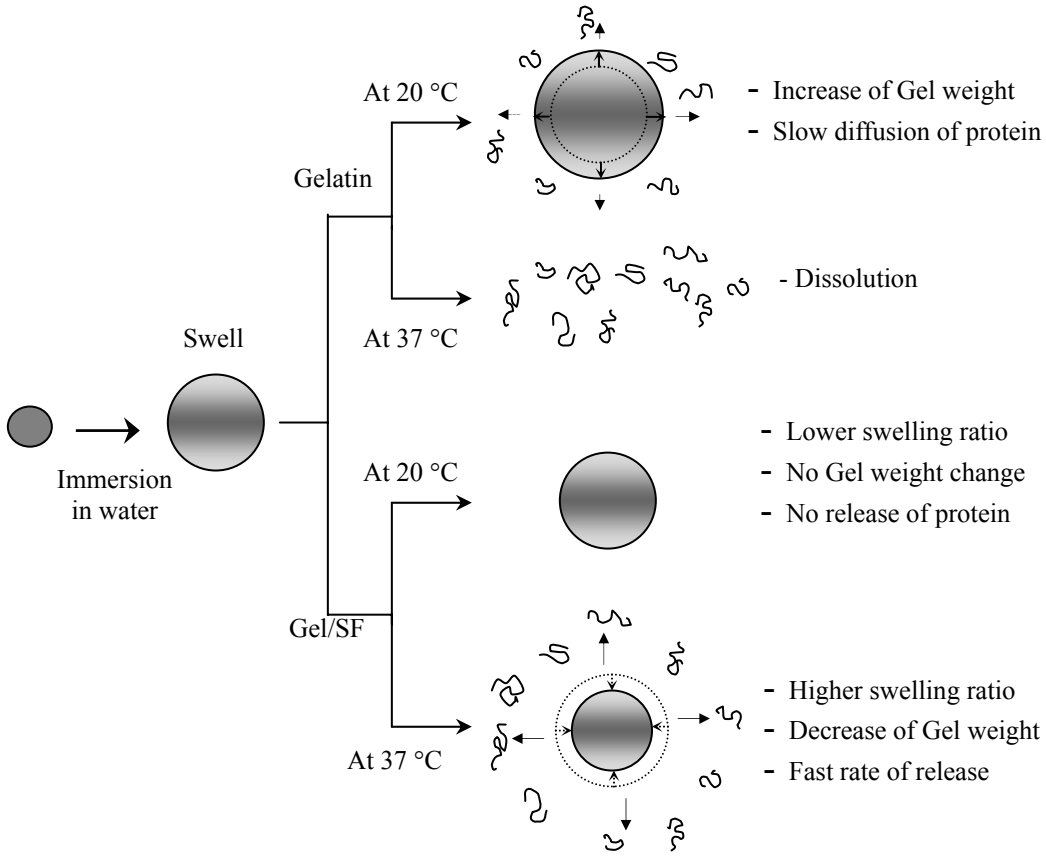

Scheme 2-2-1 Schematic Illustration for swelling and protein release properties of pure gelatin gel and Gel/SF complex hydrogels at ambient and body temperature.

3. Poly(*N*-isopropylacrylamide) Hydrogels in Interpenetrating Networks with β-Sheet Crystalline Structure: Improved Viscoelastic Properties and Fast Deswelling Rate

Abstract

Protein-synthetic polymer hybrid interpenetrating networks (IPNs) of poly(*N*-isopropylacrylamide) (PNIPAAm) with *Bombyx mori (B. mori)* silk fibroin (SF) are described. These IPNs have the β-sheet crystalline structure of SF, showing improved storage and loss modulus. The IPN hydrogels show volume phase transition behavior at the same temperature and NaCl concentration as pure PNIPAAm hydrogels. The PNIPAAm/SF IPNs keep the swelling kinetics of PNIPAAm, while showing increased deswelling kinetics, with the internal water molecules rapidly released through the induced β-sheet networks. The IPNs with SF β-sheet structure successfully decrease the formation of skin layer observed in conventional PNIPAAm hydrogels. Therefore, the proposed IPN hydrogels can provide three benefits; improved mechanical properties, biocompatibility, and deswelling rates. The effect of SF β-sheet networks on the IPNs composed of IPAAm and acrylic acid (AAc) is compared with that on the PNIPAAm/SF IPNs and the parameters controlling the deswelling kinetics of the IPNs are investigated. The manufacture of porous scaffolds bearing stimuli sensitivity was proposed by freeze-drying the IPNs. Three parameters, the skin layer formation, the restriction of SF β-sheet networks, and the aggregation force of NIPAAm chains, complexly work in the deswelling process of IPN hydrogels and scaffolds according to SF content and incorporation of AAc moiety.

3.1. Introduction

Stimuli-responsive polymers have been vigorously investigated due to their attractive properties: they undergo relatively large and abrupt, physical or chemical changes in response to small external changes in environmental conditions. These polymer systems have been utilized in bio-related applications such as drug delivery [1-8], biotechnology [9, 10], and chromatography [11-13]. Stimuli-responsive polymers can be applied in different forms as follows [14]; cross-linked (permanently) hydrogels [15-18], theromoreversible hydrogels [19-21], micelles [22, 23], modified interfaces [24-26], and conjugated solutions [27-28]. Recently we reported a systematic review of the molecular designs of stimuli-responsive polymers according to types of responding stimulus and physical forms with their bio-related applications [14]. Among these physical forms, hydrogels, which are formed with a three-dimensional (e.g. chemically or physically cross-linked) network of hydrophilic polymer chains, provide the interesting property that they swell, but do not dissolve in aqueous environment. In stimuli-responsive hydrogels, the cross-linked networks could dramatically change their dimensions by an alternative change of hydrophobicity and hydrophilicity [3, 18].

Poly(*N*-isopropylacrylamide) (PNIPAAm) has been the most actively investigated temperature-responsive polymer due to its sharp phase transition in water (a lower critical solution temperature (LCST)) at around 32°C [29]. The limitations to hydrogels composed of PNIPAAm have been disscussed, such as biocompatibility, deswelling rate, and mechanical properties [14]. The need to improve these properties led to the introduction of

other functionalities. The PNIPAAm-based hydrogels have been modified to be more versatile materials by incorporating more hydrophilic moieties in the polymer backbone or the graft chain [30, 31], and by introducing hybrid forms with silica [32] or interpenetrating networks (IPNs) with protein [33-34].

In versatile applications, such as biomimetic actuators, rapid sensitivity to stimulus is necessarily demanded. Changing the physical forms of hydrogel has been suggested to provide rapid deswelling kinetics. Macropore structures and phase-separated structures were reported to increase swelling-deswelling sensitivity of hydrogels, by increasing the surface area [35, 36]. The fabrication of hydrogel on the microstructure scale could lead to shorter response time to stimuli [37]. Especially, PNIPAAm hydrogels have a very slow deswelling rate due to the formation of a skin layer, which interrupts the release of internal water molecules in the deswelling process. Chemical modification of PNIPAAm networks, such as copolymerization with acrylic acid (AAc) and incorporation of graft chains with PNIPAAm [18] or poly(ethylene oxide) (PEO) [30], has been reported to accelerate the deswelling kinetics by suppressing the formation of skin layer. IPNs of PNIPAAm was introduced to improve the deswelling rate [38].

Silk fibroin (SF), which can be obtained by degumming silkworm silk from *B. mori*, is a fibrous protein of silk fiber and consists of heavy (350 kDa) and light (25 kDa) chain polypeptides, connected by a disulfide link [39]. The heavy chain consists of a high content of Gly–Ala–Gly–Ala–Ser repeats constructing β-sheet structures in the fibrous form [39]. SF has been reported to be dissolved in neutral salt solutions such as LiBr and $Ca(NO_3)_2$

[40, 41, 42]. The regenerated SF film [40], fiber [41], and scaffold [42] have been introduced for biomaterials due to good mechanical strength in the wet state [42], biocompatibility for the growth of cells [43], high dissolved-oxygen and water-vapor permeability [44] and resistance against enzymatic degradation [45]. Also, non-textile applications for biomedical fields have been explored for surgical sutures [46], cosmetics [47], enzyme immobilization [48], wound covering materials [49], substrate for cell culture [43], controlled drug-delivery carriers [50], and scaffolds for tissue engineering. [42]

To obtain PNIPAAm hydrogels with high mechanical strength, superior biological properties and, moreover, accelerated deswelling kinetics by suppressing the skin layer formation, interpenetrating polymer networks of SF and PNIPAAm we synthesized and examined. Also, the hydrophilic AAc moiety was incorporated in PNIPAAm backbones and the IPNs with the P(NIPAAm-co-AAc) and SF were synthesized and compared with PNIPAAm/SF IPNs. From the incomparison, we elucidate the parameters controlling the deswelling kinetics of the IPN hydrogels. A three dimensional scaffold can be developed by fabricating a porous SF membrane [42]. One strategy of manufacturing SF scaffold is the freeze-drying method [42, 51]. Therefore, the three dimensional scaffolds with stimuli responsiveness can be developed by freeze-drying PNIPAAm/SF and P(NIPAAm-co-AAc)/SF IPNs. The swelling and deswelling behaviors of the freeze-dried IPNs are examined and the interpretation of the deswelling process is focused on the role of skin layer formation, restriction of SF β-sheet networks, and aggregation forces between NIPAAm chains.

3.2. Experimental Section

3.2.1. Materials

N-Isopropylacrylamide (NIPAAm; Aldrich Chemical Co., Milwaukee) was recrystallized twice from the *n*-hexane. Acrylic acid (AAc; Aldrich Chemical Co., Milwaukee) was purified by distillation at 55°C in high vacuum. *N*,*N*'-methylenebis (acrylamide) (BIS), ammonium persulfate (APS), and *N*,*N*,*N*',*N*'-tetramethylethylenediamine (TEMED), sodium lauryl sulfate, sodium carbonate, poly(ethylene oxide) (PEO, M*v*: ca. 600,000; Aldrich Chemical Co., Milwaukee) and calcium nitrate were purchased from Aldrich or Fisher and used as received. Grade 5A raw silk with an average denier of 20.86 produced in Brazil by the Fiaçào de Seda Bratac S.S. was used. All chemicals were of analytical grade. Phosphate-buffered saline solution (PBS; pH7.4) was used for all the experiments.

3.2.2. Preparation of SF aqueous solution

The *Bombyx mori* silk was degummed with 0.25 % w/v sodium lauryl sulfate and 0.25% w/v sodium carbonate in boiling water, bath ratio of 1:10(w/v), for 1 hour. The dried silk fibroin (20 g) was dissolved in $Ca(NO_3)_2$-$4H_2O$/MeOH 75/25 w/w solution (180 g) at 67°C for 6 hr. The silk fibroin solution (10 w/w %) was dialyzed with cellulose membrane tube (MWCO 6,000-8,000) for 4 days by changing the deionized water daily. The concentration of dialyzed SF solution was controlled to 10 w/v % by dialyzing reversely with PEO powder.

3.2.3. Preparation of PNIPAAm/SF Hydrogels

PNIPAAm and SF blend solutions were prepared to a final total concentration of 10 % w/v by mixing aqueous NIPAAm (10 % w/v) and SF (10 % w/v) solution.

PNIPAAm/SF IPN gels were prepared by free radical polymerization of NIPAAm and additional organic solvent treatment to induce β-sheet crystalline network of SF. BIS (2.7 wt % of NIPAAm) as a cross-linker, and TEMED (10 μL) as an accelerator were additionally dissolved in 10 mL of NIPAAm/SF solution, and dry argon gas was bubbled into the solution for 10 min to remove the dissolved oxygen. After APS (10 mg) as an initiator was added, the solution was thoroughly stirred and immediately poured into a glass mould (3 mm thick) and covered with a glass plate. The solution mixture was polymerized at 10 °C for 1 day. The PNIPAAm/SF gel membrane which formed was immersed in methanol (gel weight/methanol: 1/3 (w/w)) for 1 day to introduce β-sheet conformation of SF in PNIPAAm networks and dried in air for 2 days. The dried membrane was immersed in pure water for 7 days by changing pure water daily to remove unreacted chemicals. The swollen IPN hydrogels were cut into disks (1.2 mm diameter) with a cork borer. The disk type gels were dried in air for 2 days and additionally dried in vacuum for 1 day.

3.2.4. Preparation of P(NIPAAm-co-AAc)/SF Hydrogels

P(NIPAAm-co-AAc)/SF Hydrogels were synthesized by the same method as PNIPAAm/SF IPN hydrogels. Aqueous monomer mixture solution (10% w/v of monomers) of NIPAAm (98.7% wt) and AAc (1.3% wt) was used instead of NIPAAm solution.

3.2.5. Preparation of Freeze-Dried Hydrogels

PNIPAAm/SF and P(NIPAAm-co-AAc)/SF Hydrogels were freeze-dried before methanol treatment. The freeze-dried samples were treated in Methanol/Water (3/1 w/w)

bath for 2 hours. The dried samples were immersed in pure water for 7 days as discussed above.

3.2.6. X-ray Studies

The Wide Angle X-ray Diffraction (WAXD) curve of PNIPAAm/SF film was obtained with a Seimens type F X-ray diffractometer. Ni-filtered Cu Kα radiation was used for the X-ray source at 35 kV and 25 mA. All scans were performed from 5 ° to 40 ° (2θ) at a speed of 1.0°/min.

3.2.7. Rheology Studies

The viscoelastic properties of PNIPAAm/SF semi-IPN and IPN hydrogles we investigated by dynamic shear oscillation measurements at small constant shear strain. These measurements we carried out with REOLOGICA rheometer (REOLOGICA Instruments AB), using parallel plates of 25 mm diameter. The loaded normal force onto each hydrogel film was automatically adjusted at 2.0 N. Mechanical spectra we measured with a constant shear strain of 1×10^{-3} over frequency range of 0.1 ~ 10 Hz at 17 °C.

3.2.8. Measurement of the Swelling Ratio

The swelling ratios of hydrogel samples were gravimetrically monitored as a function of composition (PNIPAAm to SF) in the temperature range from 20 ° to 45°C and NaCl concentration range from 0 ~ 4 M. The experimental plots were obtained from averages of three samples. The equilibrium swelling ratio was defined as the weight of absorbed water (W_w) per weight of dried gel (W_g). Water content is defined as $(W_w/W_h)\times100$, where W_h is the weight of hydrogel.

For a dynamic swelling kinetic study, the hydrogels were swollen in PBS (pH7.4) at 20 and 45 °C, removed, wiped with moistened tissue paper, and weighted at regular intervals. For a temperature dependence study on swelling ratios, the swelling ratios of the IPN hydrogels were monitored by lowering the temperature step-wise from 45 to 10 °C after at least a 2 day soaking at each targeted temperature. The desired temperature was controlled by a thermostated water bath (Precision digital water bath) with a resolution of ±0.05 °C.

3.2.9. Measurement of the Deswelling and Oscillating swelling-deswelling kinetics

To measure the deswelling kinetics, the IPN hydrogles were equilibrated in PBS at 20 °C and quickly transferred into PBS at 45 °C. The IPN hydrogels were taken out of PBS at regular intervals and weighed after removing excess water from the IPN hydrogels surface. Deswelling kinetics were defined by the temperature dependent weight changes of the IPN gels and were illustrated between equilibrium swollen (100%) states at 20 °C and equilibrium shrunken (0%) states at 45 °C. The Initial deswelling rate of hydrogels was calculated from the weight decreases of hydrogels for the initial 5 min and defined as the decreased gel weight for 5 min per swollen gel weight at 20 °C per 5 min ([g/g]/min).

For the measurement of the oscillating swelling-deswelling kinetics of the IPN hydrogels in response to a temperature jump, the IPN hydrogels were rapidly transferred between 20 °C and 45 °C PBS solution over 4-min temperature cycles. The IPN hydrogels were taken out and wiped with moistened tissue paper, and weighed at regular intervals.

3.3. Results and Discussion

3.3.1. Preparation of Hydrogels

PNIPAAm/SF hydrogels were prepared by radical polymerization of NIPAAm monomer and BIS as a cross-linker in the presence of SF molecules with random coil structure in aqueous solution. The weight ratio of SF to NIPAAm monomer was chosen to be from 0.05 to 0.8. Pure PNIPAAm gel was also prepared without adding SF. Before methanol treatment, the prepared hydrogels were clear and transparent, which means the absence of macroscopic phase separation and crystalline structure of SF. In the process of methanol treatment, the PNIPAAm/SF IPN gel membrane (7 g) was immersed in 21 g of methanol in order to adjust the weight ratio of methanol to the absorbed water as ca. 3/1 (w/w). After 1 day treatment, the dried gels were immersed in pure water for 7 days by changing water everyday to remove any remaining reagents. The pure PNIPAAm gel was clear and transparent, but the IPN gels looked more turbid with increasing SF content, which should originate from the induced β-sheet crystalline structure of SF in these IPN hydrogels.

P(NIPAAm-co-AAc)/SF hydrogels were also prepared by radical polymerization with additional AAc. The copolymerization of hydrophilic monomer with PNIPAAm has been reported to accelerate the temperature responsive hydrogel deswelling rates [30, 31]. Especially, 1.3 wt % AAc-containing PNIPAAm hydrogel showed maximum rapid deswelling, since the AAc segments interupted long linear NIPAAm segments, and their hydrophobic aggregation forces decreased [30]. The deswelling rate rebounded over a certain threshold of AAc content, enough to suppress skin layer formation. Therefore, 1.3 wt % of AAc to PNIPAAm was selected to investigate the effect of SF crystalline structure on the AAc-containing PNIPAAm hydrogels with rapid deswelling kinetics. The pure

P(NIPAAm-co-AAc) gel was clear and transparent, but the IPN gels also looked more turbid with increasing SF content. The synthesis of PNIPAAm/SF and P(NIPAAm-co-AAc)/SF IPN hydrogels was summarized and their sample codes are listed in Table 3-1.

Table 3-1 Preparation of PNIPAAm/SF and P(NIPAAm-co-AAc)/SF IPN hydrogels

Sample code	Weight fraction		Sample code	Weight fraction	
PN/SF IPNs	NIPAAm[1]	SF[2]	PNA/SF IPNs	NIPAAm/AAc[3]	SF
PN100	1.0	0	PNA100	1.0	0
PN95	0.95	0.05	PNA95	0.95	0.05
PN90	0.9	0.1	PNA90	0.9	0.1
PN80	0.8	0.2	PNA80	0.8	0.2
PN70	0.7	0.3	PNA70	0.7	0.3
PN60	0.6	0.4	PNA60	0.6	0.4
PN40	0.4	0.6	PNA40	0.4	0.6
PN20	0.2	0.8	PNA20	0.2	0.8

1: In 10 mL aqueous solution, 1g of NIPAAm, 0.027 g of BIS, 10 mg of APS, and 10μL of TEMED
2: 10 % w/v of SF aqueous solution
3: In 10 mL aqueous solution, 0.987 g of NIPAAm, 0.013 g of AAc, 0.027 g of BIS, 10 mg of APS, and 10μL of TEMED

PNIPAAm/SF (PN/SF) and P(NIPAAm-co-AAc)/SF (PNA/SF) IPNs are developed by the permanent entanglement of β-sheet crystalline (physical cross-links) and PNIPAAm (chemical cross-links) networks. Schematic structures of PN/SF IPN hydrogels are provided in Scheme 3-1. SF crystalline networks are proposed to increase physical properties as well as biocompatibility. Moreover, SF networks are proposed to produce drain channels for internal water molecules from the hydrogel matrix in the deswelling process by suppressing the skin layer effect, a signifcant drawback in PNIPAAm hydrogels.

3.3.2. Induced β-sheet Crystalline Structure of SF in PNIPAAm Networks

To investigate the induced β-sheet crystalline structure of SF in PNIPAAm networks, WAXD was used. Figure 3-1 shows the WAXD curves of PN40 dried film after the methanol treatment as the described above. It was reported that a broad peak is shown

at 2θ = 20° in regenerated SF as a typical characteristic pattern of an amorphous structure, and a major peak is observed at 2θ = 21° and two minor peaks at 9° and 24° in a methanol treated SF, assigned as characteristic peaks of a β-sheet crystalline structure [41]. The treated PN/SF shows a strong peak at 2θ = 21° and small peaks at 9 ° and 24 °, indicating that β-sheet conformation of SF was induced in PNIPAAm networks to produce an IPN structure. This result supports the conclusion that β-sheet crystalline structure of SF is successfully introduced in PNIPAAm networks, and that the PNIPAAm networks do not interrupt the conformational change of SF by increased topological constraints such as entanglements.

3.3.3. Improved viscoelastic properties of IPN hydrogels

Figure 3-2-a) and b) shows the storage modulus (G') and loss modulus (G'') of the untreated PN/SF hydrogels as function of frequency at 17 °C. In the frequency range investigated, all the mechanical spectra showed a pronounced plateau. In these mechanical spectra, G' are considerably higher than G'' in all compositions of PNIPAAm and silk fibroin, which means that the hydrogels represent typical characteristics of well developed polymeric networks. The PN/SF hydrogels, prepared without methanol treatment, shows lower G' and G'' with higher content of SF. Because these SF molecules contribute amorphous structure without physical cross-links in PNIPAAm networks, the SF component should not govern the viscoelastic property of the hydrogels and only PNIPAAm networks mainly affect the gel property. These complex hydrogels represent a semi-IPN structure. Gel network density (PNIPAAm) should be lower with higher content

of SF, so that the moduli of complex hydrogels would be lower than pure PN100 hydrogel. The effect of SF content in PN networks on the storage modulus and loss modulus is represented in Figure 3-3. The presented G' and G'' of the hydrogels were observed at a frequency of 1 Hz. Both G' and G'' decrease with more SF content, exhibiting typical S-type curves.

By contrast, the methanol treatment leads the PN/SF hydrogels to show fully developed IPN structure as shown in the X-ray result, resulting in increased viscoelastic properties with more SF content. Figure 3-4-a) and b) exhibit the storage modulus (G') and loss modulus (G'') of the treated PN/SF hydrogels as a function of frequency at 17 °C. As expected, the fully developed IPN hydrogels show considerably smaller G'' than G', which is observed as characteristic of well-developed gel-networks. The treated PN100 hydrogel shows unchanged G' and G'', compared with the untreated one. However, the treated complex hydrogels exhibit higher G' and G'' than pure PN100 hydrogel. Interestingly, the order of the moduli increases from lower content of SF to higher content of SF, which is an opposite tendency with the untreated complex hydrogels, because the untreated ones showed the lower moduli with higher content of SF. The comparison of G' and G'' of the IPN hydrogels in SF weight fraction at the frequency of 1 Hz is represented in Figure 3-5. Both G' and G'' increase with more SF weight fraction, showing pronounced S-type curves. This indicates that the β-sheet crystalline structure of SF in PN/SF IPN hydrogels enhanced the viscoelastic properties of PNIPAAm networks. One drawback of PNIPAAm hydrogel has been its physical properties in the gel state. The G' increases 1.6 times with only 10

wt % of SF, 7 times with 30 wt% of SF and 14 times with 40 wt% of SF, compared with the G' of PNIPAAm hydrogel.

3.3.4. Dynamic swelling of IPN hydrogels

Figure 3-6-a) and b) show the dynamic swelling of the PN/SF and P(NIPAAm-co-AAc)/SF IPN hydrogels in PBS (pH 7.4) at 20 °C, below the LCST. At 20 °C, below the phase transition temperature (T_p), the IPN hydrogels with the higher content of SF shows lower swelling ratios in both PN/SF and P(NIPAAm-co-AAc)/SF. When the swelling ratios of P(NIPAAm-co-AAc)/SF are compared with those of PN/SF, the AAc component, which shows more hydrophilic characteristic, leads the hydrogels to swell more in the whole range of SF content. However, all IPN hydrogels reach an equilibrium state within 1 day, which represents almost the same swelling behaviors to reach equilibrium as pure PN and P(NIPAAm-co-AAc) hydrogels.

Figure 3-7 exhibits the plots for the equilibrium swelling ratios versus SF weight fraction for the PN/SF and P(NIPAAm-co-AAc)/SF IPN hydrogels, respectively. The relation of SF content to equilibrium swelling ratios represents almost a linear decrease.

Also the dynamic swelling kinetics in PBS (pH 7.4) at 45 °C, above the LCST, are shown in Figure 3-8-a) and b) for PN/SF and P(NIPAAm-co-AAc)/SF IPN hydrogels, respectively. At 45 °C, above the T_p, the swelling ratios of the IPN hydrogels are very low, but the order of swelling ratios to SF content is totally opposite to that of swelling ratios at 20 °C. This means that the shrunken conformation of PNIPAAm or P(NIPAAm-co-AAc) networks provide more repulsive force for dehydration than even very fine β-sheet crystalline

networks of SF, so that the more content of PNIPAAm or P(NIPAAm-co-AAc) leads to a lower equilibrium swelling ratio above the T_p. All IPN hydrogels reaches equilibrium swelling within 9 hr. P(NIPAAm-co-AAc)/SF IPNs swell more than PN/SF IPNs even at 45 °C, at which temperature the gels are shrunken, due to their hydrophilic property of AAc component.

3.3.5. Phase Transition temperature with equilibrium swelling test

Figure 3-9-a) shows equilibrium swelling ratios for PN/SF IPN hydrogels in PBS (pH 7.4) in the temperature range from 45 to 20 °C. The PN/SF IPN hydrogels are swollen at lower temperature and shrunken above the T_p. The T_p of PN/SF IPN hydrogels is observed at 31 °C, at which pure PN100 hydrogel shows the T_p. This indicates that SF crystalline networks do not interfere with the forces triggering conformational changes of PNIPAAm, even though the amount of absorbed water into the IPN networks is changed by the SF crystalline structure. The fact that the entanglement does not change the T_p implies that the intra-molecular interaction of PNIPAAm operates at a smaller scale than the entanglement lengths. However, PN20 shows a small increase of swelling without significant phase transition behavior. This indicates that high content of SF might suppress abrupt hydration caused by conformational change of PNIPAAm molecules.

The equilibrium swelling ratios for the P(NIPAAm-co-AAc)/SF IPN hydrogels in PBS (pH 7.4) are shown in Figure 3-9-b). The T_p of P(NIPAAm-co-AAc) gel is observed at 37 °C, a higher temperature than the T_p of PN100 gel. In general, the LCST of a temperature responsive polymer is known to be influenced by hydrophobic or hydrophilic comomomers

in its molecular chains. Copolymerization with a small ratio of hydrophilic monomers, such as acrylamide and acrylic acid [52] has been reported to increase T_p to higher temperature as well as their swelling properties. More hydrophilic moiety in PNIPAAm chain would make the LCST increase and even disappear [53]. There is the no significant change in T_p of P(NIPAAm-co-AAc)/SF IPN hydrogels with SF β-sheet crystalline networks, demonstrating that entanglement in IPN structure does not interrupt the conformational change of P(NIPAAm-co-AAc).

3.3.6. Salt effects on phase transition of IPN hydrogels

PNIPAAm has been investigated not only for its temperature-responsive phase transition but also for its salt-responsive phase transition [34]. Usually, the salt effect on hydrogels has been reported for polyelectrolyte polymers such as a block copolymer composing *N,N'*-dimethyl aminoethyl methacrylate (DMAEMA) [54]. However, it is interesting that nonionic PNIPAAm hydrogels shows a volume phase transition responding to salt concentration. Pack et al. explained that the chloride ion plays a role to induce dehydration of the hydrogels by the mechanism of interfering with the bound water around PNIPAAm chains [55]. Dhara et al. reports that PNIPAAm hydrogels in IPNs with gelatin exhibit phase transition at the same salt concentration as pure PNIPAAm hydrogels without hindering the dehydration of PNIPAAm chains by the more hydrophilic characteristic of gelatin [34]. In the case of our PN/SF IPNs, fine SF β-sheet crystalline networks could disrupt the salt effect on PNIPAAm chains. Therefore, the effect of NaCl concentration on the water content of the PN/SF IPN hydrogels is investigated to reveal this supposition and

represented in Figure 3-10. However, the IPN hydrogels except PN20 showed the same phase transition as pure PN100 hydrogel at 1.0 M NaCl. The IPN hydrogels abruptly shrink above 1.0 M NaCl, but only PN20 does not show abrupt phase transition at 1.0 M NaCl despite dehydration with higher NaCl concentration. This result suggests that even though a too high content of SF can interrupt the phase transition by increased topological constraints, other IPNs keep the salt responsive phase transition property of PNIPAAm without disrupting the conformational change related to salt concentration.

3.3.7. Transparency and surface roughness of hydrogels

Table 3-2 shows the changes of transparency and surface roughness of PN/SF and PNA/SF IPN hydrogels after transferring the swollen gels at 20 °C into PBS at 45 °C. Both PN/SF and PNA/SF IPNs lost the transparency of pure PN100 or PNA100 hydrogels as SF content increased. This result should be because of the induced β-sheet crystalline structure in the IPN networks. However, the β-sheet crystalline did not make the IPNs completely opaque, because even pure SF film treated in methanol is not completely opaque. Pure PN100 hydrogels exhibited the most dramatic change in the transparency and surface roughness with temperature jumping, indicating that PN100 hydrogel show a skin layer formation in the deswelling process. The hardened surface blocks the water flow from the interior of the hydrogels above T_p, resulting in the increased hydrodynamic internal pressure and accumulation of water molecules near the surface of hydrogels [18].

Table 3-2 Changes of transparency and surface roughness of PNIPAAm/SF and P(NIPAAm-co-AAc)/SF IPN hydrogels in deswelling process

SF Content	PN/SF IPNs				P(NIPAAm-co-AAc)/SF IPNs			
	Swollen (20 °C)		Collapsed[3] (45 °C)		Swollen (20 °C)		Collapsed(45 °C)	
	Transparency[1]	Surface roughness[2]	Transparency	Surface roughness[2]	Transparency	Surface roughness	Transparency	Surface roughness
0	+++	–	– – –	+++	+++	–	++	–
0.05	++	–	– – –	+++	++	–	+	–
0.1	++	–	– – –	+	++	–	+	–
0.2	+	–	– – –	–	+	–	+	–
0.3	+	–	– – –	–	+	–	+	–
0.4	–	–	– – –	–	–	–	–	–
0.6	–	–	–	–	–	–	–	–
0.8	–	–	–	–	–	–	–	–

1: +++: very transparent, – – –: very opaque. 2: +++: very rough, –: smooth.
3: measured by transferring swollen gels at 20 °C into PBS at 45 °C.

The surface of PN100 hydrogels became rough and showed bubbles, which should occur for the reason described above. PN95 shows almost the same appearance change as PN100 does by putting the gels above T_p. During the deswelling, PN90 looked completely opaque and still had a little roughening surface. In the deswelling process, the other PN/SF IPN hydrogels also looked completely opaque except PN40 and PN20, but showed smooth surfaces. PN40 and PN20 kept their translucent and smooth surface.

By contrast, in the deswelling process, pure PNA100 and PNA/SF IPNs kept their translucent appearance, though they showed a small decrease of their transparency. Also, they did not exhibit any bubble-like structures and rough surfaces with temperature jumping. In PN/SF and PNA/SF IPNs with the same composition of SF, their transmittance changes with temperature jumping above T_p were different. If the size of hydrophobic aggregates is larger than the wavelength of visible light, the hydrogels become opaque in the deswelling process. The reason that PN100 and PN/SF IPNs looked opaque in the deswelling process is because PNIPAAm networks in PN/SF IPNs aggregate with larger

size than the wavelength of visible light. However, PN40 and PN20 kept the translucent appearance after temperature jumping, resulting from the relatively smaller composition of PNIPAAm. By contrast, PNA100 and PNA/SF IPNs retained their translucent appearance in the deswelling process, indicating that the hydrophobic aggregate size of P(NIPAAm-co-AAc) chains is smaller than the wavelength of visible light. The AAc moiety should divide the PNIPAAm backbone when incorporated in PNIPAAm chains, and make the hydrophobic aggregate size smaller. From these results, we notice that the SF networks do not affect the hydrophobic aggregate size of PNIPAAm or P(NIPAAm-co-AAc) chains in the IPN structure and the aggregate size only depends on PNIPAAm or P(NIPAAm-co-AAc) networks.

3.3.8. Deswelling kinetics of IPN hydrogels

Figure 3-11 exhibits the deswelling kinetics of PN/SF IPNs after moving quickly the hydrogels swollen in the equilibrium state at 20 °C, below T_p, to the PBS bath at 45 °C, above T_p. The swelling degree of PN100 hydrogel decreases very slowly to reach a new equilibrium. As mentioned in the previous section, the clear and transparent PN100 hydrogel swollen at 20 °C changed its appearance to opaque and its smooth skin at 20 °C became hardened and rough at 45 °C. This indicates that PN100 hydrogels show pronounced skin layer formation, which blocks the water flow from the hydrogel in spite of the gradually increased hydrodynamic internal pressure [18]. The skin layer formation of PN100 hydrogels has been reported as improvable by modifying its chemical structure by copolymerization [30] and grafting [30, 31]. Incorporation of a hydrophilic moiety such as AAc to the PNIPAAm backbone could disrupt the skin layer structure observed in

pure PN100 hydrogels. However, the hydrophobic aggregation force decreased with more AAc content due to the division of the NIPAAm chains into multiple short segments, leading to a lower deswelling rate [30]. Hydrophilic graft chains such as PEO were reported to act as releasing channels for water molecules from the skin layer and to sustain a strong hydrophobic attraction of PNIPAAm without the weakening of the backbone aggregation force. However, the deswelling rate of the hydrogels decreased with 11 wt % of PEO as graft chains. The higher content of hydrophilic graft chain broke the hydrophilic/hydrophobic balance, leading to a decrease of deswelling rate.

On the other hand, IPN structure provides a different influence on PNIPAAm hydrogels. The entanglement of the network structures would provide a physical restriction for gel shrinkage rather than causing a change of PNIPAAm chain aggregation force or a change of hydrophilic/hydrophobic balance, as caused by the modification of chemical structure. As shown in Figures 3-7 and 8, the swelling ratio of PN/SF hydrogels decreases at 20 °C and increases at 45 °C with more SF content, suggesting that a physical restriction of the induced SF crystalline networks acts against expansion or aggregation of PNIPAAm network. Actually, there is no pronounced force to expand or shrink SF networks with a temperature change. Therefore, hydrophilic expansion forces and hydrophobic aggregation force of PNIPAAm networks produced by thermal change have an additional burden to move SF networks with their own changes. In the deswelling process, there are three factors to control the deswelling kinetics: lowered skin layer formation by SF networks, the strong aggregation force of PNIPAAm chains, and the physical restriction of SF networks, which would act as sustaining force against the volume change of IPN

networks. In Figure 3-11, PN95 does not show a significant difference with PN100 in the deswelling curve, indicating that only 5 wt % of SF networks are not enough to remove skin layer formation. However, deswelling process becomes faster in PN/SF IPN hydrogels containing more than 10 wt % SF without significant skin layer formation. However, the transparent PN90 hydrogel at 20 °C changed to opaque and showed a slightly rough surface at 45 °C, which means it still has a weak skin layer. PN80, PN70 and PN60 show faster deswelling kinetics than PN100, PN95 and PN90. Even though PN70 has more physical restriction by SF networks than PN95 and PN90, thus, the decrease of skin layer effect should overwhelm the physical restriction of SF networks in PN/SF IPNs. However, PN40 and PN20 show decreased deswelling kinetics, because the restriction of SF networks might exceed the aggregation force of PNIPAAm chains at higher SF content. The initial deswelling rates of PN/SF IPN hydrogels are shown in Figure 3-12. The initial swelling rate was calculated from the decreased gel weight within 5 min after transferring gels to 45 °C per the swollen gel weight at 20°C. A maximum is shown at PN70, but PN80, PN70 and PN60 exhibit very similar initial swelling rates.

It is a very exiting result that SF networks increase not only the viscoelastic properties of PNIPAAm hydrogels (shown in section 3.3.3.), but also enhance their deswelling rates. The SF β-sheet crystalline networks act as drain channels for water molecules, so that the increased hydrodynamic internal pressure at higher temperature drives internal water to be quickly expelled.

The deswelling curves of PNA/SF IPN hydrogels under the same conditions described

above in PN/SF IPNs are represented in Figure 3-13. Pure PNA100 hydrogels shows very fast dewelling kinetics upon increasing temperature above the T_p. Also, PNA100 hydrogel swollen at 20 °C kept its transparency and smooth skin even in the process of deswelling at 45 °C. This suggests that pure PNA100 hydrogel does not show a considerable skin layer formation in the deswelling process. In PNA/SF IPN hydrogels, SF networks decreased the deswelling kinetics, compared with pure PNA100 hydrogel. As described above, three factors, the decreased skin layer formation, the restriction of SF networks and the aggregation force of PNIPAAm chains, could be considered to also control the deswelling process in PNA/SF IPNs. However, the first factor, skin layer formation, should not be a major factor to control the deswelling process in PNA/SF IPNs, because P(NIPAAm-co-AAc) networks themselves do not have a significant skin layer formation in the deswelling process. Therefore, the restriction of SF networks should operate as a major factor governing the deswelling process of PNA/SF IPN hydrogels, resulting in lower deswelling kinetics of PNA/SF IPNs than pure PNA100. Figure 3-14 shows the initial deswelling rates of PNA/SF hydrogels. It is surprising that the initial deswelling rate curve of PNA/SF IPNs shows a maximum peak at PNA70 even though the peak of PNA/SF IPNs is not as notable as the peak of PN/SF IPNs. This means that the first factor still controls the deswelling kinetics in PNA/SF IPNs: a weak skin layer effect remains in PNA100 and PNA/SF IPN hydrogels. The fact that PNA95 show a lower initial deswelling rate than a PNA70 suggest the following: only 5 wt % of SF networks disrupt the aggregation force of P(NIPAAm-co-AAc) chains in PNA/SF IPNs, similar to 30 wt % of SF networks, and the 30 wt % of SF networks reduce skin layer formation more effectively than do the 5 wt% of SF

networks. This result matches PN95, which showed skin layer formation like pure PN100, which means 5 wt % of SF is not sufficient to prevent skin layer effect in both PN/SF and PNA/SF IPNs. Although there are slight differences of initial deswelling rate among PNA90, PNA80, PNA70 and PNA60, PNA70 represents a maximum. This result coincides with PN/SF IPNs, which showed a maximum peak of initial swelling rate at PN70. PNA40 and PNA20 exhibit decreased initial deswelling rates on a relatively large scale, indicating that the aggregation force of P(NIPAAm-co-AAc) chains compete with the physical restriction force of SF networks as shown in PN40 and PN20.

When the dewelling rates of PNA/SF IPNs are compared with those of PN/SF IPNs, we can observe the effect of AAc components on the aggregation force of PNIPAAm networks without consideration of skin layer effect (Figure 3-12). Only PNA95 shows faster deswelling rate than PN95 because of more skin layer formation in PN95 than PNA95. However, PN/SF IPN hydrogels exhibit faster deswelling rate than PNA/SF IPN hydrogels at other compositions except 5 wt % of SF, indicating that the AAc component decreases the aggregation force of PNIPAAm chains, when the skin layer effect is not considerable. Especially, PN70 and PNA70 show the biggest difference between their initial deswelling rates: PNA70 exhibit 31 % decrease of initial deswelling rate, compared with PN70. Both have low skin layer formation and well-developed SF network channels with same physical restriction force of SF networks due to the same content of SF. This result is because the hydrophilic AAc moiety should retain more water in the deswelling process, and the strong hydrophobic aggregation force of PNIPAAm backbone should be weakened due to the division of PNIPAAm long chains into short sequences by incorporation of

hydrophilic AAc units. Therefore, if a skin layer effect is not considerable, incorporation of AAc moiety should negatively affect the deswelling process, leading to a decrease of deswelling rate.

3.3.9. Swelling and Deswelling properties of freeze-dried IPN hydrogels

One strategy for increasing the deswelling rate of PNIPAAm hydrogels is to develop macroporous structures by increasing surface area [35, 36]. The strategies to develop macroporous structure of PNIPAAm hydrogels have been suggested by irradiation polymerization above LCST [36] and incorporation of poly(ethylene glycol)s as the pore-forming agent [56]. On the other hand, porous SF matrix has been reported as a potential cell culture substrate and a scaffold for artificial tissue [42, 51]. Nazarov and Kaplan reported porous SF scaffolds manufactured by salt leaching, gas forming or freeze-drying [42]. A freeze-dried SF/poly(vinyl alcohol) blend membrane was reported to form a macroporous structure [51]. The freeze-drying method can be easily utilized to develop not only porous SF but also a porous blend membrane containing SF.

A freeze-dried PN70 (FPN70) and a freeze-dried PNA70 (FPNA70) were selected to investigate the effect of freeze-drying on the swelling ratio and deswelling rate of the IPN hydrogels and compare them with PN70 and PNA70. Figure 3-15 exhibits the equilibrium swelling ratios of PN70, PNA70, FPN70 and FPNA70 at 20 °C and 45 °C. FPN70 and FPNA70 show higher swelling ratios than PN70 and PNA70, respectively. This indicates that freeze-dried IPN hydrogels have more volume space to reservoir water molecules in their expanded and collapsed networks. There are two possibilities for the increased

swelling ratio: the increased volume space for water can be considered microscopically and macroscopically. Macroscopically generated volume space might be the macropores and microscopically induced volume space might be attributed to the decreased restriction of SF networks, resulting in the more expanded PNIPAAm or P(NIPAAm-co-AAc) networks and more bound water. Figure 3-16 shows the deswelling kinetics after jumping FPN70 and FPNA70 swollen in equilibrium state at 20 °C to 45 °C, compared with PN70 and PNA70. The FPN70 exhibits lower deswelling kinetics than PN70. By contrast, FPNA70 shows faster deswelling kinetics than PNA70. The initial deswelling rates of FPN70 and FPNA70, calculated by the same method as above, support the opposite effect of freeze-dring (Figure 3-17). FPN70 shows lower initial deswelling rate than PN70 (9.5 (g/g)/min (PN70); 5.3 (g/g)/min (FPN70)), but FPNA70 exhibits a higher initial deswelling rate than PNA70 (6.5 (g/g)/min (PNA70); 10.8 (g/g)/min (FPNA70)). This contrast in the behavior of freeze-dried FPN70 and FPNA70 can not be explained macroscopically, because the macroporous structure should increase the surface area of the hydrogels, resulting in the increased deswelling kinetics of both FPN70 and FPNA70. Therefore, the freeze-drying process may affect the microscopical structure of the IPNs. If the FPN70 and FPNA70 have more bulky SF crystalline networks, the physical restriction of SF networks on PNIPAAm or P(NIPAAm-co-AAc) networks should decrease. In the case of FPNA70, there is a negligible effect of skin layer formation in P(NIPAAm-co-AAc) chains, so that the deswelling process is governed by the decreased physical restriction of SF networks. Therefore, the macroscopically and microscopically changed structure of FPNA70 should

act positively to increase the deswelling rate. However, FPN70 has another major factor: the skin layer effect of PN chains. This means that FPN70, which bears the more expanded SF networks, have a higher skin layer effect than PN70. Despite the macroporous structure and the reduced restriction of SF networks, the increased skin layer effect should drop the deswelling rate of FPN70 lower than that of PN70. However, the deswelling rate of FPN70 is faster than pure PN hydrogels.

3.3.10. Oscillating swelling-deswelling properties

In actual applications of stimuli responsive hydrogels to function as actuators regulating drug release or controlling artificial muscles, rapid oscillating properties to stimuli change is critically demanded. From the dynamic swelling and deswelling investigations, it was observed that the SF β-sheet networks in PN/SF IPNs improved the deswelling rate without decrease of the swelling rates. From these results, it is intriguing to investigate the swelling-deswelling properties of the PN/SF IPN hydrogels in response to short term temperature cycles below and above T_p. The oscillating swelling-deswelling properties of PN, PN90 and PN70 were measured and the results are represented in Figure 3-18. PN100 and PN/SF IPN hydrogels are swollen until equilibrium state in PBS at 20 °C and jumped into PBS at 45 °C, and these hydrogels are then transferred to each PBS bath over 4-min cycles. Pure PN100 hydrogels shows a small decrease of weight in every deswelling cycle, resulting in no significant decrease of swelling degree over repeated temperature jumping cycles. The swelling degree of PN100 oscillates between 85% and 75 % from the second cycle. This indicates that in short temperature cycles, the deswelling rate of PN100 is

similar to its swelling rate. However, PN90 and PN70 exhibit the more rapid decreases of swelling degree in the deswelling process, than PN100, in every cycle. The oscillating curves of PN90 and PN70 gradually decrease. The gradual decrease of the swelling degree of PN90 and PN70 can be explained in terms of their swelling rates not being as fast as their deswelling rates. PN70 shows the faster decrease of swelling degree than PN90 in every cycle, indicating a faster deswelling rate. Even though the IPN hydrogels shows faster response in every deswelling cycle, their swelling process is not notably different from that of pure PN100. This result shows that in every temperature cycle, the SF networks accelerate deswelling process by decreasing the skin layer effect and do not interrupt the swelling rate of PNIPAAm networks.

3.3.11. Three parameters affecting the deswelling kinetics of the IPNs

From the above experiments, we can conclude that there are three parameters affecting the deswelling kinetics of the PN/SF and PNA/SF IPNs.

1. Skin layer formation
2. Restriction of SF β-sheet networks
3. Aggregation force of PNIPAAm or P(NIPAAm-co-AAc) networks

At first, the skin layer formation in the deswelling process decreased with more SF networks that act as water draining channels. Second, the restriction effect of SF β-sheet networks increased with higher SF content. Third, the aggregation force of PNIPAAm networks was higher than that of P(NIPAAm-co-AAc) with AAc moiety that is more hydrophilic and interupts long PNIPAAm backbone chains.

However, these three parameters act with different influences on PN/SF, PNA/SF and their freeze-dried IPNs. In the case of PN/SF IPNs, the most overwhelming parameter was skin layer formation. The more SF β-sheet networks the PN/SF IPNs contained, the less formation of skin layer they showed, resulting in the increased deswelling rate. When SF β-sheet networks significantly decreased the skin layer formation in PN/SF IPNs, the restriction force of SF β-sheet networks competes with the strong aggregation force of PNIPAAm networks, showing a maximum deswelling rate at PN70. On the other hand, PNA/SF IPNs showed very low influence of skin layer formation, because P(NIPAAm-co-AAc) networks originally do not have significant skin layer formation. Therefore, in PNA/SF IPNs, the restriction force of SF β-sheet networks competes with the aggregation force of P(NIPAAm-co-AAc) networks weakened by incorporation of AAc, exhibiting lower deswelling rates than PN/SF IPNs. However, there exist skin layer effects even in PNA/SF IPNs, which decrease with more SF networks, showing a weak maximum among their deswelling rates at PNA70. Freeze-drying might produce more expanded SF β-sheet networks in IPNs as well as macropores. The expanded SF β-sheet networks should increase the skin layer formation effect and decrease the restriction force of SF networks. By this reason, the freeze-dried PN/SF IPNs showed the decreased deswelling rate, because the skin layer formation is the most predominant parameter in their system. By contrast, the deswelling rate of the freeze-dried PNA/SF IPNs increased, because the restriction force of SF networks is the more important parameter in their system.

3.4. Conclusions

In this study, we introduced novel protein-PNIPAAm hydrogels as interpenetrating networks with SF β-sheet crystalline structure. The PN/SF IPNs with the β-sheet crystalline structure of SF have improved viscoelastic properties. 30 wt % of SF increased the storage modulus 7 times over pure PN100. The IPN hydrogels show the same volume phase transition behavior responding to temperature and salt concentration as pure PN100. This means that the SF β-sheet networks do not interfere with the volume phase transition of PNIPAAm networks. With the SF β-sheet networks, the IPNs show the increased deswelling kinetics and exhibit maximum rate at PN70. This result indicates that the water molecules are rapidly released through the induced β-sheet networks and with the skin layer effects reduced by more SF content, the aggregation force of PNIPAAm chains competes with the restriction of SF networks. The proposed IPN hydrogels improve the deswelling rate as well as the mechanical strength and biocompatibility of pure PN100 hydrogels. These PN/SF IPN hydrogels can be applied as rapidly responding actuator systems demanding higher mechanical properties and more biocompatibility. The swelling and deswelling behaviors of PNA/SF IPNs we investigated and compared with those of the PN/SF IPNs. Even though the swelling kinetics of the PNA/SF IPNs showed a similar tendency with pure PNA100, PNA/SF IPNs showed the lower deswelling rate than PN/SF IPNs as well as PNA100.

The freeze-dried PNA/SF IPN hydrogels showed higher swelling ratios than PNA/SF IPN hydrogels and almost recovered the deswelling rate of PNA100 hydrogels. By contrast, the freeze-dried PN/SF IPN hydrogels exhibit lower deswelling rates than PN/SF IPN

hydrogels, even though their swelling ratios were higher than those of PN/SF IPNs. The porous IPN hydrogels can be utilized as a temperature responsive scaffold in tissue engineering.

In our research, we propose that three parameters control the deswelling kinetics of the IPNs: the skin layer formation, the restriction of SF β-sheet networks, and the aggregation force of PNIPAAm networks. These work complexly together in the deswelling process according to SF content and incorporation of AAc moiety.

3.5. References

[1] Gupta P, Vermani K and Garg S. Hydrogels: from controlled release to pH-responsive drug delivery. Drug discovery today 2002; 7, 569-579.

[2] Jeong B and Gutowska A. Lessons from nature: stimuli-responsive polymers and their biomedical applications. TRENDS in Biotechnology. 2002; 20, 305-311.

[3] Qiu Y and Park K. Environment-sensitive hydrogels for drug delivery. Advanced Drug Delivery Reviews. 2001; 53, 321–339.

[4] Sershen S and West J. Implantable, polymeric systems for modulated drug delivery. Advanced Drug Delivery Reviews. 2002; 54, 1225–1235.

[5] Yokoyama M. Gene delivery using temperature-responsive polymeric carriers. Drug Discovery Today. 2002; 7, 426-432.

[6] Chilkoti A, Dreher M R, Meyer D E, and Raucher D. Targeted drug delivery by thermally responsive polymers. Advanced Drug Delivery Reviews. 2002; 54, 613–630.

[7] Bromberg L E and Ron E S. Temperature-responsive gels and thermogelling polymer matrices for protein and peptide delivery. Advanced Drug Delivery Reviews. 1998; 31, 197–221.

[8] Weidner J. Drug targeting using thermally responsive polymers and local hyperthermia. Drug discovery today. 2001; 6, 1239-1248.

[9] Galaev L Y and Mattiasson B. ‘Smart’ polymers and what they could do in biotechnology and medicine. Trends in Biotechnology, 2000; 17, 335-340.

[10] Sharma S, Kaur P, Jain A, Rajeswari M R, and Gupta M N. A smart bioconjugate of chymotrypsin. Biomacromolecules. 2003; 4, 330-336.

[11] Kikuchi A and Okano T, Intelligent thermoresponsive polymeric stationary

phases for aqueous chromatography of biological compounds, Progress in Polymer Science. 2002; 27, 1165-1193.

[12] Kobayashi J, Kikuchi A, Sakai K, and Okano T. Aqueous chromatography utilizing hydrophobicity-modified anionic temperature-responsive hydrogel for stationary phases. Journal of Chromatography A. 2002; 958, 109–119.

[13] Anastase-Ravion S, Ding Z, Pelle A, Hoffman A S, and Letourneur D. New antibody purification procedure using a thermally responsive poly(*N*-isopropylacrylamide)–dextran derivative conjugate. Journal of Chromatography B. 2001; 761, 247–254.

[14] Gil E S, Hudson S M, Stimuli-reponsive polymers and their bioconjugates, Progress in Polymer Science. 2004; 29, 1173–1222.

[15] Diez-Pena E, Quijada-Garrido I, and Barrales-Rienda J M. On the water swelling behaviour of poly(*N*-isopropylacrylamide) [P(NIPAAm)], poly(methacrylic acid) [P(MAA)], their random copolymers and sequential interpenetrating polymer networks (IPNs). Polymer. 2002; 43, 4341–4348.

[16] Varga I, Gilanyi T, Meszaros R, Filipcsei G, and Zrinyi M. Effect of cross-link density on the internal structure of poly(*N*-isopropylacrylamide) microgels. J Phys Chem B. 2001; 105, 9071-9076.

[17] Annaka M, Tanaka C, Nakahira T, Sugiyama M, Aoyagi T, and Okano T. Fluorescence study on the swelling behavior of comb-type grafted poly(*N*-isopropylacrylamide) hydrogels. Macromolecules. 2002; 35, 8173-8179.

[18] Yoshida R, Uchida K, Kaneko Y, Sakai K, Kikuchi A, Sakurai Y, and Okano T. Comb-type grafted hydrogels with rapid de-swelling response to temperature changes. Nature. 1995; 374, 240-242.

[19] Jeong B, Lee K M, Gutowska A, and An Y H. Thermogelling biodegradable copolymer aqueous solutions for injectable protein delivery and tissue engineering. Biomacromolecules. 2002; 3, 865-868.

[20] Lin H and Cheng Y. *In-situ* thermoreversible gelation of block and star copolymers of poly(ethylene glycol) and poly(*N*-isopropylacrylamide) of varying architectures. Macromolecules. 2001; 34, 3710-3715.

[21] Jeong B. Bae Y H, Lee D S, and Kim S W. Biodegradable block copolymers as injectable drug-delivery systems. Nature. 1997; 388, 860-862.

[22] Zhang R, Liu J, He J, Han B, Zhang X, Liu Z, Jiang T, and Hu G. Compressed CO_2-assisted formation of reverse micelles of PEO-PPO-PEO copolymer. Macromolecules. 2002; 35, 7869-7871.

[23] Chung J E, Yokoyama M, Aoyagi T, Sakurai Y, and Okano T. Effect of molecular architecture of hydrophobically modified poly(*N*-isopropylacrylamide) on the formation of thermoresponsive core-shell micellar drug carriers. Journal of

Controlled Release. 1998; 53, 119–130.

[24] Magoshi T, Ziani-Cherif H, Ohya S, Nakayama Y, and Matsuda T. Thermoresponsive heparin coating: Heparin conjugated with poly(*N*-isopropylacrylamide) at one terminus. Langmuir. 2002; 18, 4862-4872.

[25] Rama Rao G V, Krug M E, Balamurugan S, Xu H, Xu Q, and Lopez G P. Synthesis and characterization of silica-poly(*N*-isopropylacrylamide) hybrid membranes: switchable molecular filters. Chem Mater. 2002; 14, 5075-5080.

[26] Nath N and Chilkoti A. Interfacial Phase Transition of an environmentally responsive elastin biopolymer adsorbed on functionalized gold nanoparticles studied by colloidal surface plasmon resonance. J Am Chem Soc. 2001; 123, 8197-8202.

[27] Lackey C A, Murthy N, Press O W, Tirrell D A, Hoffman A S, and Stayton P S. Hemolytic activity of pH-responsive polymer-streptavidin bioconjugates. Bioconjugate Chem. 1999; 10, 401-405.

[28] Benns J M, Choi J, Mahato R I, Park J, and Kim S W. pH-sensitive cationic polymer gene delivery vehicle: *N*-Ac-poly(L-histidine)-graft-poly(L-lysine) comb shaped polymer. Bioconjugate Chem. 2000; 11, 637-645.

[29] Schild H G. Poly(*N*-isopropylacrylamide): Experiment, theory and application. Prog Polym Sci. 1992; 17, 163–249.

[30] Kaneko Y, Nakamura S, Sakai K, Aoyagi T, Kikuchi A, Sakurai Y, and Okano T. Rapid deswelling response of poly(*N*-isopropylacrylamide) hydrogels by the formation of water release channels using poly(ethylene oxide) graft chains. Macromolecules. 1998; 31, 6099-6105.

[31] Annaka M, Sugiyama M, Kasai M, Nakahira T, Matsuura T, Seki H, Aoyagi T, and Okano T. Transport properties of comb-type grafted and normal-type *N*-isopropylacrylamide hydrogel. Langmuir. 2002; 18, 7377-7383.

[32] Suzuki K, Yumura T, Tanaka Y, and Akashi M. Thermo-responsive release from interpenetrating porous silica–poly(*N*-isopropylacrylamide) hybrid gels. Journal of Controlled Release. 2001; 75, 183–189.

[33] Wang C, Stewart R J and Kopeček J. Hybrid hydrogles assembled from synthetic polymers and coiled-coil protein domains. Nature. 1999; 397, 417-420.

[34] Dhara D, Rathna G V N, and Chatterji P R. Volume phase transition in interpenetrating networks of poly(*N*-isopropylacrylamide) with gelatin. Langmuir. 2000; 16, 2424-2429.

[35] Wu A S, Hoffman A S, Yager P J. Synthesis and characterization of thermally reversible macroporous poly(*N*-isopropylacrylamide) hydrogels. J Polym Sci, Polym Chem. 1992; 30, 2121-2129.

[36] Kishi R, Hirasa O, and Ichijo H. Fast responsive poly(*N*-isopropylacrylamide)

hydrogels prepared by γ-ray irradiation. Gels Networks. 1997; 5, 145.

[37] Beebe D J, Moore J S, Bauer J M, Qing Yu Q, Robin H. Liu R H, Chelladurai Devadoss C, and Jo B. Functional hydrogel structures for autonomous flow control inside microfluidic channels, Nature, 2000, 404, 588-590.

[38] Zhang X, Wu D, Chu C, Synthesis, characterization and controlled drug release of thermosensitive IPN-PNIPAAm hydrogels, Biomaterials, 2004, 25, 3793-3805.

[39] Zhou C Z, Confalonieri F, Medina N, Zivanovic Y, Esnault C, Yang T, Jacquet M, Janin J, Duguet M, Perasso R, and Li Z G. Fine organization of Bombyx mori fibroin heavy chain gene, Nucleic Acids Res. 2000, 28, 2413-2419.

[40] Baggha A, Tonelli A and Hudson S. The Dissolution and Characterization of Bombyx Mori Silk in Calcium Nitrate/Methanol Solution and Regeneration and Characterization of Thin Films. Biopolymers, 1997, 42, 61-74.

[41] Ha S, Park Y H., Hudson M S. Dissolution of Bombyx mori Silk Fibroin in the Calcium Nitrate Tetrahydrate-Methanol System and Aspects of Wet Spinning of Fibroin Solution. Biomacromolecules, 2003, 4, 488-496.

[42] Nazarov R, Jin H, and Kaplan D. Porous 3-D Scaffolds from Regenerated Silk Fibroin. Biomacromolecules, 2004, 5, 718-726

[43] Gotoh Y, Tsukada M, Minoura N, and Imai Y. Synthesis of poly(ethylene glycol)-silk fibroin conjugates and surface interaction between L-929 cells and the conjugates. Biomaterials, 1997, 18, 267-271.

[44] Minoura N, Tsukada M, Nagura M. Fine structure and oxygen permeability of silk fibroin membrane treated with methanol. Polymer, 1990, 31, 265-269.

[45] Gu J, Yang X, and Zhu H. Surface sulfonation of silk fibroin film by plasma treatment and in vitro antithrombogenicity study. Materials Science and Engineering: C, 2002, 20, 199-202.

[46] Vonfraunhofer J A, and Sichina W J. Characterization of surgical suture materials using dynamic mechanical analysis. Biomaterials, 1992, 13, 715-720

[47] Padamwar M N, and Pawar A P. Silk sericin and its applications: A review, Journal of scientific and industrial research, 2004, 63, 323-329

[48] Zhang Y Q. Natural silk fibroin as a support for enzyme immobilization. Biotechnology advances, 1998, 16, 961-971.

[49] Santin M, Motta A, Freddi G, and Cannas M. In vitro evaluation of the inflammatory potential of the silk fibroin. Journal of biomedical materials research, 1999, 46, 382-389.

[50] Rujiravanit R, Kruaykitanon S, Jamieson A M, Tokura S. Preparation of crosslinked chitosan/silk fibroin blend films for drug delivery system. Macromolecular bioscience 2003, 3, 604-611.

[51] Li M, Lu S, Wu Z, Tan K, Minoura N, Kuga S. Structure and properties of silk fibroin–poly(vinyl alcohol) gel. International Journal of Biological Macromolecules, 2000, 30, 89–94.

[52] Shibayama M and Tanaka T. Volume phase transition and related phenomena of polymer gels. Adv Polym Sci. 1993; 109, 1–62.

[53] Hoffman A S et al. Really smart bioconjugates of smart polymers and receptor proteins, J Biomed Mater Res. 2000; 52, 577–586.

[54] Lee A S, Butun V, Vamvakaki M, Armes S P, Pople J A, and Gast A P. Structure of pH-dependent block copolymer micelles: Charge and ionic strength dependence. Macromolecules. 2002; 35, 8540-8551.

[55] Park T G, Hoffman A S. Sodium chloride-induced phage-transition in nonionic poly(N-isopropylacrylamide) gel, Macromolecules, 1993, 26, 5045-5048.

[56] Zhuo R, and Li W. Preparation and Characterization of Macroporous Poly(Nisopropylacrylamide) Hydrogels for the Controlled Release of Proteins. J Polym Sci Part A: Polym Chem, 2003, 41: 152-159.

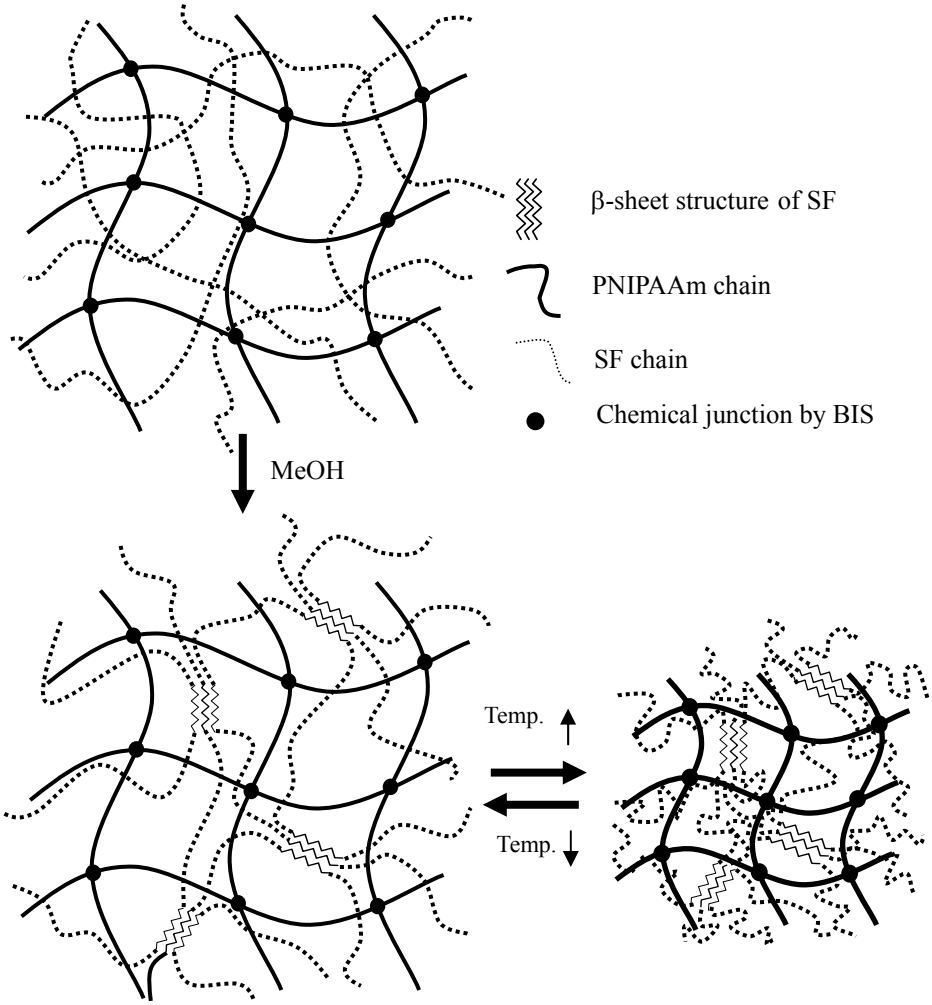

Scheme 3-1 Schematic structures of proposed PNIPAAm/SF IPN hydrogels.

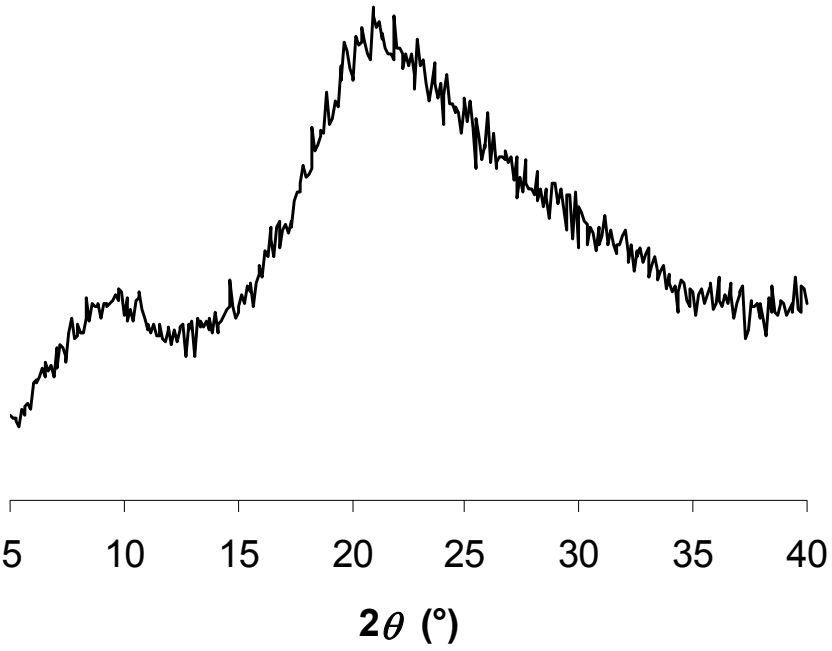

Figure 3-1 Wide Angle X-ray Diffraction (WAXD) curve of PNIPAAm/SF IPNs (40/60) (PN40).

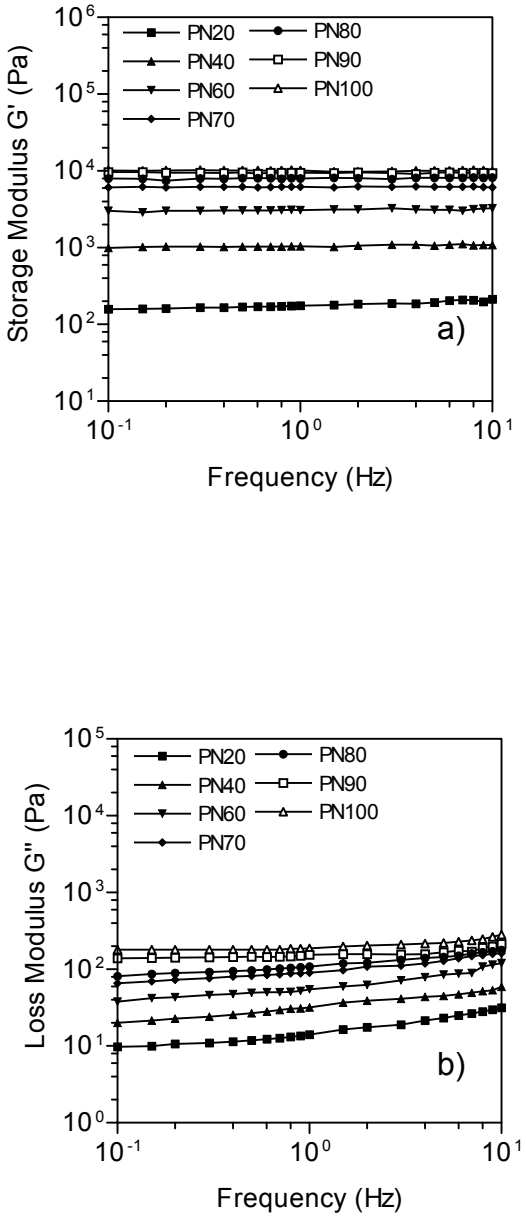

Figure 3-2 Viscoelastic properties of the untreated PNIPAAm/SF hydrogels, a) plot of storage modulus (G') vs frequency, b) plot of loss modulus (G'') vs frequency.

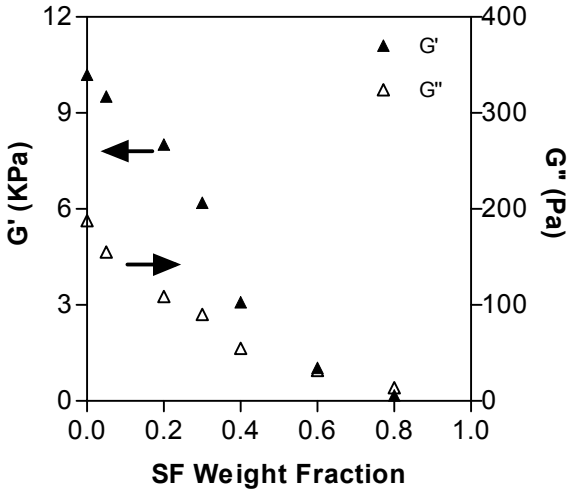

Figure 3-3 Storage modulus and loss modulus of the untreated PNIPAAm/SF hydrogels at the frequency of 1 Hz according to SF weight fraction.

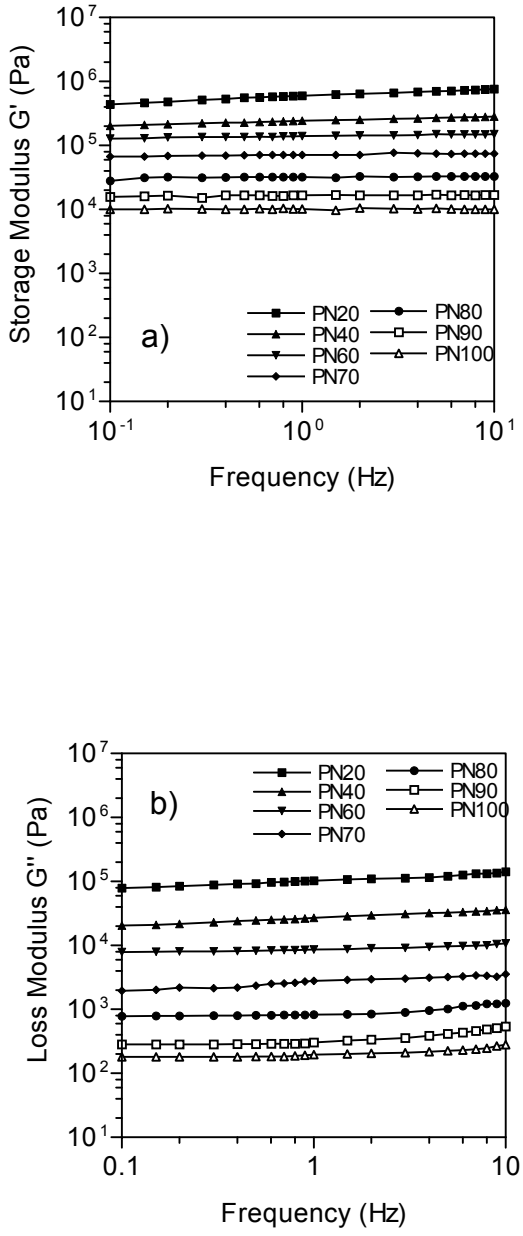

Figure 3-4 Viscoelastic properties of the treated PNIPAAm/SF hydrogels, a) plot of storage modulus (G') vs frequency, b) plot of loss modulus (G'') vs frequency.

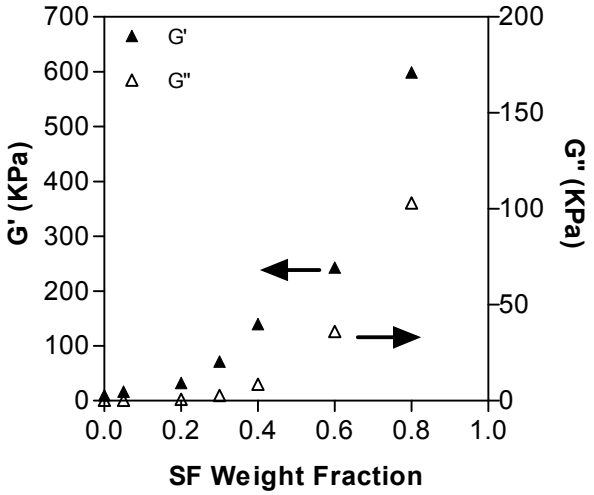

Figure 3-5 Storage modulus and loss modulus of the treated PNIPAAm/SF hydrogels at the frequency of 1 Hz according to SF weight fraction.

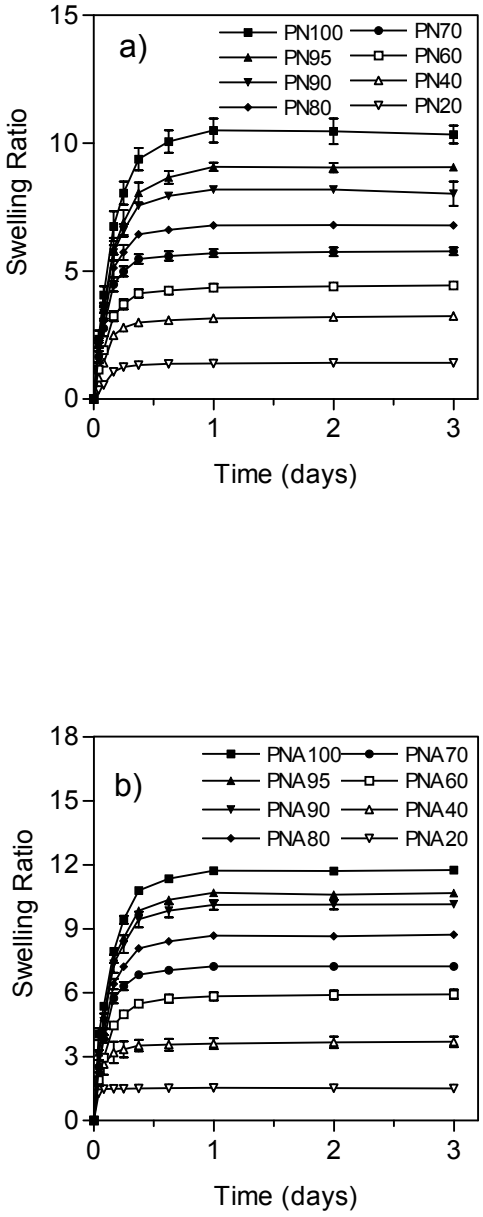

Figure 3-6 Dynamic swelling curves of a) PNIPAAm/SF and b) P(NIPAAm-co-AAc)/SF IPN hydrogels in PBS (pH 7.4) at 20 °C

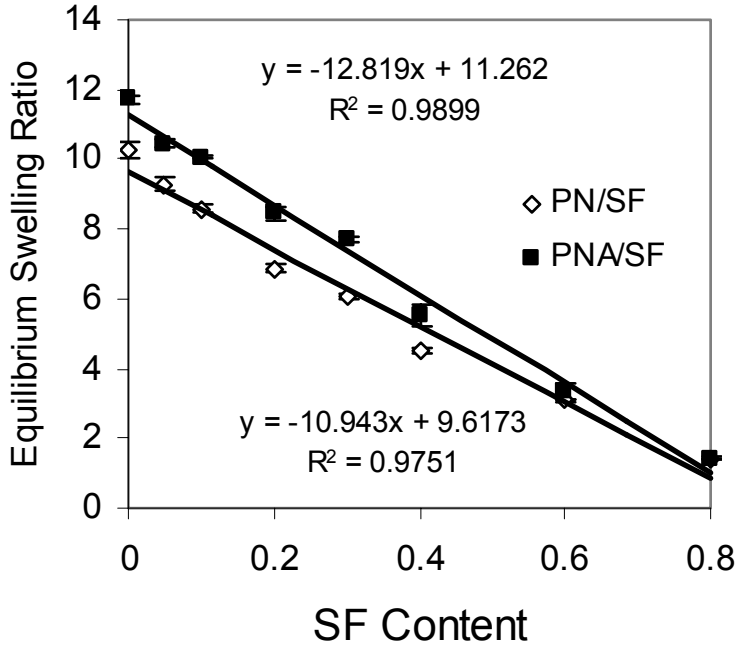

Figure 3-7 Plots of the equilibrium swelling ratios vs SF weight fraction for the PNIPAAm/SF and P(NIPAAm-co-AAc)/SF IPN hydrogels.

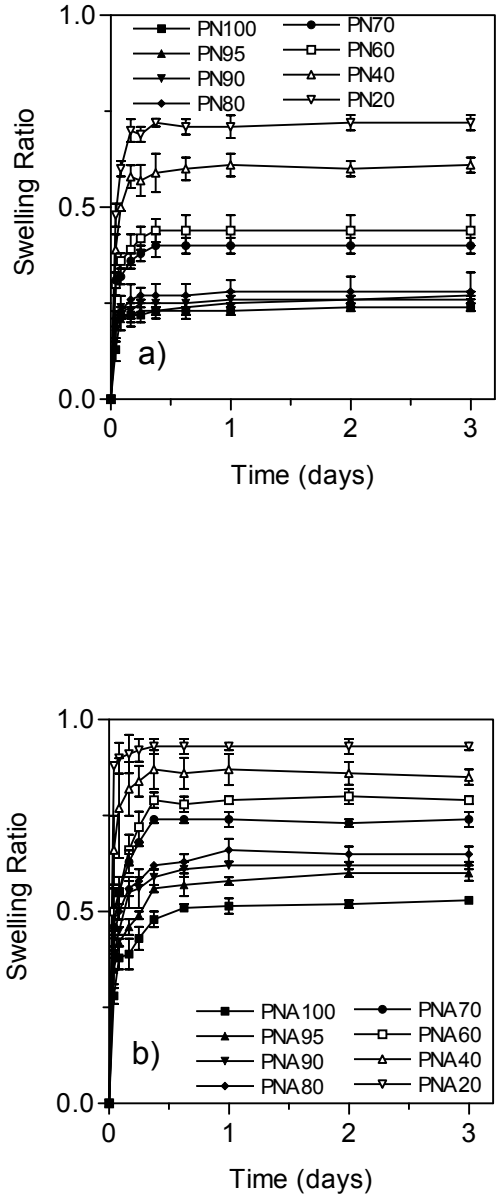

Figure 3-8 Dynamic swelling curves of a) PNIPAAm/SF and b) P(NIPAAm-co-AAc)/SF IPN hydrogels in PBS (pH 7.4) at 45 °C.

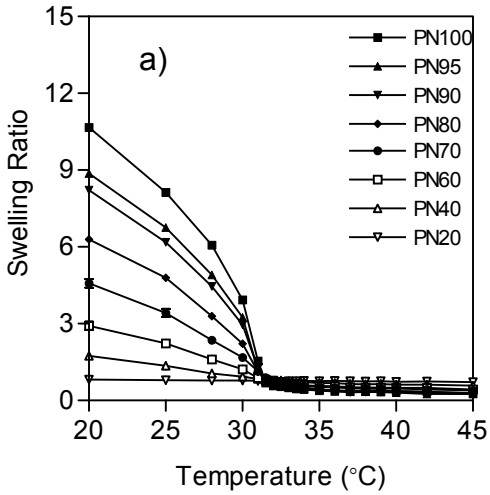

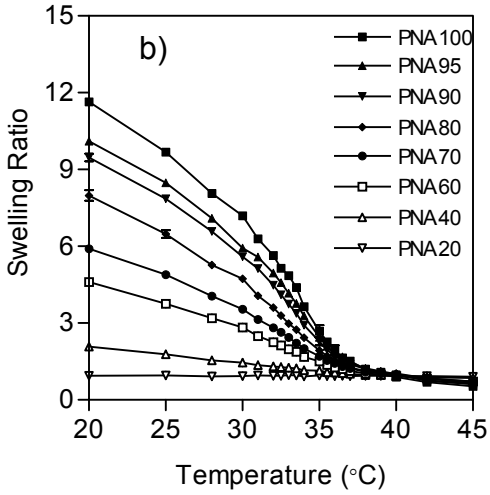

Figure 3-9 Equilibrium swelling ratios for a) PNIPAAm/SF IPN hydrogels and b) P(NIPAAm-co-AAc)/SF IPN hydrogels in PBS (pH 7.4) at the temperature range from 45 °C to 20 °C.

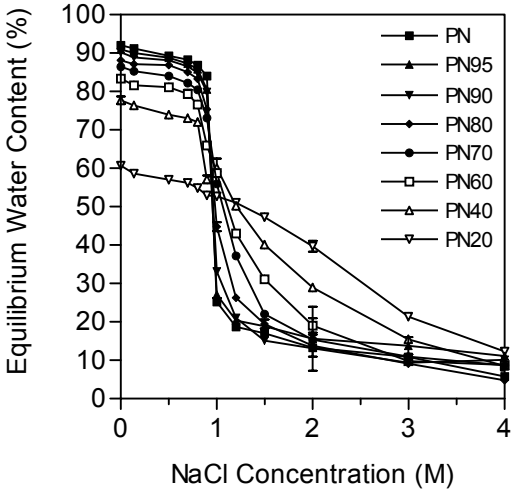

Figure 3-10 Effect of NaCl concentration on the water content of the PNIPAAm/SF IPN hydrogels.

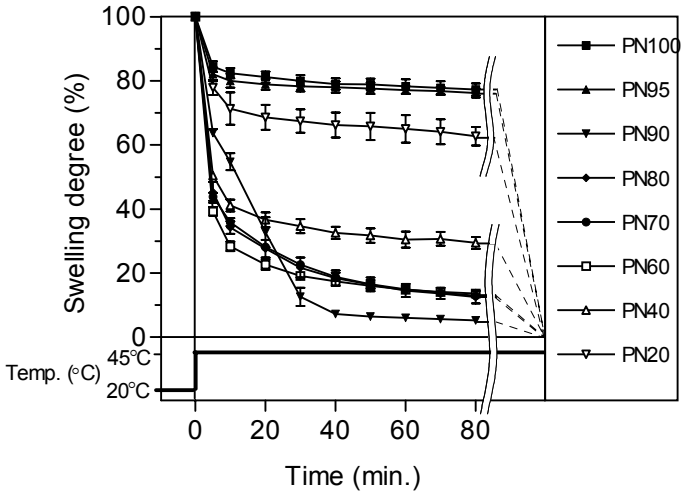

Figure 3-11 Deswelling kinetics of PNIPAAm/SF IPNs after temperature jumping from 20 °C to 45 °C.

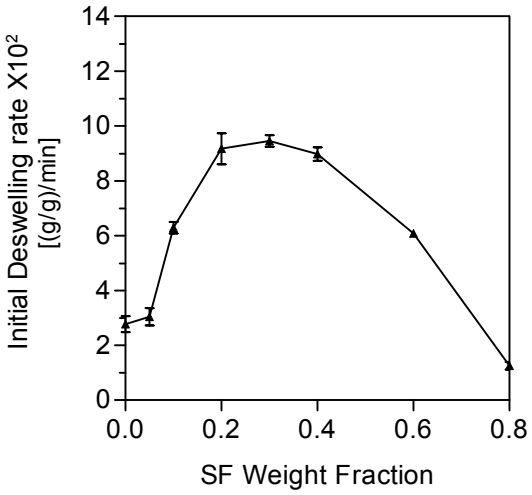

Figure 3-12 Initial deswelling rates of PNIPAAm/SF IPN hydrogels calculated from the decreased gel weight within 5 min after transferring gels to 45 °C per the swollen gel weight at 20°C.

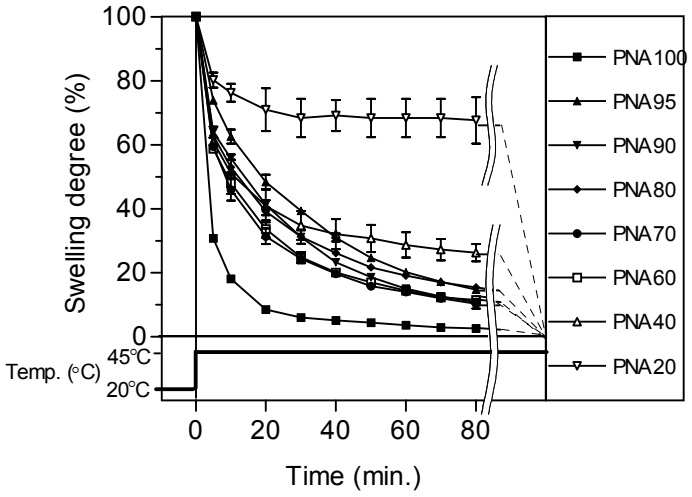

Figure 3-13 Deswelling kinetics of P(NIPAAm-co-AAc)/SF IPNs after temperature jumping from 20 °C to 45 °C.

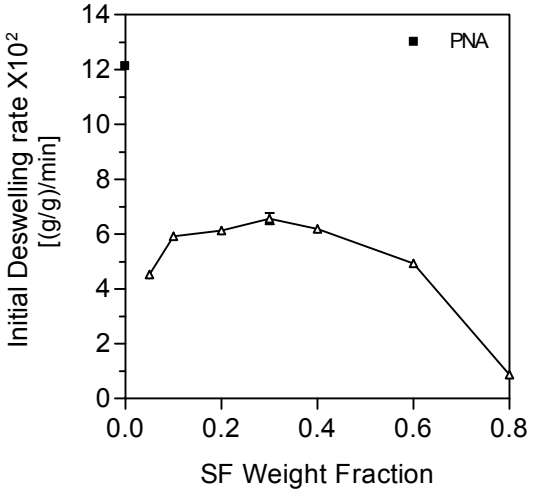

Figure 3-14 Initial deswelling rates of P(NIPAAm-co-AAc)/SF IPN hydrogels calculated from the decreased gel weight within 5 min after transferring gels to 45 °C per the swollen gel weight at 20°C.

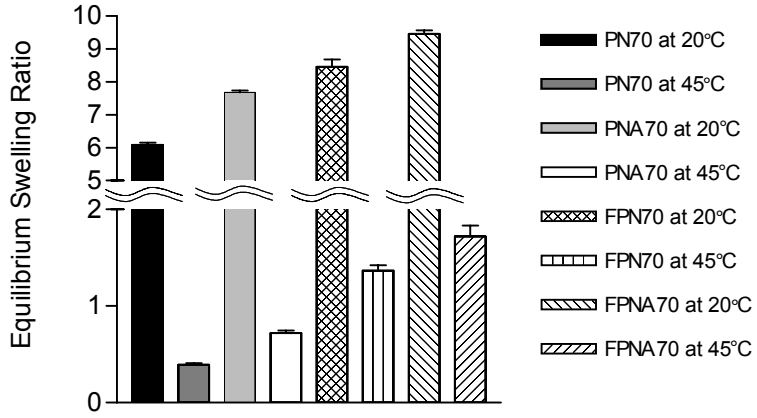

Figure 3-15 Equilibrium swelling ratios of PN70, PNA70, FPN70 and FPNA70 at 20 °C and 45 °C.

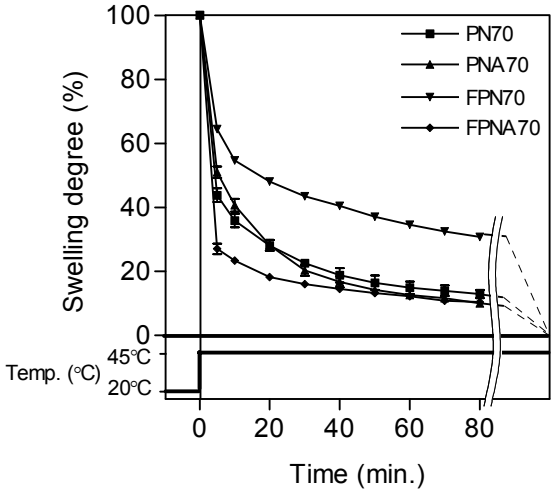

Figure 3-16 Deswelling kinetics of the FPN70 and FPNA70 after temperature jumping from 20 °C to 45 °C.

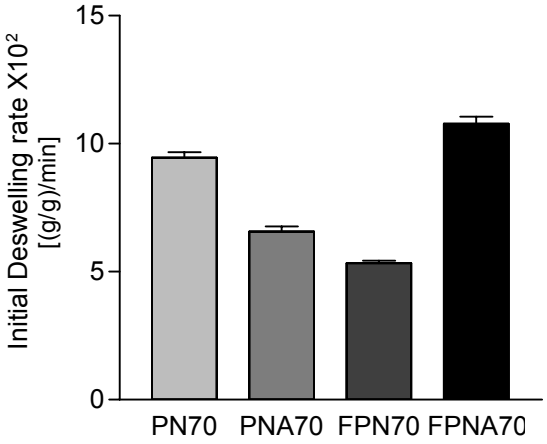

Figure 3-17 Initial deswelling rates of FPN70 and FPNA70 calculated from the decreased gel weight within 5 min after transferring gels to 45 °C per the swollen gel weight at 20°C.

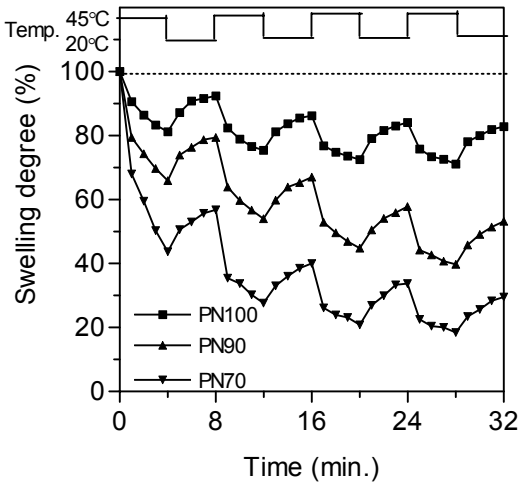

Figure 3-18 Oscillating swelling deswelling properties of PN, PN90 and PN70 over 4-min cycles between 20 °C and 45 °C.

4. Recommendations for future research

The first recommendation for future research is to test drug release from Gel/SF hydrogels in vitro and in vivo. Also, the morphological investigation can be recommended to observe the morphological change between before and after treatment. Also, the effect of soaking time and treatment condition on the Gel/SF complex hydrogels can be investigated by morphological test with SEM and AFM.

The other recommendation for Gel/SF is to fabricate macroporous Gel/SF complex scaffolds for tissue engineering. Freeze-drying method can be used for manufacturing the scaffolds. The porosity, mechnical strength, degradation, and drug release should be important factors for this material.

In the case of PN/SF hydrogels, I would like to recommend morphological test the fractures and sufaces of the swollen hydrogels and collapsed hydrogels after freeze-drying. These morphologica tests should provide more information about the swelling and deswelling process. More investigation about the macroporous PN/SF and PNA/SF scaffolds should give us more valuable information for real applications such as temperature responsive scaffolds as artificial tissue.

Most of all, I would like to recommend to utilize SF β-sheet networks in fabricating IPNs with the other fuctional polymers such as poly(acrylic acid), poly(L-lactic acid), and poly(N,N'-diethyl aminoethyl methacrylate).